UNIVERSIDADE DE LISBOA
FACULDADE DE CIÊNCIAS
DEPARTAMENTO DE QUÍMICA E BIOQUÍMICA

Development of nanosystems for HIV vaccine delivery

Ana Isabel Neves de Matos

Dissertation
Master in Biochemistry
Specialization: Biochemistry

2014

UNIVERSIDADE DE LISBOA
FACULDADE DE CIÊNCIAS
DEPARTAMENTO DE QUÍMICA E BIOQUÍMICA

Development of nanosystems for HIV vaccine delivery

Ana Isabel Neves de Matos

Dissertation
Master in Biochemistry
Specialization: Biochemistry

Supervisors: Carla Real Afonso, PhD, FCUL
Helena Florindo, PhD, FFUL

2014

Acknowledgements

The progress of this master thesis was only possible with teamwork. For this reason, I want to thank all people that worked with me this year.

I express my deepest gratitude to my supervisor, Prof. Helena Florindo, not only for the opportunity to develop this project in her laboratory, but also for the unconditional help, support and friendship throughout this year.

I am grateful to my supervisor, Prof. Carla Afonso, for accepting embarks on this adventure and for helping me with confocal microscopy, as well as Filipe.

I thank to all my group colleagues by teaching, advice and guidance, especially Carina Peres, Eva Zupančič and Joana Silva. Your friendship has made everything much easier.

A special thanks to Melissa Sirage by strong friendship attained this year that will remain for live.

I am grateful to Prof. Liana Silva for all the advice given.

I am very thankful to Ana Salgado and Prof. Ana Viana for helping me with HPLC and AFM analysis, respectively.

I would like to thank Fundação para a Ciência e a Tecnologia (FCT) for the financial support: PTDC/SAU-FAR/119389/2010 and Pest- OE/SAU/UI4013/2011.

Finally, my sincere gratitude to my family and friends for their patience, strength and care at all times. A special thank you to my parents for the unconditional love. An extra special thanks to João, my safe haven.

Thank you all!

Abstract

Purpose: Despite the improvements achieved in the current therapy regimens, the development of prophylactic, safe and highly immunogenic vaccines to control and eradicate the Human Immunodeficiency Virus (HIV) remains one of the most exigent and challenging tasks. To prevent HIV infection, highly specialized antigen presenting cells, as dendritic cells (DCs), have to elicit effective humoral and cellular immune responses. In fact, the induction of both virus-specific neutralizing antibodies (IgG and IgA), at the site of viral entry, and cytotoxic T lymphocyte along with a Th1 response seem to be crucial to impair the dissemination of the virus. As a promising strategy for HIV delivery systems, polymeric nanoparticles (NPs) can protect HIV-1 antigens from unfavorable conditions after administration, in addition to acting as adjuvants by enhancing the antigen uptake by DCs. T20 and T1249 antigenic peptides are HIV-1 fusion inhibitors derived from the gp41 helical region adjacent to the C-terminal sequence that have never been associated to a particulate delivery system. This project aims to design a HIV-1 vaccine throught the entrappement of HIV-1 antigenic peptides (T20 and T1249) into polymeric NPs.

Materials and Methods: Polymeric NPs were prepared by the double emulsion solvent evaporation method and characterized. Polyvinyl alcohol, block co-polymer Pluronic® F127 and glycol chitosan were included in vaccine formulation to promote their potential adjuvant effect and/or improve NP stability. Model antigen ovalbumin and HIV-1 gp41 peptides, T20 and T1249, were entrapped or co-entrapped into NPs. Characterization of NPs was performed in terms of size, zeta potential and surface morphology by Dynamic Light Scattering, Laser Doppler Electrophoresis and Atomic Force Microscopy, respectively. Entrapment efficiency (EE, % (w/w)) and loading capacity (LC, µg/mg) of the entrapped agents were quantified by MicroBCA®, High Performance Liquid Chromatography and fluorescence. DCs were used to evaluate the *in vitro* cytotoxicity of NPs by the AlamarBlue® assay and the cellular uptake and intracellular trafficking of rhodamine-labeled NPs by confocal microscopy. The peptide integrity was also assessed by sodium dodecyl sulphate polyacrylamide gel electrophoresis.

Results: NPs presented mean diameters in the range of 170-180 nm, with a narrow size distribution (PdI < 0.15), surface charge close to neutrality and spherical shape. These antigen delivery systems presented high EE and LC, and no cytotoxic

effect on DCs, in the range of tested concentrations (0.125-1 mg/mL), after 24, 48 and 72 h of incubation. According to NP physicochemical characteristics, PLGA-PEG_GCs formulation was selected for further studies. Peptide structure was maintained intact, not being affected by the double emulsion procedure. Confocal microscopy confirmed the internalization of NPs, demonstrating their endosomal localization and a tendency to accumulate close to the endoplasmic reticulum.

Conclusions: The results herein described show that stable and reproducible PLGA-PEG_GCs NPs produced using a modified double emulsion solvent evaporation method constitute a promising platform for the successful delivery of HIV antigens to DCs, in order to develop a HIV-1 vaccine.

Keywords

HIV-1 vaccine, PLGA-PEG nanoparticles, HIV-1 gp41 peptides, targeted delivery systems, dendritic cells, intracellular trafficking

Resumo

Objetivo: Apesar dos avanços alcançados nas terapêuticas atuais, o desenvolvimento de vacinas profiláticas, seguras e altamente imunogénicas para controlar e erradicar o vírus da imunodeficiência humana (HIV) continua a ser uma das tarefas mais exigentes e desafiantes. Para prevenir a infeção por HIV, as células apresentadoras de antigénio (APCs) altamente especializadas, têm de induzir respostas imunitárias humorais e celulares eficazes. Mais especificamente, a indução de anticorpos neutralizantes específicos contra o vírus (nomadamente as imunoglobulinas (Ig)G, IgA e IgE) secretados pelos linfócitos B, especialmente no local de entrada do vírus (resposta tipo Th2), e a estimulação de linfócitos T citotóxicos juntamente com uma resposta do tipo Th1 parecem ser cruciais para travar a disseminação deste vírus. Deste modo, a persistência da infeção por HIV parece estar intimamente associada à inadequada estimulação de uma resposta imunológica eficaz e específica capaz de destruir o vírus. Esta resposta é bastante complexa, não existindo uma correlação directa entre a infeção por este agente e eventuais mecanismos de proteção ou controlo da disseminação da doença.

O HIV liga-se ao receptor CD4 via glicoproteína gp120 do invólucro viral, a qual sofre uma alteração conformacional, facilitando a sua ligação a um dos dois co-recetores de referência, CCR5 ou CXCR4. A interação da gp120 com o recetor CD4 e os co-recetores é vital para que o vírus se ligue à célula. Contudo, para finalizar o processo de infeção vírus-célula, a glicoproteína gp41 do invólucro viral terá posteriormente de interagir com um recetor de fusão na célula. Após a fusão, o conteúdo viral é libertado para o interior da célula com a subsequente transcrição do RNA viral em DNA, que será transportado até ao núcleo e integrado no genoma celular, sendo posteriormente traduzido em proteínas. Estas proteínas virais, juntamente com o RNA viral, são transportados para a superfície celular iniciando a formação de novos viriões maduros. Os linfócitos T e B, os macrófagos e as células dendríticas (DCs) podem expressar os co-recetores CCR5 ou CXCR4, estando portanto suscetíveis à infeção por HIV. No entanto, apenas as DCs podem ligar-se à glicoproteína gp120 sem que haja fusão membranar.

As DCs são atualmente reconhecidas como entidades fundamentais para a estimulação de uma resposta imunológica robusta e específica contra o HIV, a qual se deve à sua capacidade de migração para os órgãos linfáticos, zonas ricas em linfócitos

T, onde apresentarão os antigénios fagocitados e consequentemente levarão à estimulação dos linfócitos T $CD4^+$ e $CD8^+$, promovendo um eficiente e prolongado controlo da replicação do vírus no hospedeiro. No entanto, o papel destas APCs na imunologia do HIV está longe de ser um tema consensual. Estas células podem capturar, processar e apresentar o HIV desencadeando uma resposta eficaz e específica. Contudo, uma vez infetadas, as DCs podem infetar os linfócitos T, promovendo a disseminação do vírus e a progressão da doença. A fase crónica e assintomática da doença é caracterizada por um decréscimo da carga viral, persistindo o vírus latente em tecidos extravasculares, nódulos linfáticos, DCs e nos linfócitos T $CD4^+$. Embora seja reconhecido o papel dos linfócitos T no controlo da infeção crónica por HIV-1, a imunidade especificamente induzida contra este microrganismo decresce após períodos prolongados da supressão do vírus, não conseguindo controlar a replicação do vírus e consequentemente originando a progressão da doença. Apesar destes doentes serem tratados com medicamentos antiretrovirais, reconhecidos como a melhor opção terapêutica atualmente disponível, estes tratamentos são dispendiosos, apresentam efeitos secundários significativos inerentes à sua toxicidade, dificultando a adesão à terapêutica por parte do doente por longos períodos. Mesmo na presença de medicamentos antiretrovirais, o vírus permanece latente no organismo em níveis não detetáveis, nomeadamente em linfócitos T $CD4^+$ memória. Estes estão inativos, constituindo reservatórios que protegem o vírus da resposta imunológica e da terapêutica antiretroviral, tornando praticamente impossível a eliminação total do vírus com as abordagens terapêuticas actualmente disponíveis.

O desenvolvimento de vacinas preventivas e de abordagens imunoterapêuticas contra a infeção por HIV tem sido bastante dificultado pela complexidade dos mecanismos imunológicos associados. De fato, a mutação do vírus, a capacidade deste ultrapassar a resposta imunológica humoral, bem como a manipulação das APCs evitando a maturação destas e portanto a eficaz apresentação dos antigénio aos linfócitos T, têm contribuído para a falta de eficácia obtida por inúmeros candidatos. Deste modo, torna-se desejável o desenvolvimento de novas estratégias capazes de modelar a resposta imunológica contra a infeção por HIV. As nanopartículas (NPs) poliméricas constituem sistemas promissores para o transporte de antigénios HIV-1. De fato, estes nanosistemas protegem os antigénios de HIV-1 das condições desfavoráveis após a sua administração e podem atuar como adjuvantes, aumentando o reconhecimento e a internalização de antigénios pelas DCs. Assim, este projeto único e

inovador tem como objetivo criar uma vacina contra o HIV-1 através da encapsulação dos péptidos antigénicos inibidores de fusão do HIV-1, derivados da sequência da região helicoidal adjacente ao C-terminal da gp41, T20 e T1249 em NPs poliméricas. É importante referir que estes péptidos de HIV-1 nunca foram associados a partículas poliméricas.

Materiais e Métodos: As NPs poliméricas foram preparadas utilizando o método de dupla emulsão com a evaporação do solvente. O álcool polivinílico, o co-polímero Pluronic® F127 e o glicol quitosano foram incluídos na formulação da vacina para promover o seu potencial efeito adjuvante e/ou aumentar a estabilidade das NPs. O antigénio modelo ovalbumina e os péptidos de HIV-1 gp41, T20 e T1249, foram incorporados ou co-incorporados nas NPs. A caracterização da NPs foi realizada tendo em conta o tamanho, a carga e morfologia da sua superfície por Dispersão Dinâmica de Luz, Dispersão Electroforética da Luz e Microscopia de Força Atómica, respetivamente. A eficiência de incorporação (EE, % (w/w)) e capacidade de carga (LC, µg/mg) dos agentes incorporados foram quantificados por MicroBCA®, Cromatografia Líquida de Alta Eficiência e fluorescência. As DCs foram usadas para avaliar a citotoxicidade *in vitro* das NPs através do ensaio AlamarBlue® e a captura e tráfego intracelular das NPs marcadas com rodamina foram estudados por microscopia confocal. A integridade da estrutura dos péptidos foi ainda confirmada por electroforese em gel de poliacrilamida em condições desnaturantes, utilizando o dodecil sulfato de sódio.

Resultados: As NPs apresentaram diâmetros médios compreendidos entre 170-180 nm, com uma distribuição de tamanhos restrita (PdI < 0,15), carga superficial próxima da neutralidade e forma esférica. Estes sistemas de transporte de antigénios apresentaram elevados EE e LC, e nenhum efeito citotóxico em DCs, na gama de concentrações testadas (0,125-1 mg/mL), após 24, 48 e 72 h de incubação. Tendo em consideração os resultados previamente descritos, nomeadamente as características físico-químicas das NPs, a formulação PLGA-PEG_GCs foi selecionada para os restantes estudos. A estrutura dos péptidos foi mantida intacta, não sendo afetada pelo processo de dupla emulsão. A microscopia confocal confirmou a internalização das NPs, demonstrando a sua localização endosomal e uma tendência para se acumularem perto do retículo endoplasmático.

Conclusões: Os resultados aqui descritos mostram que NPs estáveis e reprodutíveis foram produzidas utilizando um método de dupla emulsão com evaporação de solvente modificado. Importa no entanto realçar que as NPs PLGA-

PEG_GCs constituem uma plataforma promissora para o transporte e eficaz apresentação de antigénios de HIV, tendo em vista o desenvolvimento de uma vacina eficaz contra a infeção por HIV-1.

Palavras-chave

Vacina contra a infeção por HIV-1, nanopartículas PLGA-PEG, péptidos de HIV-1 gp41, sistemas de transporte, células dendríticas, tráfego intracelular

List of Contents

List of Figures

List of Tables

List of Abbreviations

η: Yield

λ_{max}: Maximum wavelength

Abs: Antibodies

AFM: Atomic Force Microscopy

AIDS: Acquired Immune Deficiency Syndrome

AP: Alkaline phosphatase

APs: Ammonium persulfate

APCs: Antigen presenting cells

ART: Antiretroviral therapy

ATCC: American Type Culture Collection

BCA: bicinchoninic acid

BMDCs: Bone marrow dendritic cells

bNAbs: Broadly neutralizing antibodies

BSA: Bovine serum albumin

BSP: Betamethasone sodium phosphate

$CaCl_2$: Calcium chloride

CD40L: CD40 ligand

CHR: Helical region adjacent to the C-terminal

CLRs: C-type lectin receptors

CNS: Central nervous system

CpG: Unmethylated cytosine-phosphate-guanine oligodeoxynucleotides

Cs: Chitosan

CTL: Cytotoxic T lymphocytes

DCM: Dichloromethane

DCs: Dendritic cells

DC-SIGN: Dendritic cell specific intercellular adhesion molecule-grabbing non-integrin

DLS: Dynamic Light Scattering

DNA: deoxyribonucleic acid

DPBS: Dulbecco's PBS

dsRNA: Double stranded RNA

EE: Entrapment efficiency

EFV: Efavirenz

EMA: European Medicine Agency

EP: External aqueous phase

ER: Endoplasmic reticulum

FBS: Heat inactivated fetal bovine serum

FDA: Food and Drug Administration

FGF: Fibroblast growth factor

GALT: Gut-associated lymphoid tissues

GCs: Glycol chitosan

GM-CSF: Granulocyte-macrophage colony stimulating factor

gp: Glycoprotein

6HB: Six-helix bundle

HAART: Highly active ART

HCl: Hydrochloric acid

HIV: Human Immunodeficiency Virus

HIV-1: Human Immunodeficiency Virus type 1

HIV-2: Human Immunodeficiency Virus type 2

HPLC: High Performance Liquid Chromatography

HR: Helical region

HSV-2: Herpes Simplex Virus type 2

ICH: International Conference Guidelines

ID: Intradermal

IFN: Interferon

Ig: Immunoglobulin

IL: Interleukin

IM: Intramuscular

IN: Intranasal

IP: Internal aqueous phase

IS: Infectious synapse

ISCOMs: Immunostimulating complexes

LB: Loading buffer

LC: Loading capacity

LCs: Langerhans cells

LDE: Laser Doppler Electrophoresis

LPS: Lipopolysaccharide

M1 and M2: Mander's coefficients 1 and 2

MALP: Macrophage-activating lipopeptide

MBD: Methyl-CpG binding domain protein

$MgCl_2$: Magnesium chloride

MHC: Major histocompatibility complex

MIP: Macrophage inflammatory protein

MPLA: Monophosphoryl lipid A

MRI: Magnetic Resonance Imaging

mRNA: Messenger RNA

MTT: Thiazolyl blue tetrazolium bromide

Mw: Molecular weight

Na_2HPO_4: sodium phosphate dibasic

NaCl: sodium chloride

NaH_2PO_4: sodium phosphate monobasic

NHR: Helical region adjacent to the N-terminal

NK: Natural killer

NPs: Nanoparticles

NPs-Rho: Rhodamine-labeled NPs

OVA: Ovalbumin, albumin from chicken egg white

PALS: Phase Analysis Light Scattering

PAMP: Pathogen associated molecular patterns

PBS: Phosphate buffered saline

PCL: Poly(caprolactone)

PdI: Polydispersity index

pDNA: Plasmid DNA

PEG: Poly(ethylene glycol)

PEI: Poly(ethyleneimine)

PEST: Penicillin/streptomycin

PG: Poly(γ-glutamic acid)

PGA: Poly(glycolic acid)

PI: Protease inhibitors

PL: Pluronic® F127

PLA: Poly(lactic acid)

PLGA: Poly(lactic-co-glycolic)

PLL: Poly-L-lysine

PMMA: Poly(methyl methacrylate)

pNPP: p-nitrophenylphosphate

poly(I:C): Poly(inosinic-cytidylic) acid

PRR: Pattern recognition receptors

PVA: Poly(vinyl alcohol)

RAL: Raltegravir

RES: reticuloendothelial system

Rho-grafted PLGA: Rhodamine 6G derivative-grafted PLGA

RNA: Ribonucleic acid

Rr: Pearson's correlation coefficient

RTI: Reverse transcriptase inhibitors

SC: Subcutaneous

SD: Standard deviation

SDS: Sodium dodecyl sulfate

SDS-PAGE: SDS-polyacrylamide gel electrophoresis

SHIV: Simian and human immunodeficiency chimeric virus

Siglec-1: Sialic acid-binding immunoglobulin-type lectin-1

siRNA: Small interfering RNA

SIV: Simian immunodeficiency virus

STAT: Signal transducer and activator of transcription

TAP: Transporter associated with antigen processing

Tc: T cytotoxic

TC: Transcutaneous

TEMED: N,N,N',N'-tetramethylethylenediamine

TGF: Transforming growth factor

Th: T helper

TLR(s): Toll-like receptor(s)

TNF: Tumor necrosis factor

Treg: T regulatory

UNAIDS: Joint United Nations Program on AIDS

VS: Virological synapse

w/o/w: *water-in-oil-in-water*

Z-Ave: Z-Average (size)

ZP: zeta-potential (surface charge)

1. State of art

1.1. Incidence and mortality

The Human Immunodeficiency Virus (HIV), the causative agent of Acquired Immune Deficiency Syndrome (AIDS) was identified in the early 1980s and became an increasing global health, social, and economical concern (1). HIV/AIDS has high prevalence rates in developing nations, such as sub-Saharan African countries and other important regions including the Caribbean, Latin America, and South and Southeast Asia, with important socioeconomic, family, and public health burdens (2).

In 2007, it was estimated that 33 million of people were infected by HIV and 25 million have died since the first reported cases. Moreover, two million of new infections as well as deaths per year are annually reported. Despite the increased number of new infectious per year, Joint United Nations Program on AIDS (UNAIDS) reported a slight decrease in HIV pandemic since the beginning of the 21st century (2.7 million in 2007 vs. 3.0 million in 2001), justified by the expanding access to antiretroviral drugs that increased lifespan and the quality life of HIV infected people (3).

1.2. Biology of HIV

HIV belongs to the genus Lentivirus and the family of Retroviridae (4). The virus is a spherical nanostructure (around 100-150 nm) composed by an outer viral envelope and an inner nucleocapsid enclosing the genetic material in the form of two copies of single stranded ribonucleic acid (RNA). The RNA genome (9.5 kB) contains nine genes that code for structural (Gag, Pol and Env), regulatory (Tat and Rev) and accessory (Nef, Vif, Vpr and Vpu) proteins (5). Gag protein is cleaved into matrix (p17), capsid and nucleocapsid (p24) proteins. Env is a homotrimeric type I integral membrane protein cleaved into glycoprotein 160 (gp160) that forms two noncovalently attached envelope glycoproteins embedded in the lipid bilayer of outer viral membrane, gp120 surface protein and gp41 transmembrane protein, responsible for the virus/cell fusion subsequent to the recognition of CD4 receptor and CCR5 or CXCR4 coreceptors present on host cell membrane (6). The Pol protein encodes essential viral enzymes such as reverse transcriptase, integrase and protease that are enclosed within a cage of capsid and matrix (4). Regarding accessory proteins, Vif can infect otherwise non-permissive cell types inducing productive infections and allowing the increase of viral

infectivity; Vpr transport the viral genome to the nucleus in the viral life cycle; and Vpu and Nef degrade cellular CD4 receptor and increase virus budding/spreading (7). Summarizing, HIV retrovirus contains the RNA genome into the nucleocapsid, which is converted to deoxyribonucleic acid (DNA) by reverse transcriptase and inserted into host cell genome, causing an extended and lethal disease.

Two distinct types of HIV (HIV-1 and HIV-2) were identified as causative agents for HIV infection and disease in humans (8). Apart from other differences, such as their geographical origin and the organization of their genome, HIV-1 is the most prevalent and efficiently transmitted, associated with a faster progression to immunodeficiency (9). HIV-1 is divided into three groups: the prevalent M, N and O. The M group is responsible for most of the epidemic and contains eleven subtypes termed A-K, where B causes the majority of infections in America, Europe, Asia and Australia, whereas subtypes A, C, D and E are widely founded in Africa (10). HIV-2 mostly prevalent in West Africa, India, Portugal and Portuguese African colonies is diversified into eight virus groups termed A–H, being group A the most prevalent (11).

1.3. HIV infection process

HIV infects preferably cell types that express cell-surface protein CD4 such as macrophages, lymphocyte T-cells and dendritic cells (DCs) (12). HIV entry into the target cell can be divided into three steps: attachment, coreceptor interaction and fusion. Attachment of HIV-1 to host cell membrane is not an easy task and is mediated by the Env protein (13). Env is synthesized as gp160, a complex of noncovalently associated glycoproteins that is cleaved during the transport to the cell surface into two vital glycoproteins for viral binding to human cells, gp120 and gp41 (120 and 41 kDa, respectively). At the beginning of HIV entry process, the viral envelope gp120 interact with the host cell-surface receptor CD4. Consequently, conformational changes and structural rearrangements are induced in gp120 exposing the coreceptor-binding site and allowing its binding to a chemokine coreceptor (CXCR4 or CCR5) on the host cell surface (14). Together, CD4 and coreceptor binding trigger additional fusogenic conformational changes in gp41 that cause its release and insertion into the host cell membrane, completing the fusion process between virus and target cell (15, 16). Specifically, HIV-1 gp120 contains an inner core constituted by five conserved protein domains (C1-C5) that interact noncovalently with gp41 transmembrane protein, forming

a i) trimeric envelope spikes; ii) an outer structure composed by five variable protein domains (V1-V5); and iii) numerous N-linked glycosylation sites that forms the most part of the spike-exposed surface. This surface protein mediates virus binding to cellular receptors. Particularly, the interaction between gp120 and CD4 receptor induces a conformational change leading to the formation of a third domain or bridging sheet, responsible for the interaction of inner and outer domains with viral coreceptors (14). HIV-1 gp41 is composed of three domains (an extracellular termed ectodomain, a transmembrane and an intracellular named endodomain) that constitute the transmembrane subunit of Env, embedded in the viral membrane by their transmembrane domains. Through the ectodomains, gp41 and the Env surface subunits constituted by gp120 molecules remains noncovalently associated. Immediately after gp120-coreceptor binding, the gp120-gp41 complex is dissociated and the unstable gp41 structure is released, exposing a fusion domain. Subsequently, the fusion peptide present on gp41 ectodomain is inserted into the lipid cell membrane, eliciting the virus-cell anchoring. Following the insertion, two heptad-repeated helical regions (HR) adjacent to the N- and C-terminal (NHR and CHR, respectively) of the ectodomain are energetically reorganized under conformational changes, creating a thermostable trimer of heterodimers termed six-helix bundle (6HB) structure. This 6HB consists of three NHR domains in the inner core and three CHR domains packed on the outside and associated with NHR domains in an antiparallel manner, representing the fusion-active core of gp41 (17). As a result, the fusion peptide and transmembrane domain of gp41, along with their associated membranes, are brought into close proximity producing a juxtaposition of viral and host cell membranes and their complete fusion (18, 19).

Following the fusion process, the capsid core is disrupted and the viral content containing RNA, reverse transcriptase and integrase, is released inside the host cell cytoplasm. After the successful entry of the content, the viral RNA template is degraded and reverse transcribed into its complementary DNA strand by the viral enzyme reverse transcriptase associated with other viral proteins, producing a double-stranded viral DNA. The newly synthesized viral DNA is then transported to the host cell nucleus where is processed and inserted into the host cell genome by viral enzyme integrase (20). Once transferred viral DNA, the target cell is permanently infected. Without cell stimulation, the HIV can persist as a provirus in a latent state for several years (21). However, host cell activation will elicit the transcription of proviral DNA into viral RNA by RNA polymerase, the viral RNA transport outside the nucleus and its

translation into viral proteins by the ribosome. The newly produced viral proteins (capsid, envelope and auxiliary proteins) together with two copies of the viral genomic RNA are transported to the cell surface beginning the assembly of new virus particles (22). This assembly induces a curvature in plasma membrane allowing that non-infectious and immature virions sprouting from host cell, with its consequent explosion. The immature virion is then reorganized into its mature form with the help of HIV protease that cleaves the Gag and Pol polyproteins into their structural proteins and functional enzymes (10). The HIV entry process described above is illustrated on Figure 1.

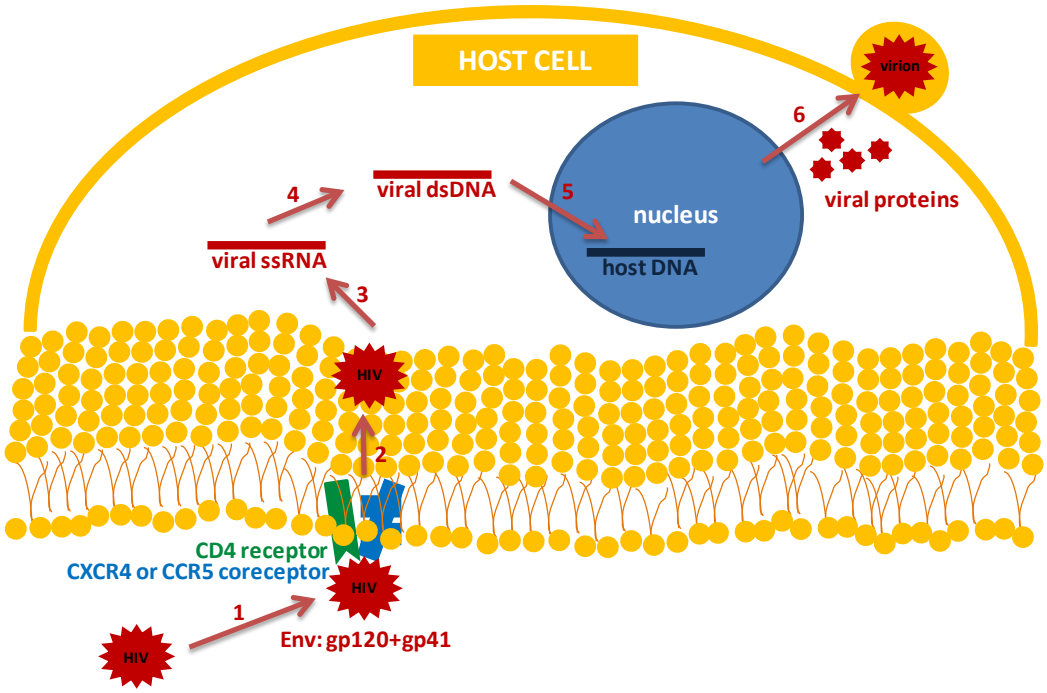

1. Entry 2. Fusion 3. Core release 4. Reverse transcription 5. Viral DNA insertion 6. Virions production

Figure 1 – HIV infection process.

1.4. HIV transmission

HIV-1 is transmitted through the horizontal route, that includes hetero- or homosexual contact (vaginal or anal sexual intercourse), or contaminated blood contact (blood transfusions, drug addiction: sharing of contaminated needles among injected drug users, accidents); or vertical route from mother to child during pregnancy, at childbirth or during breastfeeding (23). Overall, the efficiency of HIV-1 transmission is dependent on the concentration of virus in body fluids (blood, semen, vaginal secretions

and breast milk contain higher virus load) and the immunological and cellular host vulnerability (24).

Regarding the sexual contact, HIV can penetrate in vaginal and cervical mucosa either as free virions or cell associated, being macrophages the primary transmission carriers (25). In the genital mucosa, the presence of several immune cells mainly DCs, macrophages, T and B lymphocytes that express either CXCR4 or CCR5 coreceptors, enhance the spread of the virus (26). In addition, the unique capacity of DCs to binding HIV gp120 without the membrane fusion process due to the presence of a dendritic cell-specific HIV-1 binding protein, DC-SIGN (dendritic cell specific intercellular adhesion molecule-grabbing non-integrin), facilitates the viral transport to secondary lymphoid organs increasing the infectivity of HIV in T cells (27). Moreover, epidermal immature DCs, named Langerhans cells (LCs), are abundant in the cervico vaginal epithelium and can extend the initial HIV replication (local amplification) through the uptake of HIV antigens, mediating its transmission across intact genital epithelium and presenting them to specific T cells in the surrounding tissues (28). The capacity of all DCs, including infected/HIV-bearing LCs, to carry virions across the epithelium due to their ability to migrate to T cell-rich lymph nodes, has highlighted their crucial role in vaginal HIV transmission (29).

Rectal transmission is also a straightforward route for viral infection enhanced by the presence of a single columnar epithelial lining in rectum and terminal colon. Mainly, M cells abundant in these tissues can present antigens to sub-epithelial lymphocytes and macrophages ensuring its constant lumen sampling (30).

It has been known that HIV-1 replicates more promptly in target cells co-cultured with infected cells, unlike cell-free virus inoculation (31). HIV-1 cell-to-cell transmission requires transient adhesive junctions between infected and target cells (32). Two types can be differentiated by the infection status of the donor cell. Virological synapse (VS), also known as cis-infection, is formed by HIV-infected cells. The binding of Env expressed by the infected donor cell to CD4 receptor on the target cell is a characteristic of transmission via VS. VS assembly and target cell infection is also co-receptor and fusion-dependent (33). In contrast, infectious synapse (IS) is formed by uninfected cells that have captured free HIV-1. This process also known as trans-infection is mediated by a variety of DC receptors (DC-SIGN, sialic acid-binding immunoglobulin-type lectin (Siglec)-1 and heparin sulphate proteoglycans) used to capture HIV-1 virions and to maintain them in an infectious state adsorbed within

complex surface-connected plasma membrane invaginations. The surface-bound virus will be released after the contact between DCs and uninfected target cell, such as a $CD4^+$ T helper (Th) lymphocyte, interacting with receptors on the target cell (34). In addition, the transfer either via VS (infected immature DCs) or IS (uninfected mature DCs) can be directed by DC maturation cycle, where DC phenotype varies from an immature state with higher phagocytic ability in the mucosal tissues to a mature state with higher ability to present antigen in lymph nodes. It has also been reported that mature DCs are resistant to HIV-1 infection but also much more efficient at HIV-1 trans-infection, whilst immature DCs are capable of limited HIV-1 replication (35).

1.5. HIV pathogenesis and immune response

Clinically, HIV-1 infected patients may undergo three stages: acute phase, chronic phase (first asymptomatic and later non-AIDS defining symptoms) and terminal or illness phase, defined by AIDS.

During the following days post initial infection, the virus readily infects $CD4^+$ Th cells to produce new virions (up to 10^{10} new virus particles/day) being locally amplified, at the mucosal site. Accordingly, virus spreads as free or infected cell-associated form, via regional lymph nodes from the local entry to lymphoid organs, principally the gut-associated lymphoid tissues (GALT), spleen and bone marrow, being accompanied by a burst in viral replication (acute infection) (36). Until the first six weeks, a high viral load expressed as several million of viral genomic RNA copies/mL plasma and the fast depletion of $CD4^+$

Th and $CD8^+$ T cytotoxic (Tc) cells are particularly observed in the peripheral blood and gastrointestinal tract, where there is a massive viral production (37). During this acute phase exists an increased risk for sexual HIV transmission consequence of high blood and genital viral load (38). Moreover, a proportion of the newly infected patients have experienced the clinical “acute phase syndrome” described by fever, fatigue, sore throat, skin rash, enlarged lymph nodes, diarrhea, nausea and general malaise symptoms. Within six months post infection, the immune system reacts with specific cellular responses and HIV-1 specific antibodies, which recovers immediately and gradually $CD4^+$ Th and $CD8^+$ Tc cell levels, respectively. Never completely depleted, viral load is reduced attaining a steady state viremia (viral setpoint) defined by

the equilibrium between viral replication (fitness) and viral suppression by the intense immune response (latent phase) (39).

During the chronic phase, characterized initially by the absence or presence of residual clinical symptoms, in addition to the high viral mutation rate and virus persistence in several reservoir sites, is observed an exhaustion of the immune system accompanied by T-cell depletion. The last, especially the continuous decrease of $CD4^+$ Th cells is a result of the i) limited regeneration capacity of the immune system (including thymic atrophy in adults), ii) direct morphologic alterations of infected cells (cytopathic effects), iii) loss of $CD8^+$ Tc cell response efficacy, iv) apoptosis of uninfected $CD4^+$ Th and $CD8^+$ Tc lymphocytes and v) lymphoid organs degeneration. Moreover, the depletion of T cells, especially the massive loss of $CD4^+$ Th cells in gastrointestinal tract, may affect the protective barrier of the intestinal mucosa, allowing bacteria and bacterial toxins such as lipopolysaccharide (LPS, a cell-wall component of Gram-negative bacteria) and possibly gastrointestinal viruses to cross into blood circulation, inducing a pathological over-activation of the immune system (40). Furthermore, T regulatory (Treg) lymphocytes, a subset of T cells with suppressor activity capable of blocking the activation (proliferation and cytokine production) of T cells (41), have appeared increased in the GALT during HIV infection. Treg cells were reported as protectors from productive infection and pathogenic disease (42); but, on the other hand, Treg cells were associated with the establishment of HIV infection in humanized mice (43). Therefore, whether this accumulation prevents disease progression by inhibition of immune activation or increases opportunistic infections probability in gastrointestinal tract remains unclear. Consequently, immune response influenced by Treg cells against HIV infection may be destructive, resulting in diseases such as lymphoid interstitial pneumonitis and autoimmunity (e.g. immune thrombocytopenic purpura), or protective. (44) A possible explanation for such diverging results is arguably the heterogeneity of this population, not exclusive to HIV-infection. Treg cells are mostly characterized based in the expression of surface markers ($CD4^+$, $CD25^+$, $CD127^-$) and the transcription factor FoxP3. However, the phenotypic characterization of HIV, wherein different CD4 subsets become infected with different kinetics, can affect the expression of Treg surface markers, $CD4^+$ Th cell plasticity and FoxP3 stability (45).

Finally, the loss of immune surveillance characterized by decreased $CD4^+$ Th cell counts and rising viral load, causing the appearance of opportunistic infections normally

prevented by cell-mediated immunity (i.e. infections with mycobacteria, fungi, protozoa and viruses), leads to a symptomatic clinical stage, designated by AIDS, within about ten years after primary infection for the majority of rapid progressors (46). The progression of infection is also encouraged by the increase of HIV genetic diversity due to intense error-prone reverse transcription and evolutionary pressure to evade the immune system, generating viruses resistant to cellular and humoral immune responses. Nevertheless, a curious small number of individuals named long term survivors or non progressors remain without symptoms, with stable $CD4^+$ Th cells number and low to intermediate viral loads, for more than ten years (47). The rapid progressors and long term non-progressors differ in the immune system ability to control virus infection. More curiously, in normal survey people it was discovered an apparently harmless mutation (the D32 mutation), which results in $CD4^+$ Th cells not presenting CCR5, capable to confer a natural resistance to HIV infection (48).

1.5.1. HIV reservoir sites

Reservoir sites are cellular or anatomical locations able to protect the virus from biological elimination ensuring a persistent and undetected replication. Overall, cellular reservoirs are particularly composed by macrophages, lymph node DCs and memory $CD4^+$ Th cells and allow the residence and surviving of HIV infection for long periods (49). Mainly, macrophages are important viral reservoirs outside the bloodstream able to transport HIV and infect the central nervous system (CNS), causing neurocognitive disorders, namely HIV-associated dementia. This cell population is also the key in maintaining the HIV replication cycle when $CD4^+$ Th cells are largely depleted, at later stages of infection (50). Anatomical reservoir sites of HIV include mainly lymphoid organs (in particular the spleen, lymph nodes, and GALT) and CNS, but also testicles and female genital tract (51). As discussed above, lymphoid organs are directly implicit in the circulation and production of HIV-susceptible lymphocytes, being its destruction well correlated with progressive HIV disease.

1.5.2. Humoral immune response against HIV

In order to control viral transmission preventing infection of host cells, the adaptative immune system induces a humoral immune response mediated through the production of virus-specific antibodies by B lymphocytes (52). Post infection, extracellular viral proteins are taken up by antigen presenting cells (APCs), essentially

DCs, macrophages and B cells; and processed into small peptides that will be presented to $CD4^+$ Th cells once complexed with major histocompatibility complex (MHC) class II molecules at cell surface. In particular, the activation of Th2 cells will stimulate naïve B cells through the production of cytokines, including interleukin (IL)-4, IL-5, IL-6, IL-10 and transforming growth factor (TGF)-β. Therefore, specific epitopes or intact virus recognize the surface of immunoglobulin (Ig)M on naïve B cells inducing their differentiation into both antibodies-producing plasma cells (IgG, IgA, IgE) and memory B cells. Within the antibodies produced a few weeks to several months after HIV-1 infection against gp120, gp41, the nucleocapsid (p24) and the matrix (p17), mainly anti-HIV Env antibodies predominantly target one of the three crucial regions for viral entry into $CD4^+$ Th cells (gp120, gp41 or the binding sites for CD4 and CXCR4 or CCR5 co-receptors), presenting a neutralizing capacity able to prevent virus attachment or inhibit the viral entry. Moreover, antibodies can attach and kill HIV infected cells via antibody dependent cellular cytotoxicity mediated by their Fc moiety and natural killer (NK) cells (53, 54). However, the virus easily mutates and escapes from immune pressure exerted by autologous neutralization, which uses a minority of anti-HIV Env antibodies (55). In addition, the ability to neutralize heterologous viruses using generated broadly neutralizing antibodies (bNAbs) is achieved by only 20% of infected individuals during the chronic infection, being insufficient to control or eliminate established HIV-1 infection (56). As expected, long-term non-progressor individuals present a strong neutralizing antibody response.

1.5.3. Cellular immune response against HIV

When the viremia peak attain the maximum level within 1-2 weeks, specific cellular immune responses mediated by $CD8^+$ Tc lymphocytes are triggered as other arm of the adaptative immune system to combat viral infection. MHC class I molecules at cell membrane display peptide fragments resulting from intracellular processing of viral proteins, by the proteasome, for recognition by $CD8^+$ Tc lymphocytes. In this case, the engagement of T cell receptors with MHC-peptide complexes activates Th1 cells, producing IL-2, interferon (IFN)-γ and tumor necrosis factor (TNF)-α, which induce $CD8^+$ Tc lymphocytes maturation and differentiation into memory or effector cells. $CD4^+$ Th cells induced by APCs are a crucial help in an optimal $CD8^+$ Tc cell response through the secretion of cytokines and the modulation of cellular functions. Specifically,

after massive depletion during acute phase, the remaining $CD4^+$ Th cells need to produce at least IL-2 and IFN-γ to proliferate after antigen stimulation and provide help to $CD8^+$ Tc lymphocytes (57). Polyfunctional $CD8^+$ Tc cells producing IFN-γ, TNF-α, IL-2, macrophage inflammatory protein (MIP)-1β, perforines and granzymes display the capacity to exert different effector functions such as: i) directly eliminate HIV-infected cells; ii) induce apoptosis of infected cell through the interaction between the Fas ligand on $CD8^+$ Tc cells and Fas receptor on infected T cells; and iii) suppress virus replication and block viral entry into $CD4^+$ Th cells, controlling partially the viremia (58). To promote polyfunctional $CD8^+$ Tc cells and initiate target cell lysis more rapidly, a strong avidity of T cell receptor for the epitope-MHC class I-complex is necessary (59). However, the introduction of escape mutations in specific $CD8^+$ Tc cell epitopes (60), the Nef-mediated down-regulation of MHC class I, the rate of cytokine production and T-cell signaling, and the $CD4^+$ Th cell function weakness (61) become responsible for virus escape from $CD8^+$ Tc mediated cell response, resulting in a reduced control of the infection and an increased viral load.

1.6. Antiretroviral therapy

Despite the HIV ability to persist in cellular and anatomical reservoir sites (latent state), currently the best option to preserve the immune system after HIV infection, prolonging and maximizing viral suppression, is the antiretroviral therapy (ART) (62). The first antiretroviral drug, a nucleotide mimic that targets HIV-1 reverse transcriptase, was introduced in the mid-1980s (63). Over the years, more than 30 individual antiretroviral drugs to treat HIV infection were developed, being inserted into different classes such as reverse transcriptase inhibitors (RTI), protease inhibitors (PI), entry inhibitors (CCR5 antagonists and fusion inhibitors), and integrase inhibitors.

Usually, antiretroviral treatment leads to increase levels of $CD4^+$ Th cell, improving their function and immune competency (64). Additionally, the application of highly active antiretroviral therapy (HAART), that involves the use of agents from at least two distinct classes of antiretrovirals, can suppresses viremia and partially restores $CD4^+$ Th cell number, improving the lifespan expectancy of patients infected with HIV-1 (65). However, most of these antiretroviral drugs displays inadequate physicochemical properties (e.g. poor solubility, permeability and stability) which affect the optimal absorption, biodistribution and sustained antiretroviral effect. Furthermore,

these therapies presents several disadvantages such as the inherent toxicity caused by the lifelong treatment with important adverse effects (cardiovascular complications (66), renal and hepatic diseases, lipodystrophy and diabetes mellitus (67)), insufficient efficacy, drug resistance, drug interactions, poor bioavailability, increase in viral load post therapy cessation and high costs (~US$10 000 per patient per year), particularly for drugs recently approved (68). Predominantly, drug resistance has been reported for each antiretroviral drug currently used in HIV therapy, being the most common cause of antiretroviral treatment failure (69). As a result, it is necessary the continual development of new inhibitors that can be used against resistant strains of HIV-1 virus, as well as, new classes of drugs against unexploited targets. Also, cheaper and more widely available therapies to suppress and/or eliminate the viral reservoirs, even if the treatment is stopped or interrupted, are a clearly need.

Taking into account the lifelong treatment exposure, costs, the risk of antiretroviral drugs and the incapacity to restore effective HIV-specific T cell responses, vaccination is a generally considered approach to tackle all these problems.

1.7. HIV vaccine development

The future control of the HIV-1 pandemic is based on the development of a safe, effective and inexpensive HIV vaccine for therapeutic and/or prophylactic use. HIV vaccine development is perhaps the most important and challenging goal remaining in HIV-AIDS research and its discovery will contribute to the solution of one of the major global health problem of our time. The RV144 trial (Thailand) recently reported the successful use of a prime-boost combination of two vaccines: a canarypox-HIV recombinant vector encoding Gag, Pro and gp120 followed by a recombinant gp120 protein, which prevented HIV infection (31.2% efficacy) (70). In fact, a HIV vaccine development is a major research challenge due to the numerous infection-related hurdles including the virus latency, the high genetic variability, the potential cell-to-cell transmission and the down-regulating MHC class I in infected cells (71). Accordingly, a HIV vaccine must prevent the acquisition of infection, inducing a durable and robust protective immunity (prophylactic effect) and/or stimulate sufficiently potent immune responses that limits virus replication in infected persons in order to diminish disease progression and viral transmission (therapeutic effect) (72). To prevent or control HIV infection, the new vaccine have to induce the production of bNAbs, activate HIV-

specific $CD4^+$ and $CD8^+$ T cells, polyfunctional T cell responses and induce long-term memory cells (73).

In fact, prophylactic vaccines focus on limiting viral entry into host cells through the production of broadly reactive anti-HIV neutralizing antibodies (mainly IgG and IgA) that bind to free virus particles, crucially on mucosal tissues. Despite the extreme variability of HIV Env antigenic epitopes complicating the induction of bNAbs, HIV-neutralizing IgA antibodies have been isolated in uninfected individuals frequently exposed to the virus (74). In addition, the passive transfer of human neutralizing antibodies in animal models can protect against viral challenge (75). However, an enormous quantity of antibodies is needed for the protection of viral transmission. The strategy is also based on high quality $CD8^+$ Tc memory and effector cells to eliminate infected cells if cellular infection prevented by antibodies fails, stimulating polyfunctional and sustained $CD4^+$ Th responses (76). Moreover, such vaccine should induce HIV specific $CD8^+$ Tc cell to eliminate infected cells and $CD4^+$ Th cells to help in the induction and maintenance of B and $CD8^+$ Tc cell responses (77).

Therapeutic vaccine have to enhance HIV-1 specific $CD4^+$ Th and $CD8^+$ Tc cell-mediated immune responses in infected individuals to control virus replication and eliminate infected cells (78).

1.7.1. Antigens, adjuvants and delivery systems

Vaccine strategies use antigens to be recognized by the immune system promoting the induction of an adaptive immune response. Traditional HIV vaccines designed to mimic natural infection are mainly composed of live attenuated or inactivated virus, which often cause many undesired side effects for human use (79). Unsafety of these vaccines and advances in biotechnology encouraged the development of new vaccine strategies using part of the pathogen, such as recombinant or synthetic proteins or peptides, or nucleic acids such as plasmid DNA (pDNA) or messenger RNA (mRNA) encoding viral proteins. As compared to pDNA, mRNA is easier to engineer, effective in protein production not needing to cross the nuclear membrane (80), and eliminates the insertion of mutations on cell genome (81). Despite the greater safety of these antigens comparing with live attenuated or killed pathogens, they are typically insufficiently immunogenic to initiate adaptative immune responses when administered

alone; therefore, adjuvants or vaccine delivery systems are necessary to induce an adequate immunity (82).

The development of long-lasting antigen-specific immune responses implies an adjuvant which stimulates the innate and adaptative immune system, more specifically by activating APCs. Therefore, an effective adjuvant will help the long-term efficacy of antigen vaccines (83). Furthermore, delivery systems are also required to insure an optimal, protector and modulator delivery of single or multiple vaccine antigens and/or adjuvants to APCs, in a targeted and prolonged manner (84). In fact, when administered alone, antigens tend to elicit a Th2-type immune response or even tolerance to the antigen, while when co-administered with adjuvants tend to induce Th1-type immune response. Aluminium-based adjuvants (generally referred to as alum) were the first vaccine adjuvants to be widely used worldwide, being the only ones approved by the Food and Drug Administration (FDA) for human use more than 60 years (85). Although alum adjuvants are generally well tolerated, they have important side effects and safety concerns such as the formation of granulomas after injection, increase of vascular permeability, toxic effects to macrophages, and if renal function is poor, their higher toxicity can be linked to neurodegenerative disorders, including Alzheimer's disease (86, 87). Alum is not suitable for all antigens and is a weak adjuvant for producing antibodies and initiating cell-mediated immunity (88). Consequently, a great need exists for new, safe and potent immunostimulatory adjuvants and antigen delivery systems able to stimulate both Th1 and Th2-type immune responses. There are several other experimental adjuvants that have been shown to activate APCs more directly, including LPS and unmethylated cytosine-phosphate-guanine oligodeoxynucleotides (CpG). However, the administration of high doses of these adjuvants seems to cause toxic effects. Particularly, repeated daily injections of CpG in mice for 14 days of treatment damaged lymphoid tissues and caused hepatic toxicity (89). Other types of adjuvants, including microemulsions (MF59 or Freund incomplete adjuvant) and saponins (QS-21) were approved for human use in Europe (90). However, adjuvant safety and efficacy on a wide scale have yet to be confirmed. Thus, improved adjuvants such as particulate systems have demonstrated both non-toxic and strongly immunogenic characteristics required for developing new vaccine technology. The latter also act as a delivery system carrying immunostimulatory molecules and promoting the presentation of vaccine antigens to the immune system. HIV vaccine delivery systems based on particulate adjuvants, such as liposomes, virosomes, immunostimulating complexes (ISCOMs),

emulsions and biocompatible polymeric nano- and microparticles have been widely investigated due to their safety profile, ability to protect and enhance immunogenicity of antigens, when delivered by diverse administration routes (e.g. intramuscular (IM), subcutaneous (SC), intradermal (ID), and intranasal (IN)) (91).

1.7.1.1. Polymeric nanoparticles as HIV vaccine delivery system

Biodegradable polymeric nanoparticles (NPs) or nanospheres are colloidal nanosystems composed of natural or synthetic macromolecular substances, having a size range between 10 and 1000 nm (92). Hydrophobic or hydrophilic HIV drugs, as well as biomolecule-like proteins, peptides, pDNA and small interfering RNA (siRNA) can be loaded into polymeric NPs through dissolution, encapsulation, adsorption or conjugation (93). These nano-scaled polymeric particles have shown a great potential to become the next generation vaccine delivery systems/adjuvants due to the protection of antigens from proteolytic degradation *in vivo* after systemic or mucosal immunization and the enhancement of antigen uptake by APCs in a targeted manner, facilitating the induction of potent immune responses comparing to soluble molecules (94). Furthermore, polymeric NPs facilitate co-delivery of other immunomodulators or adjuvants. Moreover, these nanocarriers are a sustainable source of retained antigens releasing them in a sustained manner for a long period to APCs (depot effect), avoiding the need for repeated administrations (95). In addition, formulation process and scaling-up of polymeric NPs are much easier and less expensive than liposomal formulations, especially in terms of ability to manipulate several physicochemical properties (96). In summary, polymeric nanosystems present good toxicity profile, possibility of drug-release modulation, high drug payloads, relative low cost, easiness to produce and possible scaling up. Using polymeric nanocarriers, the drug uptake is increased and cell toxicity is diminished, due to the slow-release properties of these systems. Particularly, synthetic polymers such as poly(lactic acid) (PLA), poly(γ-glutamic acid) (PG), poly(lactic-co-glycolic) acid (PLGA), poly(caprolactone) (PCL), poly(methyl methacrylates) (PMMA) and natural polymers like chitosan (Cs) are widely used for the formulation of nanoparticulate delivery systems for HIV vaccines.

Liard *et al.* (2011) investigated the cellular and humoral immune responses in mice after injection of HIV-1 p24 antigen-coated PLA NPs by three different skin layers, transcutaneous (TC), ID and SC application. Regarding the cellular response, TC

and ID routes induced significant levels of p24-specific $CD8^+$ effector T cells producing IL-2, TNF-α and IFN-γ cytokines, as well as p24-specific $CD4^+$ Th cells. Higher levels of systemic p24-specific IgG1 and IgG2a antibodies were produced by ID and SC immunization (humoral immunity). As a primary line of protection, a higher number of vaginal mucosa $CD8^+$ Tc cells was found after TC and ID skin immunizations. Significant levels of vaginal p24-specific IgA were generated choosing ID and TC skin routes for priming. Thus, systemic and mucosal cellular and humoral responses are influenced by the skin route of p24-coated PLA NPs vaccine administration (97).

Caputo and colleagues (2009) developed anionic surfactant-free nanospheres as HIV-1 vaccine carriers composed of a PMMA polymeric-inner core with Tat antigen electrostatically linked onto hydrophilic anionic Eudragit L 100-55 outer surface. HIV-1 vaccines administered by IM, SC or IN routes revealed efficient and long-lasting cellular (Tat-specific cytotoxic T lymphocytes) and humoral (IgG) immune responses in mice elicited by particulate systems as opposed to Tat alone or Tat delivered with alum adjuvant (98).

Another example was shown by Himeno *et al.* (2010) evaluated immune responses and protective efficacy against an inoculation of simian and human immunodeficiency chimeric virus (SHIV) after rhesus macaques' immunization with HIV gp120-carrying PG NPs. Despite PG NPs did not offer protection against SHIV in macaques, maintaining higher values of viral load, they induced stronger responses for both gp120-specific cellular and humoral immunity than gp120 in solution (99).

Zhu *et al*. (2012) developed PLGA NPs encapsulating a $CD4^+$ Th cell epitope fused with an HIV Env $CD8^+$ Tc lymphocyte epitope and toll-like receptor (TLR) ligands (macrophage-activating lipopeptide (MALP)-2 + Poly(inosinic-cytidylic) acid (poly(I:C)) + CpG). These NPs were subsequently encapsulated in Eudragit FS-30D microspheres for oral administration to mice. These microparticles induced colorectal immunity and protection of animals against rectal and vaginal viral challenge. The induction of mucosal immunity and protection of antigens from gastrointestinal environment by PLGA NPs demonstrate their great potential for delivery of HIV vaccines (100). Furthermore, as mentioned before, nanosystems are able to develop multivalent vaccines carrying several antigenic substances simultaneously. Accordingly, Lamalle-Bernard *et al.* (2006) developed surfactant-free anionic PLA NPs acting as delivery system coadsorbing two vaccine antigens, HIV-1 p24 and gp120 proteins. Divalent PLA-p24/gp120 induced high antibody-mediated responses in mouse after SC

administration, suggesting its potential application as multivalent vaccine delivery systems (101).

DermaVir (Genetic Immunity LLC, United States/Hungary) is a topical therapeutic vaccine in development (human phase II clinical trials) for patients being treated with antiretroviral drugs composed of HIV pDNA material encapsulated in mannosylated poly(ethyleneimine) (PEI) NPs. Dermavir is able to target mice epidermal LCs upon topical administration (102) allowing the induction of $CD8^+$ Tc response and efficiently inhibiting and controlling Simian immunodeficiency virus (SIV) replication in infected rhesus macaques (103).

1.7.1.2. HIV nanovaccine based on dendritic cells targeting

Next generation of vaccines and immunotherapy technology is based on the ability to deliver antigens and immune stimuli to the most effective APCs, DCs, in a targeted and prolonged manner to develop a protective immune response against infection with subsequent activation of T-cell mediated immunity (104). DCs represent the sentinels of the immune system, residing in most peripheral tissues and bridging innate and adaptative immunity. Known as the most potent activators of naïve T cells, DCs are able to modulate the adaptative immunity by antigenic peptide presentation to $CD4^+$ and $CD8^+$ T lymphocytes through MHC class I and class II pathways, respectively (105). However, several complex processes including antigen transport to DC-rich areas across physiological barriers, DC binding, and antigen uptake, processing and presentation, as well as the immunogenicity and integrity of antigens influence immune responses.

Biodegradable polymeric NPs have been designed to target DCs in new nanovaccine strategies, enhancing the antigen uptake process compared with soluble antigen alone. First of all, nanovaccine (foreign substance) induces an inflammatory or innate immune response, involving inflammatory mediator secretion. In particular, the secretion of MIP-1α in the peripheral tissues activates and recruits immature DCs, through their exclusive chemokine receptors, CCR1 and CCR5 (95, 106). Subsequently, immature DCs localized strategically in peripheral tissues (skin and mucosal surfaces) capture efficiently the nanovaccine and are activated to migrate into local secondary lymphoid tissues (spleen, lymph nodes and mucosal lymphoid system, mucosa's and gut) to interact with naïve T cells for an adaptative response. This DC-maturation

process, induced by exposure to "danger signals", is accompanied by a reduction of uptake capacity, acquisition of cellular motility with the development of characteristic dendrites, and migration to lymph nodes to efficiently present the antigen and further activate naïve T cells (107, 108). These issues are also accompanied by the down regulation of immature receptors and up regulation of CCR7, which directs DCs into the T cell area of lymph nodes through the production of CCR7 ligand, MIP-3β, by the resident DCs in T cell areas (109). In particular, DC maturation is induced by the recognition and interaction between highly conserved portions of molecular structures produced by pathogens, termed "danger signals" or pathogen associated molecular patterns (PAMP), and specific pattern recognition receptors (PRR), such as TLRs and C-type lectin receptors (CLRs) (110). Particularly, the interaction between TLRs and hydrophobic portions of ligands is also coupled to the expression of host-derived inflammatory molecules such as CD40 ligand (CD40L), TNF-α, IL-1, IL-6, and IFN-α initiating the adaptive immune response (111, 112). In addition, the contact with TLRs also induces cytokines and chemokines (IL-12 and IFN-γ) and co-stimulatory molecules (CD80 and CD86) mediators of innate immunity that are essential for the induction of adaptative response (113). In contrast, CLRs that recognizes various saccharides, such as D-mannose, L-fucose, and *N*-acetylglucosamine help in internalization for further processing and presentation by DCs (114).

Following uptake process, antigens are released intracellularly and fragmented into peptides presenting at least 12 amino-acid by proteases in endosomes or phagosomes, which also contain high concentrations of MHC class II molecules (endolysosomal pathway). Before exported to the cell surface to bind specifically the receptors of $CD4^+$ Th lymphocytes, antigenic peptides are loaded onto MHC class II molecules (115). On the other hand, antigenic peptides encapsulated into NPs can be processed into normally 8-9 amino-acid peptides and presented on cell surface by MHC class I molecules to activate $CD8^+$ Tc lymphocytes, in a mechanism termed cross-presentation only operated by DCs. The exact mechanism is poorly understood; however, two distinct routes have been proposed: i) in a transporter associated with antigen processing (TAP)-dependent pathway, antigen escapes from the endosomes into the cytosol, before lysosomal fusion, being degraded by cytosolic proteasomes into small peptides, which are then transported via TAP into the endoplasmic reticulum (ER) and loaded onto MHC class I molecules; ii) in a TAP independent manner favored by the low pH values in endosomal vesicles, the antigen is processed by endosomal acid

proteases. Once degraded, peptides are loaded onto the MHC class I molecules inside vesicles and exported to the cell surface (116). The question is: How MHC class I molecules enter into phagocytic vesicles? The first proposal is that MHC class I can be internalized into the phagocytic vesicles through membrane invagination during phagocytosis (117). Moreover, ER can fuse with phagocytic vesicles (118).

Mature DCs are the most potent activators of naïve T cells (one DC can activate 500 different T cells in 1 h, through the extension on dendrites) (119). Apart from the down regulation of DC endocytic activity and T cell receptor and co-receptor (CD3) stimulation by the peptide-MHC complex, a secondary co-stimulatory signal is necessary for the co-stimulation and expansion of naïve T cells. More specifically, the interaction between CD28 present on T cells and co-stimulatory molecules CD80 and CD86 on DCs enhances the production of the major T cell growth hormone, IL-2, which drives the clonal expansion of naïve T cells (120). In addition, the CD80 and CD86 molecular expression is activated through the interaction between CD40 on DCs and CD40L on naïve T cells, stimulating its activation. The strength of signal transduction is also influenced by other co-stimulatory molecules such as CD27, and secreted cytokines IL-12 and IFN-γ. Once activate naïve T cell are expanded and differentiated into effector and memory cells in a manner dependent of cytokines produced (121).

Naïve $CD4^+$ Th cells can be differentiated into Th2 cells, associated with the production of IL-4, IL-5, IL-10 and TGF-β, which can induce the activation of naïve B cells (122, 123). Mature B cells proliferate and differentiate into antibody-secreting plasma cells (IgG, IgA and IgE), helped by IL-5 and IL-6, or memory B cells. Upon the re-encountering with the same pathogen or antigen, memory B cells divide very rapidly and differentiate into antibody-secreting plasma cells (82). Additionally, associated with IL-12, IFN-γ and TNF-α, Th1 cells are produced and induce the stimulation of cytotoxic response to kill infected cells. In fact, naïve $CD8^+$ Tc cells are differentiated into effector cytotoxic T lymphocytes (CTL) able to migrate to the inflamed peripheral tissue to eliminate virus-infected cells and release cytokines capable to decrease viral replication (124, 125). Particularly, the secreted IFN-γ may also promote the recruitment of cells from innate immune system, such as NK cells, granulocytes and or macrophages to eliminate infected cells (126). In addition, effector memory T cells are also developed, particularly from effector T cells. Notably, the immunological memory resultant from adaptative immunity and maintained by distinct populations of long-lived

memory cells is crucial to rapidly and effectively respond to pathogens (127). Figure 2 illustrates the immune response described above.

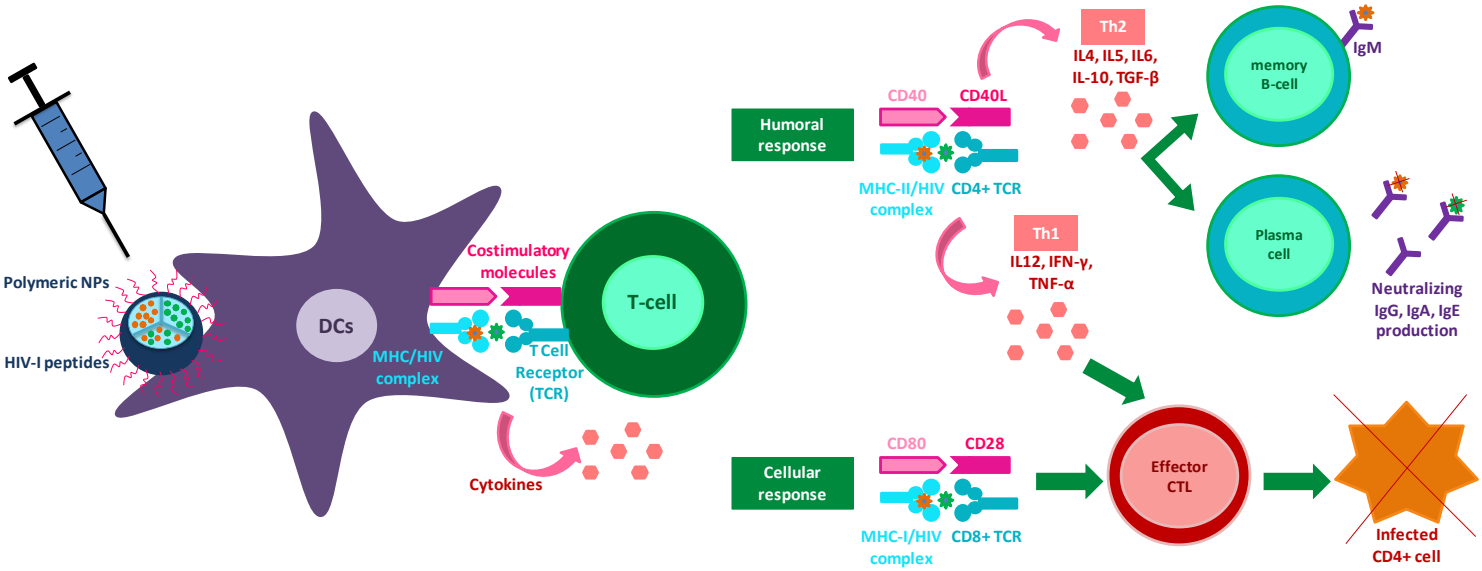

Figure 2 – The desired immune response elicited by a HIV vaccine is the combined action of $CD8^+$ Tc cells and $CD4^+$ Th cells.

Moreover, as mentioned above, a potent cytotoxic response requires the presence of $CD4^+$ Th cells to compensate for inadequate co-stimulation of naïve $CD8^+$ Tc cells by APCs and to guarantee optimal activity of the induced CTL (128). HIV infection affects DCs function by the deregulation of cytokine network. More specifically, maturation of DCs and IL-12 secretion are typically reduced, thereby suppressing T cell response (129). Otherwise, IL-10 cytokine secretion is increased in infected individuals, thus limiting the activation and proliferation of T cells, rather inducing tolerance (130, 131). Recent findings have also shown that IL-10 producing Treg cells (FoxP3-) can effectively suppress effector T-cell functions (132).

Conceptually, particulate vaccine strategy mimicking the particulate nature of pathogens, including their size (nano- to micrometer range), has been employed being preferentially directed to DCs. Particle shape, size, surface charge and coating are also important physicochemical factors playing crucial roles in the interaction, internalization and processing of polymeric-nanosized vehicles by APCs, affecting the subsequent processing of antigen via MHC class I, MHC class II or cross-presentation pathways (133). Generally, immature DCs can internalize larger particles by either macropinocytosis or phagocytosis, while smaller particles are mainly taken up by receptor-mediated endocytosis (134). However, besides the ability inherent to polymer

NPs to act as an intrinsic “danger signal” inducing DC maturation and adaptative immune responses, they are not sufficiently strong to activate a sustained immunity. To increase targeting specificity and adjuvant effects, facilitating NPs uptake and DC maturation, surface can be functionalized with specific antibodies or ligands directed against DC-surface receptors. DCs can be targeted on lectin-like receptors, such as DEC-205 and DC-SIGN, using endocytosis ligands with a terminal sugar such as mannose, fucose and *N*-acetylglucosamine conjugated on NPs surface (135). Moreover, binding of specific adjuvants (e.g. TLRs ligands) with protein antigens in NPs is essentially to alert immune system, promoting a desired immune response, and allow the use of small doses of those compounds, limiting their toxicity (136). TLRs are the most studied class of PPRs to develop effective adjuvants and can be divided into surface bound receptors (TLR1, 2, 4, 5, 6) and intracellular receptors present in the endosomes (TLR3, 7, 8, 9) (137). Extracellular TLRs recognize bacterial invaders, but also fungi and some enveloped viruses, while intracellular TLRs recognize nucleic acids from viral or bacterial pathogens. CpG adjuvant can be incorporated into NPs acting directly on DC maturation by binding intracellular TLR9 (138). Also, the poly(I:C) adjuvant mimicking a double stranded RNA (dsRNA) can bind the TLR3. This receptor contributes to the initiation of immune responses against the induction of dsRNA replication by viruses, in infected cells (139). As well, monophosphoryl lipid A (MPLA) ligand can be delivered when associated with NPs to target TLR4 (84). It has been recently shown that IL-6 secreted by TLR4-activated DCs is capable of reversing the Treg suppressive effects, activating T-cell functions (140).

Particulate delivery makes also possible simultaneous delivery of several TLR ligands in the same formulation. On the other hand, to enhance DC uptake, maturation and T-cell immunity, others ligands or cytokines can also be conjugated with the surface of polymer particles. Conjugation with DC-specific antibodies, anti-CD11c (myeloid marker) and anti-CD40, can also enhance the specificity of NPs for DCs *in vivo*, increasing the NP uptake and the subsequent immune response (141). In order to stabilize the conjugation process, the polymer “PEGylation” can be performed (142). Another important factor is premature antigen presentation on DC surface before reaching a lymph node, which can actually result in antigen tolerance. In this case, NP size can determine the antigen delivery to lymph-node-resident DCs instead of only peripheral DCs, providing a more-potent immunostimulation. In this case, the internalization and antigen processing is attained in lymph nodes due to a fraction of

resident immature DCs (143). Small NPs (<100 nm) are directly transported to lymph nodes, into the lymphatic system by interstitial flow; larger NPs (>500 nm) are predominantly internalized by skin DCs (dermis, epidermis and to a lesser extent subcutis), draining subsequently to the lymph nodes; and intermediate nanovaccines (100-500 nm) present both pathways (44). Studies have shown that NPs within viral-sized range, are preferentially internalized by DCs, whereas those presenting dimensions similar to bacteria are preferentially ingested by macrophages (144). According to the surface charge, cationic NPs display ionic attraction with negatively charged cell surface, facilitating the binding and particle internalization (145). Since DCs recognize nanovaccine as exogenous antigens, the MHC class II pathway is followed preferentially than MHC I molecules via cross-presentation. However, the induction of a strong and broad $CD8^+$ Tc cell response is a prerequisite for a therapeutic vaccine. In this context, to improve cross-presentation, promoting the antigen escape from endosomes into the cytosol, polymeric NPs based on amphiphilic PG were developed (146). Furthermore, the efficacy and nature of the immune response is also influenced by the route of administration. Polymeric NPs administered ID or SC were efficiently internalized by DCs (147). Nanovaccine size has a major impact when administered into the skin. However, retention in the skin is a drawback. Accordingly, direct administration into the lymph node might offer an attractive route. Otherwise, injection into the blood is less size dependent. It is important to highlight that the time period at which antigen and adjuvant reach DCs is crucial, affecting the immune outcome. Tolerance may be induced if the maturation stimulus is given too late after antigen capture by DCs. On the other hand, antigens will not be efficiently presented if they reach already mature DCs (84). In summary, the specific targeting of particles to DCs may not only enhance efficacy but also the specificity of interaction.

1.7.1.3. HIV nanovaccine based on peptide HIV-1 fusion inhibitors

Generation of broadly-neutralizing antibodies to prevent (new) infections of host cells is a major purpose for HIV-1 vaccine development. Consequently, the advance of new immunogens which elicit bNAbs, capable of protecting against several different strains of HIV, has stimulated the HIV vaccine research, for prevention and treatment (148). As a result, several conformational changes involved in the interaction between viral envelope glycoproteins and host receptors, resulting in the entry of HIV into host

cells, has received special attention (149). There are three categories of entry inhibitors: (1) interference with the binding of the HIV-1 gp120 to CD4 receptors is attained by attachment inhibitors; (2) inhibition of the interaction between gp120-CD4 complex and coreceptor (CCR5 or CXCR4) is achieved by coreceptor inhibitors; and (3) inhibition of fusion between viral and cellular membranes is performed by fusion inhibitors (150). Despite all the steps of viral entry being considered important for HIV-1 drug design, it is preferable to develop anti-HIV drugs targeting viral proteins (gp120 and gp41) rather than host cell molecules (CD4, CCR5 and CXCR4), because binding the cellular molecules might cause toxic or adverse effects interfering with their normal functions (150). In this regard, the investigation of different epitopes in the HIV envelope glycoproteins, blocked by new discovered bNAbs, as potential targets for vaccine development, has been explored (151). In recent years, new antiretroviral inhibitors belonging to the third class of anti-HIV-1 drugs, have been developed. The fusion inhibitors target an earlier HIV-1 life-cycle process, specifically components of the viral entry pathway, preventing and stopping HIV-1 infections more efficiently than RTI and PI. Peptide fusion inhibitors derived directly or engineered from HIV-1 gp41 NHR or CHR sequences can be made by peptide synthesis or produced as recombinant proteins or peptides, depending on their length and *in vivo* stability. Generally, the interference with the fusion process is achieved by the formation of unproductive 6HBs with HIV-1 gp41 NHR or CHR counterparts, inhibiting virus-target cell fusion and preventing HIV-1 infection. However, CHR peptide fusion inhibitors are the most exploited, showing greater anti-HIV potency than NHR peptides (152).

Since 2003, T20 (enfuvirtide, Fuzeon®), initially termed DP178 and identified by Wild's group (early 1990s), was the first HIV fusion inhibitor approved by the FDA for the treatment of HIV-infected individuals and AIDS patients (153, 154). T20 is a 36-amino acid linear peptide that mimics the sequence of the CHR domain in HIV-1 gp41 (a.a 127-162 in gp41 or a.a 638-673 in gp160 precursor) (150, 155). Its mechanism of action seems to be different of the established interaction model for HIV-1 peptide fusion inhibitors. T20 may interact either with gp41 NHR or the target cell membrane, blocking the formation of the 6HB structure and preventing viral fusion and HIV-1 infection (6, 156). Enfuvirtide presents high solubility under physiological conditions and anti-HIV-1 activity in the nanomolar range. It inhibits HIV-1 replication in human cell types such as mature and immature DCs, and macrophages, with values of IC50 (concentration required for 50% inhibition) ranging from 0.0018-0.853 μg/mL (157).

However, T20 is only used as a salvage therapy in HIV-1 infection, being injected parenterally (subcutaneously) twice daily due to the poor orally bioavailability (158). Additionally, the major problem is T20-resistant HIV-1 mutations mostly found in NHR domain of gp41, which decrease the binding efficiency between T20 and its target gp41 NHR. To overcome T20 resistance, a new generation of peptide fusion inhibitors was developed. In addition, increase the helical content of peptide fusion inhibitors, using salt bridges and helix-enhancing amino acids; increase their binding efficiency for NHR; as well as their *in vivo* stability, have been shown to improve their anti-HIV-1 potency (159). Accordingly, T1249 is a more potent second generation HIV-1-fusion inhibitor composed of 39 amino acids and derived from CHR consensus sequences of HIV-1 gp41 (11). To combat T20-resistant virus, T1249 contains conserved amino acids from SIV and HIV-2 sequences, as well as, an alanine substitution and a salt bridge to increase the helical content (160). T1249 was tested in treatment-experienced HIV-1 infected patients presenting a reduction on viral loads, non-severe side effects and enhanced anti-HIV-1 activity against T20-resistant virus (161).

Despite all those positive results, these peptides present crucial weaknesses including high degradation by proteases, poor oral availability, reactions associated with administration in the majority of patients, and complex and highly expensive manufacturing procedure. Therefore, the development of polymeric nanocarriers is essential for the transport and protection of these peptide fusion inhibitors. Moreover, the complexity of immunological events related to infectious diseases clarifies that the encapsulation of both peptides into polymeric NPs developing a divalent vaccine can be a new promising strategy for worldwide control of HIV.

1.7.2. PLGA nanoparticles as promising HIV vaccine delivery systems

PLGA is a biodegradable synthetic polymer approved by the FDA for human use, due to its favorable properties such as good biocompatibility, biodegradability and mechanical strength. The hydrolysis of PLGA results in lactic and glycolic acid monomers that are metabolites well tolerated in the human body, and depends mainly on the molecular weight, hydrophilicity and crystalinity of the polymer (162). PLGA has been used to a greater extent than PLA due to its higher degradation rate. The smaller molecular weight, the higher hydrophilicity and less crystalinity of PLGA polymers attained with higher proportions of glycolic acid (more hydrophilic and

amorphous) and less lactic acid (more hydrophobic and crystalline), tend to increase the rate of polymer degradation. Exceptionally, due to its amorphous nature, PLGA co-polymer with 50:50 glycolic:lactic acid ratio is more susceptible to hydrolysis and degradation (half-life about 2 weeks) among PLGA polymers with lower or higher glycolic:lactic acid ratios (163). Besides biomedical applications, PLGA co-polymer has been employed to fabricate NPs as delivery systems applied to different pathologies, particularly in cancer world. PLGA NPs encapsulating tumor-associated antigens (TAAs) either alone or associated with adjuvants (such as TLR ligands), as well as tumor lysates, have been tested as cancer vaccines. In order to restore immunocompetence in cancer patients, an inhibitor of signal transducer and activator of transcription (STAT)-3 (activated in tumor cells inducing immunosuppression) has been encapsulated into PLGA NPs (164). PLGA-based NPs are also currently under investigation for applications in cancer therapy, such as chemotherapy and gene therapy. PLGA NPs combined with paclitaxel (mitotic inhibitor used in the treatment of various cancers) have demonstrated *in vitro* and *in vivo* greater cytotoxic effects than paclitaxel alone (165). PLGA NPs loaded with plasmid coding for siRNA sequence targeting methyl-CpG binding domain protein (MBD)-1 showed to be taken up *in vitro* by pancreatic cancer cells up to 30%, leading to cell growth inhibition and inducing tumor cell apoptosis (166). PLGA has also been used as non-invasive molecular imaging systems for cancer diagnosis and imaging. PLGA nanocarriers were used to transport superparamagnetic iron oxides for Magnetic Resonance Imaging (MRI), improving the imaging effects (167).

In order to target inflammation sites and avoid long-term treatment, PLGA NPs were shown to deliver and release sustainably anti-inflammatory drugs into a target site. PLGA NPs encapsulating tacrolimus increased drug amounts in inflamed areas, whereas free tacrolimus was found in high concentrations in healthy tissues of two different rat colitis models (168). For rheumatoid arthritis therapy, the direct injection of PLGA NPs containing betamethasone sodium phosphate (BSP) in arthritic joints of rabbits showed a sustained release and a prolonged pharmacological efficacy than BSP administered as an aqueous solution (169). In addition, the oral administration of PLGA NPs encapsulating curcumin enhanced therapeutic effect in cystic fibrosis model mice, as compared to non-encapsulated curcumin (170).

The incorporation of bioactive molecules, which stimulate cell migration, proliferation or induce cell differentiation, such as growth and neurotrophic factors, into

PLGA NPs has been a promising tool in regenerative medicine. PLGA NPs loaded with fibroblast growth factor (FGF)-2 increased the total number of large and moderate diameter arterioles, as well as a marked luminal expansion of both the pre-existing collateral arteries and the transverse arterioles in ischemic mouse hind-limb adductor muscles (171).

Additionally, PLGA has also been investigated for the treatment of cardiovascular diseases. PLGA-based systems have been employed to develop engineered grafts used in arterial replacement when cardiovascular tissue is too damaged (172).

Insulin-loaded PLGA NPs have been extensively studied in the treatment of diabetes mellitus (type I). Their administration *in vivo* considerably decreased the blood glucose levels of diabetic mices (173).

The development of alternative treatments against infection has also involved the preparation of PLGA-based NPs. The development of antibiotic-loaded PLGA NPs has improved the treatment of bacterial infections. Nafcillin-loaded PLGA NPs demonstrated their potential use for the treatment of osteomylitis by significant reduction or destruction of intracellular *Staphylococcus aureus* infecting osteoblasts (174). Moreover, PLGA NPs loading Hepatitis B core antigen induced a stronger cellular immune response in a murine model (175, 176). PLGA-based nanocarriers encapsulating a version of the West Nile virus envelope protein elicited a robust cellular immune response and protection against West Nile encephalitis in a mouse model, being effectively endocytosed by immune cells and thus leading to proinflammatory cytokines secretion (177). In particular case of HIV infection, PLGA NPs have been employed particularly for prophylaxis. HIV prophylaxis has explored the use of PLGA NPs to deliver antiretroviral drugs and siRNA. Ham *et al.* (2009) engineered PLGA NPs containing PSC-RANTES (CCR5 chemokine receptor inhibitor) that demonstrated higher uptake by human ectocervical cells, as compared to nonencapsulated inhibitor, in *ex-vivo* studies. Furthermore, these NPs could achieve a critical component of the HIV infection - the basal layer of the cervical epithelium (178). PLGA NPs containing siRNA directed to specific genes relevant to Herpes Simplex Virus type 2 (HSV-2) infection were developed and evaluated for their *in vitro* and *in vivo* efficacy in comparison to siRNA-lipoplexes. siRNA-loaded PLGA NPs showed *in vitro* significantly higher gene silencing, which was further confirmed *in vivo* 7 days after treatment; induced higher survival when intravaginally administered to mice, before and after lethal HSV-2 challenge and disease progression, observed for 28 days; and did not

show relevant inflammation and epithelial damage in the vaginal mucosa after the treatment (179). The development of pH-sensitive PLGA NPs for vaginal delivery of tenofovir was completed with the addition of Eudragit S100, a pH-sensitive polymer that dissolves at pH 7.4. NPs were well tolerated by vaginal epithelial cells and 50% internalized by those cells after 24 h of incubation. These NPs released minimal amount of drug in simulated vaginal fluids (pH 4.5) and higher amount of drug in the simulated seminal fluid (pH 7.6), due to presence of Eudragit S100. The drug release was sustained for 24 h due to presence of PLGA polymer. Problems of tenofovir nanoencapsulation have been reported due to its extreme hydrophilicity, not being achieved entrapment efficiency (EE) greater than 40 %. This is a major challenge that still needs to be overcome (180). In the field of prophylaxis, a combination of antiretroviral drugs has gained success mainly to avoid drug resistance. Thermosensitive vaginal gel (liquid at room temperature and very viscous at 37 ºC), containing raltegravir-(RAL, integrase inhibitor) and efavirenz-(EFV, non-nucleoside reverse transcriptase inhibitor) loaded PLGA NPs (RAL+EFV–NPs), was developed for pre-exposure prophylaxis of HIV, using a combination of Pluronic F127 and Pluronic F68. RAL+EFV–NPs did not cause any cytotoxicity to HeLa cells for 14 days and have shown a sustained intracellular release of both RAL and EFV. Despite the intracellular levels of EFV above EC90 (90.3 ng/mL) for 14 days, RAL intracellular concentrations disappeared within 6 days. Fluorescent NPs fabricated similarly to the RAL+EFV–NPs demonstrated rapid transfer from the gel to transwell membrane and were taken up by HeLa cells within 30 min. Summarizing, thermosensitive vaginal gel composed of RAL+EFV–NPs demonstrated antiretroviral potential for long-term prophylaxis of HIV-1 transmission (181).

Despite the ability of PLGA NPs as drug delivery systems for HIV prophylaxis, and their extensive use in cancer vaccines, namely the study previously described and developed by Zhu *et al.* (2012) demonstrated the applicability of these particulate delivery systems, using PLGA NPs as HIV vaccine carriers. PLGA NPs mimicking viral particles represent pharmaceutically promising systems for *in vivo* antigen delivery within HIV vaccine field design. PLGA NPs provide a continuous and prolonged release of entrapped cargo for long periods of time, avoiding the risk of tolerance and the need for several boosting administrations (182). Moreover, several antigens and adjuvants can be encapsulated into the same PLGA NPs formulation (183). PLGA NPs seem to have the particular ability to rapidly escape the endolysosomal pathway, being

released into cytoplasm reaching the MHC class I pathway, after being internalized by DCs (184). PLGA-based nanosystems have been also shown to be able to induce DC maturation as well as broad and potent humoral and cellular immune responses, entrapping low doses of antigens and adjuvants (185). Furthermore, despite PLGA NPs adjuvant effects, its surface can be easily decorated with several immunomodulators and endocytosis ligands (186, 187). Additionally, PLGA can be further modified with hydrophilic moieties like hydrophilic and non-ionic polymer poly(ethylene glycol) (PEG) to form NPs with increasing lifetime *in vivo* and higher stability in gastrointestinal fluids (188). All these evidences and the studies reported above seem to confirm the possible utility of PLGA to produce nanodelivery systems for the promising development of anti-HIV vaccines.

2. Goals

AIDS remains a worldwide health threat, with more than 34 million people infected at the end of 2010. Despite the progress achieved on HIV prevention, detection and treatments, which significantly prolonged the life of HIV infected people, the complete erradication of this disease was not yet fully achieved. The main goal of several research groups worldwide has been the identification of new immunogens able to elicit the production of reactive HIV neutralizing antibodies that seems to be crucial for the development of an effective immune response against this infection agent.

Polymeric NPs are a promising strategy to deliver antigens and adjuvants to APCs, as they have the capacity to overcome cellular barriers and to target specific cells and organelles. DCs, considered highly specialized APCs, after maturation, can elicit effective humoral and cellular immune responses throught the induction of virus-specific neutralizing antibodies and cytotoxic effect, preventing HIV infection at the site of viral entry and impairing the dissemination of the virus, respectively.

This project aims to develop and characterize different types of PLGA and PLGA-PEG NPs-based HIV-1 vaccine designed to deliver incorporated HIV-1 gp41 peptides to DCs to be ultimately used to stimulate effective immune responses with the production of neutralizing antibodies that will promote the complete prevention of this infection and, enventually, contribute for the treatment of this disease.

The main tasks designed for this project include (i) the production and optimization of NPs; (ii) the physicochemical characterization of nanoparticulate candidates; (iii) the entrapment of antigens in PLGA-based nanoparticulate systems; (iv) the assessment of HIV-1 peptide integrity after entrapment; (v) the evaluation of cytotoxic effect of NPs in targeted DCs; (vi) the *in vitro* study of the uptake of nanocarriers by targeted DCs and characterization of their cellular trafficking.

3. Materials and Methods

3.1. Materials

Solutions were prepared from analytical grade reagents using Millipore Milli-Q ultrapure water (resistivity ≥ 15.0 MΩcm).

Poly(vinyl alcohol) (PVA, molecular weight (M_w) 13,000-23,000 Da), Pluronic® F127 (PL, M_w 12,600 g/mol), glycol chitosan (GCs), albumin from chicken egg white (ovalbumin or OVA, M_w 45,000 Da), bovine serum albumin (BSA, M_w 66,000 Da), phosphate buffered saline (PBS, 0.01 M pH 7.4), calcium chloride ($CaCl_2$), magnesium chloride ($MgCl_2$), sucrose, N,N,N',N'-tetramethylethylenediamine (TEMED), glycine, glycerol, ammonium persulfate (APs), sodium dodecyl sulphate (SDS), trizma® base, coomassie brilliant blue G 250, Triton X-100, paraformaldehyde, poly-L-lysine solution (PLL), sodium phosphate dibasic (Na_2HPO_4), sodium phosphate monobasic (NaH_2PO_4), sodium chloride (NaCl) and Mowiol® 4-88 (PVA, M_w 31,000 Da) were purchased from Sigma-Aldrich (St. Louis, MO, USA). PLGA Resomer® RG 502 (lactide:glycolide 50:50, M_w 7,000–17,000 g/mol) and PLGA-co-PEG Resomer® RGP d50155 (PLGA-PEG, Diblock, 15 % PEG with 5,000 Da) was purchased from Boehringer Ingelheim GmbH (Ingelheim, Germany). Acrylamide/bisacrilamide and SDS-polyacrylamide gel electrophoresis (SDS-PAGE) Mw marker (Precision Plus Protein™ standards 10-250 kDa) were supplied by Bio-Rad (Hercules, CA, USA). Bromophenol blue, dichloromethane (DCM), hydrochloric acid (HCl), acetic acid and methanol were purchased from Merck (Darmstadt, Germany). The MicroBCA™ protein assay kit was supplied by Thermo Fisher Scientific Inc. (Rockford, IL, USA).

HIV-1 antigens, T20 and T1249 peptides, were kindly provided by Prof. Nuno Taveira from iMed - Research Institute for Medicines, Faculty of Pharmacy, Universidade de Lisboa.

Rhodamine 6G derivative-grafted PLGA (Rho-grafted PLGA) polymer was synthesized as described by Freichels *et al.* (2011) and kindly provided by Prof. Carlos Afonso from iMed - Research Institute for Medicines, Faculty of Pharmacy, Universidade de Lisboa (189).

Murine immature bone marrow dendritic cells (BMDCs, JAW SII, ATCC®CRL-11904™) was purchased from American Type Culture Collection (ATCC, Manassas, VA, USA).

PBS sterile (0.01 M pH 7.4, [-]$CaCl_2$, $MgCl_2$), RPMI 1640 + Glutamax™, heat inactivated fetal bovine serum (FBS), granulocyte-macrophage colony stimulating factor (GM-CSF), trypsine EDTA 0.25 %, HEPES, sodium pyruvate, penicillin/streptomycin (PEST) 10,000 U/mL/10,000 µg/mL, β-mercaptoethanol and Trypan-Blue stain were purchased from Gibco® Invitrogen (Life Technologies, Paisley, United Kingdom).

Cell culture disposable material as cell culture flasks, cell lifters, 24- and 96-well plates were purchased by Corning® (Life Technologies, Paisley, United Kingdom).

Anti- EEA1 and anti-calnexin immunofluorescence rabbit anti-mouse antibodies for confocal microscopy were acquired from Novus Biologicals (Littleton, CO, USA). Goat anti-rabbit IgG Alexa Fluor 488® antibody and AlamarBlue® reagent were purchased from Life Technologies (Carlsbad, CA, USA).

Dulbecco's PBS (DPBS, 0.01 M pH 7.4, [+] 0.9 mM $CaCl_2$, 0.45 mM $MgCl_2$) was prepared by adding appropriate amounts of $CaCl_2$ and $MgCl_2$ to PBS.

3.2. Methods

3.2.1. Preparation of nanoparticles

OVA (model antigen) and HIV-1 antigens, T20 and T1249 peptides, were entrapped in different polymeric NPs using a double emulsion (*water-in-oil-in-water* (w/o/w)) solvent evaporation method, also named double emulsion method, as reported elsewhere, with modifications (190). Briefly, the internal aqueous phase (IP) was composed by 10 % (w/v) PVA or 8 % (w/v) PVA/0.1 % ($w_{GCs}/w_{polymer}$) GCs aqueous solutions, in which OVA (250 µg) or HIV-1 peptides (200 µg, or 100 µg of each one for co-entrapment) were dissolved for HIV antigen-loaded NP. This IP was then emulsified with an organic solution (10 mg polymer, PLGA or PLGA-PEG in DCM), under continuous sonication at 70 W, for 15 s, using an ultrasonic processor (XL 2015 Sonicator® Ultrasonic processor, Misonix, Inc, Farmingdale, NY), leading to the single w/o emulsion.

In order to form the double emulsion, a 1.25 % (w/v) PVA solution was added to the single w/o emulsion and sonicated under the same conditions. The obtained w/o/w emulsion was added dropwise to the external aqueous phase (EP) (0.25 % (w/v) PVA or 0.125 % (w/v) PL), and left under magnetic stirring for 1 h at 37 ºC, allowing DCM evaporation and NPs formation. The formulation details are shown in Table 1.

Table 1 – Composition of plain and antigen-loaded PLGA or PLGA-PEG nanoparticles.

FORMULATION	MATRIX POLYMER	INTERNAL PHASE	EXTERNAL PHASE
Polymer_PVA_plain	PLGA or PLGA-PEG	10 % (w/v) PVA	0.25 % (w/v) PVA
Polymer_PVA_antigen		Antigen/10 % (w/v) PVA	
Polymer_GCs_plain	PLGA or PLGA-PEG	8 % (w/v) PVA+0.1 % (w/w) GCs	0.25 % (w/v) PVA
Polymer_GCs_antigen		Antigen/8 % (w/v) PVA+0.1 % (w/w) GCs	
Polymer_PL_plain	PLGA or PLGA-PEG	10 % (w/v) PVA	0.125 % (w/v) PL
Polymer_PL_antigen		Antigen_10 % (w/v) PVA	

NPs were thereafter separated from the preparation media and washed with millipore ultrapure water, in order to remove the excess of surfactant and non-entrapped antigen, through three centrifugations, at 22,000 x g, 4 °C, for 45 or 20 min (Beckman Coulter Allegra 64R High Speed Centrifuge) for formulations with or without GCs, respectively. NPs were then resuspended in DPBS (20 mg/mL) and preserved at 4˚ C for following *in vitro* experiments. The yield (η, % (w/w)), was calculated according to *Equation 1*. Formulation batches were frozen overnight and freeze-dried under vacuum, for 24 h (Freezone 1 Labconco® Lyophilizator, Kansas City, MO, USA), after resuspension in lyoprotectant 10 % ($w_{sucrose}/w_{polymer}$) sucrose aqueous solution.

$$\eta\ (\%) = \frac{\text{final amount of lyophilized NPs}}{\text{total amount of polymer \& } sucrose} \times 100 \qquad \textit{Equation 1}$$

After each centrifugation, supernatants were recovered and kept at 4 ºC, or frozen at -20 ºC until future analysis. Plain NPs were formulated using the same protocol, without the dissolution of HIV-1 antigens. Fluorescent rhodamine-labeled NPs (NPs-Rho) for confocal microscopy were formulated by replacing one tenth of the PLGA-PEG mass by Rho-grafted PLGA polymer.

3.2.2. Physicochemical characterization of nanoparticles

3.2.2.1. Size and zeta potential analysis

A Zetasizer Nano ZS equipment (Malvern Instruments, Worcestershire, UK) was used to determine the mean NP size (Z-Average, Z-Ave) and polydispersity index (PdI) by Dynamic Light Scattering (DLS) in combination with cumulative analysis. The same equipment allowed the determination of NP surface charge (zeta potential, ZP) by Laser Doppler Electrophoresis (LDE) in combination with Phase Analysis Light Scattering

(PALS), at 25 ºC. In brief, each batch of NP suspension (20 mg/mL) was diluted twenty and two hundred times, in DPBS. The diluted working suspension was primarily introduced into a cuvette to evaluate the Brownian motion of NPs based on laser light scattering, measuring size and PdI. Thereafter, the same suspension was inserted into an electrode specific cell for electrophoretic mobility determination (ZP). Because ZP is extremely dependent on pH and ionic strength of the dispersant and NP concentration, measurement and working conditions were always maintained constant to obtain comparable results.

Each dilution was measured in triplicate where, each zeta potential data correspond to 100 measurements, while for size and PdI data it represents 13-16 readings. Each formulation was also prepared in triplicate, resulting in three different batches for the same particle composition.

3.2.2.2. Surface morphology analysis

The surface morphology of NPs was characterized by Atomic Force Microscopy (AFM), using a Nanoscope IIIa Multimode AFM produced by Digital Instruments (Veeco). Samples were prepared by depositing a drop of final colloidal suspension onto freshly cleaved mica at room temperature, for 15 min, and then carefully dried with pure N_2. All measurements were carried out using tapping-mode AFM with etched silicon tips (~ 300 kHz), at room temperature, obtaining topography and phase images.

3.2.3. Antigen loading analysis

The entrapment efficiency (EE, % (w/w)) is the percentage of entrapped antigen into the polymeric matrix of NPs over the initial amount of loaded antigen (*Equation 2*). On the other hand, the loading capacity (LC, μg/mg) is defined as the antigen amount (μg) present per mg of NPs (*Equation 3*).

The EE (% (w/w)) and LC (μg/mg) of model antigen, OVA, were determined indirectly by the colorimetric MicroBCA™ protein assay (191) and High Performance Liquid Chromatography (HPLC), using the supernatants obtained after washing and centrifugation steps, performed for each batch of NPs.

Regarding the protein quantification by the MicroBCA™ assay, triplicate aliquots of each supernatant were transferred to a polystyrene 96-well plate (Greiner Bio-One, Frickenhausen, Germany), including the supernatants of plain NPs to be used as controls, by subtracting the contribution of polymers and surfactants to absorbance. A

calibration curve using OVA aqueous solution in the concentration range of 2.5–40 μg/mL was prepared in triplicate, for each plate assay. Absorbance values were read at 560 nm, using a microplate reader (FLUOstar Omega, BMG Labtech, Durham, NY, USA), after incubation with the MicroBCA™ reagent at 37 °C, for 2 h.

OVA was also indirectly quantified by HPLC. Chromatographic analyzes of supernatants were performed using a Beckman System Gold: UV-vis detector (Beckman 166), Beckman 126 solvent module and a Midas autosampler. Samples (20 μL) were injected onto a Shodex PROTEIN KW-803 series column (8.0 mm ID x 300 mm, 5 μm particle size, 300 Å pore size) and eluted with sodium phosphate buffer (0.05 M pH 7.0) plus NaCl (0.3 M), at room temperature (run time: 20 min, flow rate: 1 mL/min). OVA elution from each supernatant was monitored at 220 nm by spectrophotometric analysis and their amount calculated using the standard calibration curve obtained as mentioned above. Each curve was generated by known concentrations of OVA, prepared using the first supernatant recovered after centrifugation of plain NPs. This calibration curve demonstrated to be linear over the range of 0.5–10 μg/mL of OVA, presenting a correlation coefficient $r^2 \geq 0.99$.

The EE (% (w/w)) and LC (μg/mg) of HIV-1 antigens were indirectly quantified by the intrinsic fluorescence assay of tyrosine, tryptophan and phenylalanine aminoacids present in T20 and T1249 peptides. Similarly, supernatants were placed in triplicate into a black polystyrene 96-well plate (Perhinelmer®, Walthman, MA, USA), including those obtained for plain NPs. Calibration curves for T20, T1249 or co-entrapment were prepared in triplicate, using peptide aqueous solutions in a concentration range of 2.5–40 μg/mL for each plate assay. For NPs with co-entrapped antigens, the amount of T20 and T1249 was calculated as a total amount, using a calibration curve prepared with a 1:1 mixture of both peptides. Fluorescence intensity was measured at 280 nm and 340 nm of absorbance or emission wavelengths, respectively, using a microplate reader (POLARstar OPTIMA, BMG Labtech, Durham, NY, USA). Plates were maintained at 4 ºC and protected from light until measurement.

EE (% (w/w)) and LC (μg/mg), for all studied antigens, were calculated as follows (*Equations 2 and 3*):

$$\text{EE}\ (\%) = \frac{\text{initial amount of antigen} - \text{amount of antigen in the supernatants}}{\text{initial amount of antigen}} \times 100 \qquad \textit{Equation 2}$$

$$\text{LC } (\mu g/mg) = \frac{\text{initial amount of antigen} - \text{amount of antigen in the supernatants}}{\text{initial amount of polymer}} \qquad \textit{Equation 3}$$

3.2.4. Cell culture conditions

Murine immature BMDCs were propagated in RPMI 1640 + Glutamax™ supplemented with 10 % (v/v) FBS, 1 % (v/v) PEST, 50 μM β-mercaptoethanol, 10 mM HEPES, 1 mM sodium pyruvate and 5 ng/mL GM-CSF, in a humidified incubator with 5 % CO_2, at 37 °C, using 75 cm^2 flasks (Corning®, NY, USA). Medium was replaced twice a week and cells subcultured at a 1:2 ratio when log phase of growth was achieved. BMDCs have a combination of non-adherent and adherent cells. For BMDCs subculture, non-adherent cells with old medium were transferred to a 75 cm^2 sterile Falcon® flask. Adherent cells were washed with 2 mL of PBS sterile, collected by tripsinization using 4 mL of trypsin EDTA 0.25 % at 37 °C, 5 % CO_2, for 3 minutes, and transferred to the same Falcon® flask of non-adherent cells. After centrifugation at 250 x g for 5 min using an Eppendorf® 5430 R centrifuge, supernatant was removed and the BMDCs pellet resuspended in 5 mL of fresh medium. Cell counting was performed on a haemocytometer (Neubauer, Brand, Germany), using Trypan-Blue stain.

3.2.5. *In vitro* cell viability assay

In order to evaluate quantitatively the cytotoxic effect of NPs in murine immature BMDCs, metabolic activity of mitochondrial dehyrogenase was measured by using the AlamarBlue® assay. Cells were seeded at a density of $1.5x10^4$ cells/100 μl/well in 96-well plates and incubated overnight, in a humidified incubator with 5 % CO_2, at 37 °C. Thereafter, BMDCs were treated with different concentrations of the three groups of plain PLGA-PEG NPs (0.125, 0.25, 0.5 and 1 mg/mL). Cells exposed to PBS or 0.05 % (v/v) Triton X-100 instead of NPs, were used as negative or positive controls, respectively. After 21, 45 and 69 h of incubation in a humidified incubator, AlamarBlue® reagent was added at 10 % (v/v) and incubated for 3 h. After 24, 48 and 72 h of total incubation time, absorbance values of AlamarBlue® reagent were measured at 570 nm (AlamarBlue reduced form, pink) and 600 nm (AlamarBlue oxidized form, blue), using a microplate reader (FLUOstar Omega, BMG Labtech, Durham, NY, USA). Each assay was performed in hexaplicate (n=6) and each NPs formulation was evaluate in triplicate (N=3).

Cell viability (%) was normalized and plotting versus NP concentration. Higher values are correlated to an increased total metabolic activity of cells or to the presence of phenol red in the growth medium which, according to manufacturer instructions, shifts the values approximately 0.03 units higher. The relative cell viability related to control wells was determined by the following equations:

$$\text{Cell Viability (\%)} = \frac{\text{Abs}_{570} - (\text{Abs}_{600} \times \text{R}_0) \text{ for test well}}{\text{Abs}_{570} - (\text{Abs}_{600} \times \text{R}_0) \text{ positive growth control}} \times 100 \qquad \textit{Equation 4}$$

$$\text{R}_0 = \frac{(Abs_{AlamarBlue\ in\ medium} - Abs_{medium})_{570}}{(Abs_{AlamarBlue\ in\ medium} - Abs_{medium})_{600}} \qquad \textit{Equation 5}$$

3.2.6. Peptide integrity assessment

Evaluation of peptide integrity was determined by SDS-PAGE. The SDS-PAGE gel was composed by a stacking gel (4.7 % (w/v) acrylamide) and a resolving gel (16 % (w/v) acrylamide), prepared with acrylamide:bisacrylamide solutions. NP suspensions and peptide standard solutions (control) were mixed with the SDS-containing loading buffer (LB) achieving the final concentrations of 15 mg/mL and 0.75 mg/mL for NPs and each of the peptides (T20 and T1249), respectively. Afterwards, samples were centrifuged at 1000 x g for 5 minutes, incubated at 100 °C for 10 minutes and cooled to room temperature before being loaded into the gel (20 µl). A molecular weight marker with proteins of known molecular weight, ranging from 10-250 kDa (Mw markers, Bio-Rad, Hercules, CA, USA) was loaded into the gel (10 µl), providing a reference to determine the mass of peptides entrapped into NPs. Electrophoresis was performed using a running buffer composed by 0.025 mM (w/v) trizma, 0.192 M (w/v) glycine and 0.1 % (v/v) SDS, applying a constant voltage of 150 V at room temperature, for 90 min using a Bio-Rad 300 Power pack™ electrophoresis system (Bio-Rad, Hercules, CA, USA). To reveal peptide bands, the resolving gel was stained with a coomassie blue solution containing 0.125 % (w/v) coomassie blue G, 10 % (v/v) acetic acid and 50 % (v/v) methanol. Gel was further distained using a solution of 5 % (v/v) acetic acid and 7 % (v/v) methanol.

3.2.7. Cell uptake and intracellular trafficking studies

For qualitative uptake and intracellular trafficking studies based on confocal microscopy imaging, BMDCs (2×10^5 cells/400 µL/well) were seeded in 24-well plates, on coverslips previously coated with PLL, and incubated overnight in a humidified incubator with 5 % CO_2, at 37 °C, allowing cells to become adherent. Thereafter, without removing the medium, fluorescent PLGA-PEG_GCs_plain NPs containing Rho-grafted PLGA were added at 500 µg/mL and incubated for 1, 5 and 20 h. After this period, cells were washed twice with PBS. In order to fixe and then permeabilized cells for antibody staining, without destroying cell structures, 4 % (w/v) paraformaldehyde in PBS (pH 7.4) and 0.2 % (v/v) Triton X-100 were added separately for 10 minutes, at room temperature, with removing and washing (3x with PBS) steps before each addition. To prevent unspecific binding of antibodies (Abs) and thus minimize the background, 2 % (w/v) BSA blocking solution was added to the wells and cells were incubated for 30 minutes in a humid chamber at room temperature protected from the light. After being washed with PBS, cells were stained with primary rabbit anti-mouse Abs, anti-EEA1 (1:100) and anti-calnexin (1:200), for early endosomes and ER labeling, respectively, for 2 h, in a humid chamber at room temperature and protected from light. Then, primary Abs solutions were removed, cells washed with PBS and stained with secondary goat anti-rabbit IgG Alexa Fluor 488® antibody (1:400), under the same conditions of primary Abs labeling. Confocal microscopy samples were prepared by depositing the coverslips (cell deposits face down) on clean fluorescence microscopy slides, using an excess of mounting media (Mowiol® 4-88) between the coverslip and the slide. Preparations were allowed to dry protected from light, for 30 minutes, at 4º C and conserved under the same conditions until observation. For confocal microscopy imaging analysis, images were obtained by confocal microscopy (Leica DMI 4000 B Microscope-Leica TCS SPE; Leica source CTR 4000) and processed using the WCIF ImageJ Software. Images were processed using the colocalization plug-in of this software, for colocalization analysis. Raw images from each channel were used, the background was automatically subtracted and thresholds for both channels (red and green) were calculated. Pearson's correlation coefficient (R_r) and Mander's coefficients (M_1 and M_2) were calculated after running the colocalization finder. The colocalization percentages were calculated through the number of voxels for each channel with both, green and red channel intensities, above the threshold.

3.2.8. Statistical analysis

All experimental results are expressed as mean ± standard deviation (SD). One-way ANOVA and Turkey's post test were performed to demonstrate statistical differences, using the SPSS software (version 21) for Windows®. Differences were considered statistically significant at $p < 0.05$.

4. Results

4.1. Characterization of nanoparticles

4.1.1. Ovalbumin entrapped-nanoparticles

Biodegradable polymeric NPs derived from two different polymers, PLGA and PLGA-PEG, were prepared by double emulsion-solvent evaporation method and primarily optimized using OVA as a model antigen.

Nanoparticles were physicochemical characterized for Z-Ave, PdI, ZP, η and surface morphology. Values of Z-Ave, PdI, ZP and η, measured in triplicate, are summarized in Table 2 and Table 3 according to the polymer, PLGA and PLGA-PEG, respectively. In each table, formulations were organized according to the internal aqueous phase (10 % (w/v) PVA or 8 % (w/v) PVA/0.1 % ($w_{GCs}/w_{polymer}$) GCs) or to the external aqueous surfactants utilized (0.25 % (w/v) PVA or 0.125 % (w/v) PL), as well as to the entrapment or non-entrapment of OVA.

Table 2 – Physicochemical properties of plain and ovalbumin (OVA)-entrapped PLGA nanoparticles, by size (Z-Ave), polydispersity index (PdI) and surface charge (ZP); evaluation of yield (η) (mean ± SD; N≥3; n=3). Statistical analysis: one-way ANOVA and Turkey's post test. ZP, relative to plain formulations: * $p < 0.05$, ** $p < 0.01$ and *** $p < 0.001$.

FORMULATION	DILUTION	Z-Ave (nm)	PdI	ZP (mV)	η (% (w/w))
PLGA_PVA_plain	1:20	177±2	0.029±0.005	-2.01±0.12	46.99±8.04x10^{-13}
	1:200	177±2	0.131±0.032	-2.79±0.58	
PLGA_PVA_OVA	1:20	179±2	0.046±0.009	-2.64±0.07**	49.71±0.59
	1:200	176±3	0.114±0.064	-3.19±0.08	
PLGA_GCs_plain	1:20	170±4	0.093±0.027	-2.53±0.12	77.12±3.61
	1:200	171±3	0.095±0.016	-3.25±0.05	
PLGA_GCs_OVA	1:20	171±5	0.089±0.019	-2.48±0.53	76.27±5.63
	1:200	171±3	0.117±0.003	-3.22±0.64	
PLGA_PL_plain	1:20	217±30	0.298±0.093	-1.89±0.47	nd
	1:200	222±20	0.354±0.047	-2.99±0.32	
PLGA_PL_OVA	1:20	271±56	0.357±0.089	-2.88±0.29*	nd
	1:200	252±31	0.392±0.038	-3.27±0.48	

nd, not determined.

Table 3 – Physicochemical properties of plain and ovalbumin (OVA)-entrapped PLGA-PEG nanoparticles, by size (Z-Ave), polydispersity index (PdI) and surface charge (ZP); evaluation of yield (η) (mean ± SD; N≥3; n=3). Statistical analysis: one-way ANOVA and Turkey's post test. ZP, relative to plain formulations: * $p < 0.05$, ** $p < 0.01$ and *** $p < 0.001$.

FORMULATION	DILUTION	Z-Ave (nm)	PdI	ZP (mV)	η (% (w/w))
PLGA-PEG_PVA_plain	1:20	177±4	0.039±0.011	-2.02±0.15	51.75±4.61
	1:200	181±5	0.138±0.021	-2.96±0.81	
PLGA-PEG_PVA_OVA	1:20	179±3	0.031±0.012	-2.25±0.08	51.41±5.99
	1:200	184±3	0.121±0.028	-2.74±0.78	
PLGA-PEG_GCs_plain	1:20	178±6	0.084±0.032	-1.22±0.13	72.52±2.70
	1:200	182±5	0.159±0.016	-1.63±0.18	
PLGA-PEG_GCs_OVA	1:20	171±2	0.036±0.010	-2.38±0.09***	74.23±1.18
	1:200	174±3	0.109±0.018	-2.65±0.40	
PLGA-PEG_PL_plain	1:20	186±1	0.034±0.011	-1.50±0.25	53.12±3.06
	1:200	187±2	0.100±0.028	-2.10±0.55	
PLGA-PEG_PL_OVA	1:20	184±2	0.021±0.002	-1.98±0.39	54.82±2.95
	1:200	187±4	0.088±0.010	-2.16±0.18	

Except for PLGA_PL NPs whose formulation was not stable, all different PLGA and PLGA-PEG formulated NPs presented a size range between 170 and 187 nm, a PdI below 0.150, and a slightly negative surface charge, but still close to neutrality, with ZP values ranging from -1.22 to -3.27 mV. In addition, the low SD obtained for the three parameters (Z-Ave, PdI and ZP), demonstrates that the double emulsion-solvent evaporation method used for NPs preparation is highly reproducible. Moreover, these parameters were shown to be independent on both internal (PVA or GCs) and external (PVA or PL) aqueous phase composition, since no statistically significant differences were detected between size and zeta potential (one-way ANOVA and Turkey's post test) of NPs prepared with those different external or internal phases. Formulation stability was also maintained when OVA was entrapped into NPs, not being observed statistically significant differences between the size of antigen-loaded and plain NPs (one-way ANOVA and Turkey's post test). In addition, dilutions of NP suspensions did not alter the carrier size and zeta potential. The yield obtained for formulations prepared with GCs in the internal phase was significantly higher (~ 75 % (w/w)) than those obtained for other formulations (~ 50 % (w/w)).

Plain and OVA-loaded PLGA_PVA NPs were further characterized by AFM for their size, shape and surface morphology. Section analysis corroborates the results of

DLS, presenting a homogeneous size distribution with a mean diameter close to 170 nm (Figure 3C). In addition, AFM images showed NPs with spherical shape, as can be seen in topography and 3D images (Figure 3A and 3B-left; and 3C). However, surface morphology analysis (phase images) of plain NPs is considerably different from the OVA-loaded ones. A smoother surface was examined for plain NPs (Figure 3A-right) comparing to OVA-entrapped NPs. The slight roughness observed for OVA-loaded NPs (Figure 3B-right) may suggest that the amount of protein entrapped into these carriers is not totally incorporated into the polymeric matrix, being a small portion adsorbed onto NP surface.

A.

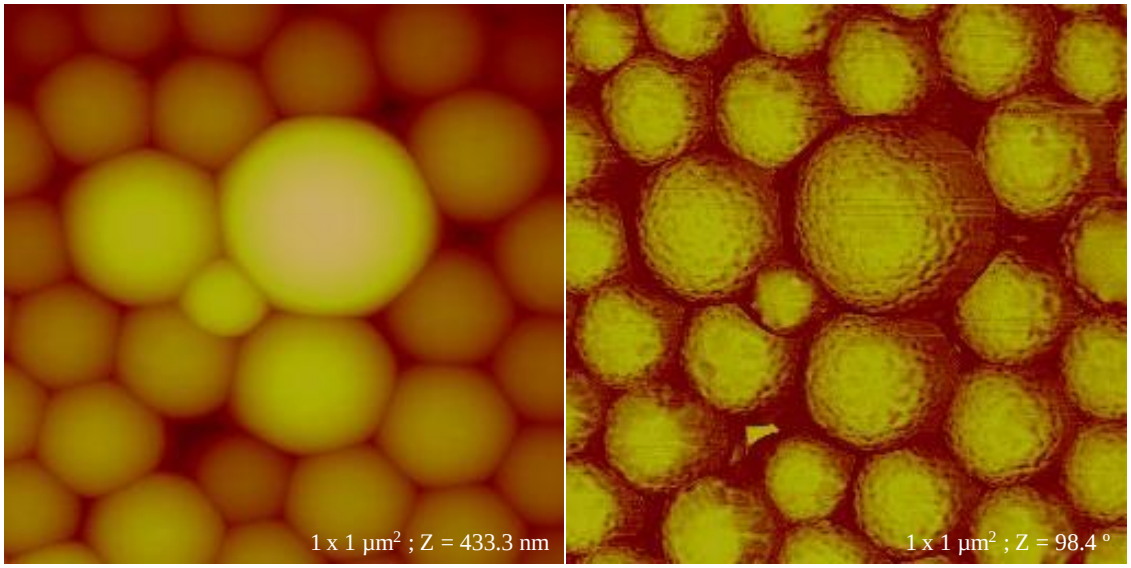

B.

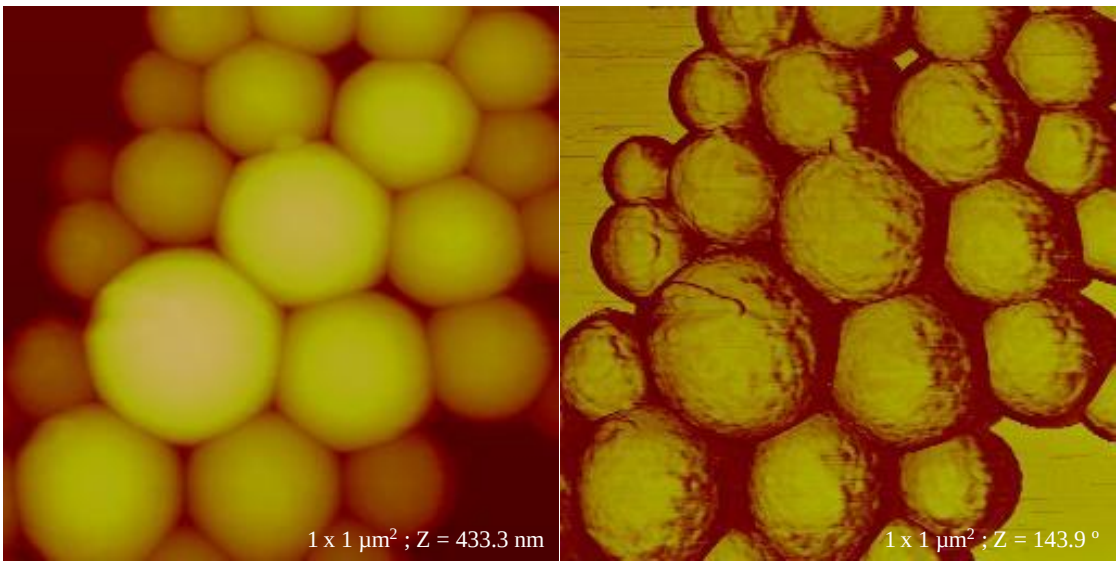

C.

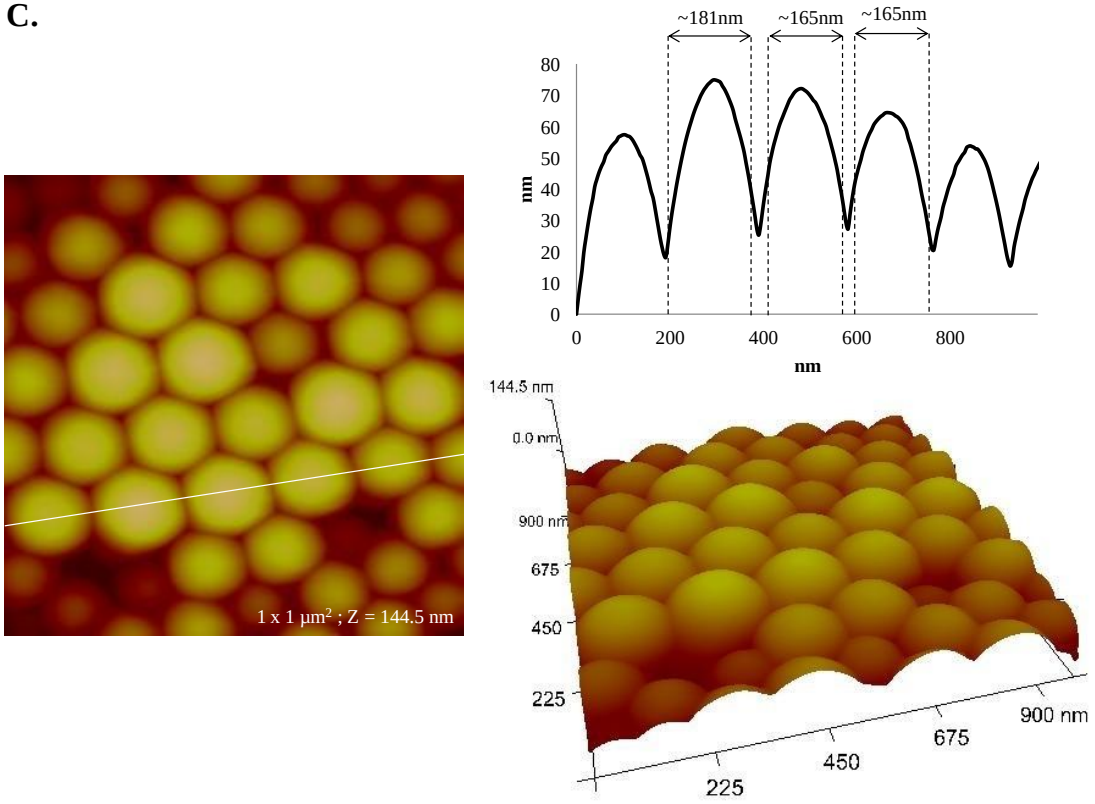

Figure 3 – Analysis of size, shape and surface morphology of nanoparticles (NPs) by Atomic Force Microscopy. Topography (left) and phase (right) images of (A) PLGA_PVA_plain NPs and (B) PLGA_PVA_OVA NPs. Section analysis and 3D image of (C) PLGA_PVA_plain NPs.

The EE (% (w/w)) and LC (µg/mg) of model antigen determined by MicroBCA™ protein assay and HPLC, are presented on Table 4, for the three different compositions of PLGA and PLGA-PEG NPs. Results were obtained indirectly through the quantification of OVA amount present in each of the three supernatants collected during the washing and centrifugation steps of NPs.

EE was calculated as the percentage of antigen mass in the NPs over the initial amount of loaded antigen, while LC was determined as mass of associated agent per mass of polymer.

EE (% (w/w)) and LC (µg/mg) analysis from both methods suggest that significantly higher values were obtained for all NPs when determined by HPLC, achieving an EE between 84 % (w/w) and 93 % (w/w), and LC close to 22 µg/mg. In fact MicroBCA™ determination evidenced EE ranging from 41 % (w/w) to 64 % (w/w) and LC values between 10 and 16 µg/mg.

Table 4 – Entrapment efficiency (EE, % (w/w)) and loading capacity (LC, µg/mg) of the ovalbumin (OVA) entrapped in PLGA and PLGA-PEG nanoparticles, determined by MicroBCA™ protein assay and High Performance Liquid Chromatography (HPLC) (mean ± SD; N≥3; n=3). Statistical analysis: one-way ANOVA and Turkey's post test. Relative to PVA and PL formulations: * $p < 0.05$, ** $p < 0.01$ and *** $p < 0.001$.

FORMULATION	EE (% (w/w)) MicroBCA™ | HPLC	LC (µg/mg) MicroBCA™ | HPLC
PLGA_PVA_ OVA	42.56±5.92 | 84.33±0.127	10.64±1.48 | 21.08±0.03
PLGA-PEG_PVA_OVA	53.43±5.73 | 92.49±2.82	13.36±1.43 | 23.12±0.70
PLGA_GCs_OVA	64.01±2.90* | 85.69±3.24	16.00±0.73* | 21.42±0.81
PLGA-PEG_GCs_OVA	62.82±3.88* | 84.37±1.11*	15.71±0.97* | 21.09±0.28*
PLGA_PL_OVA	41.60±3.96 | nd	10. 40±0.99 | nd
PLGA-PEG_PL_OVA	44.39±5.16 | 91.16±2.93	11.10±1.63 | 22.79±0.73

nd, not determined.

No statistically significant differences were seen between NPs prepared with PEGylated and non-PEGylated polymers for EE (% (w/w)) and LC (µg/mg) determined by both MicroBCA™ and HPLC. Even though the different internal phase emulsion polymers used during NP preparation seem to have a pronounced impact on the entrapment of antigens ($p < 0.05$; one-way ANOVA and Turkey's post test). In fact, results appear to be independent of the type of polymer (PLGA or PLGA-PEG), as well as, the nature of the surfactant present in the external aqueous phase (PVA or PL), since similar EE (% (w/w)) and LC (µg/mg) were observed (Table 4). However, EE (% (w/w)) and LC (µg/mg) seem to be dependent on the internal aqueous phase used, PVA or GCs, when determined by MicroBCA™. NPs containing GCs have shown values of EE and LC close to 63 % (w/w) and 16 µg/mg, respectively, while PVA stabilized NPs presented EE between 42 % (w/w) and 53 % (w/w) and LC ranging from 10 µg/mg to 13 µg/mg. Curiously, results obtained using HPLC method show that the PLGA-PEG_GCs NPs present lower EE (% (w/w)) and LC (µg/mg) values than those prepared with PVA. In fact, the use of GCs in internal phase led to EE and LC values of 84 % (w/w) and 21 µg/mg, respectively, compared with those obtained for NP presenting only PVA in the internal phase (EE of 91-92 % (w/w) and LC of 23 µg/mg).

HPLC analysis also showed that the excess of PVA is efficiently removed from the surface of NPs during the washing and centrifugation procedure (data not shown).

4.1.2. HIV-1 peptides entrapped-nanoparticles

Taking into account the previous results (Z-Ave, PdI, ZP, η, EE and LC) obtained for model antigen OVA and the advantages of PEG in NP biodistribution, HIV-1 peptides, T20 and T1249, were entrapped into biodegradable PLGA-PEG NPs using the same methodology. Results for Z-Ave, PdI and ZP are summarized in Table 5, in which formulations were also ordered according to the i) internal aqueous phase used (10 % (w/v) PVA or 8 % (w/v) PVA/0.1 % ($w_{GCs}/w_{polymer}$) GCs); ii) stabilizers present at the outer water phase, 0.25 % (w/v) PVA or 0.125 % (w/v) PL, and the iii) entrapment/co-entrapment of HIV-1 peptides. Since the evaluated parameters (size and ZP) have been shown to be independent of dilution factor for NPs obtained during the optimization procedure, the physicochemical characteristics of HIV-1 peptide-loaded NPs were determined using only the lower dilution factor (1:20).

Table 5 – Physicochemical properties of plain or HIV-1 peptides (T20 and T1249)-entrapped PLGA-PEG nanoparticles, by size (Z-Ave), polydispersity index (PdI) and surface charge (ZP); (mean ± SD; N≥3; n=3). Statistical analysis: one-way ANOVA and Turkey's post test. Relative to PLGA-PEG_plain for each formulation type: * $p < 0.05$, ** $p < 0.01$ and *** $p < 0.001$.

FORMULATION	Z-Ave (nm)	PdI	ZP (mV)
PLGA-PEG_PVA_plain	171±1	0.042±0.003	-1.72±0.15
PLGA-PEG_PVA_T20	170±2	0.064±0.016	-2.39±0.62
PLGA-PEG_PVA_T1249	163±1*	0.049±0.017	-2.15±0.29
PLGA-PEG_PVA_T20_T1249	168±3	0.078±0.011	-1.56±0.48
PLGA-PEG_GCs_plain	178±1	0.073±0.017	-1.33±0.29
PLGA-PEG_GCs_T20	171±3*	0.053±0.018	-2.36±0.30
PLGA-PEG_GCs_T1249	165±2**	0.060±0.018	-2.44±0.58*
PLGA-PEG_GCs_T20_T1249	174±2	0.062±0.012	-1.61±0.15
PLGA-PEG_PL_plain	175±3	0.036±0.019	-1.95±0.21
PLGA-PEG_PL_T20	169±3*	0.048±0.017	-1.93±0.26
PLGA-PEG_PL_T1249	164±2**	0.049±0.014	-1.31±0.31
PLGA-PEG_PL_T20_T1249	172±1	0.095±0.013	-1.17±0.36*

In general, the different PEGylated PLGA NPs presented a mean hydrodynamic diameter (Z-ave) close to 170 nm (mean size range of 163 to 178 nm), a PdI below 0.1 and a surface charge close to neutrality, with ZP values ranging from -1.17 to -2.36 mV.

The double emulsion-solvent evaporation method proved to be extremely reproducible, observing the low SD values obtained for Z-Ave, PdI and ZP. It can also

be seen that the stability of PLGA-PEG NPs was not affected by the different HIV-1 antigens entrapped, as well as by the nature of the polymers/surfactants used in the external or internal aqueous phases. In fact, the differences observed in Z-Ave, PdI and ZP values obtained for HIV peptide-loaded PLGA-PEG NPs were not statistically significant, despite the different entrapped antigens and the polymers used in the external or internal phases (one-way ANOVA and Turkey's post test).

On the other hand, statistical differences were found between size and zeta potential obtained for HIV-1 antigen-loaded NPs and those presented by plain or OVA-loaded NPs ($p < 0.05$; one-way ANOVA and Turkey's post test).

A preliminary study was conducted to infer the stability and degradation profiles of NPs. Accordingly, freshly prepared HIV-1 antigen-loaded PLGA-PEG NPs were stored at 4ºC for one month and Z-Ave, PdI and ZP parameters were measured after this period (Table 6).

Table 6 – Physicochemical properties of HIV-1 peptide-loaded PLGA-PEG nanoparticles, by size (Z-Ave), polydispersity index (PdI) and surface charge (ZP), one month after preparation (mean ± SD; N≥3; n=3).

FORMULATION	Z-Ave (nm)	PdI	ZP (mV)
PLGA-PEG_PVA_T20	176±1	0.073±0.008	-3.90±1.08
PLGA-PEG_PVA_T1249	166±5	0.076±0.015	-2.46±0.36
PLGA-PEG_PVA_T20_T1249	172±0	0.070±0.028	-2.75±0.35
PLGA-PEG_GCs_T20	179±3	0.109±0.018	-3.77±0.53
PLGA-PEG_GCs_T1249	167±1	0.066±0.009	-2.08±0.93
PLGA-PEG_GCs_T20_T1249	185±6	0.121±0.001	-2.69±0.66
PLGA-PEG_PL_T20	175±0	0.074±0.018	-3.58±0.54
PLGA-PEG_PL_T1249	170±3	0.078±0.012	-2.15±0.43
PLGA-PEG_PL_T20_T1249	176±2	0.094 ± 0.009	-3.27±1.20

From tables 5 and 6, it is evident that the physicochemical properties of HIV-1 peptide-loaded PLGA-PEG NPs remained unaltered over the one month period. HIV-1 peptide-loaded PLGA-PEG NPs did not show any tendency to aggregate, presented a mean hydrodynamic diameter close to 174 nm and a PdI below 0.1. Although the surface charge remained close to neutrality, a slight decrease in ZP was observed, which is consistent with polymer degradation and consequent exposure of carboxylic acid end-groups.

The EE (% (w/w)) and LC (µg/mg) of HIV-1 antigen-loaded NPs (Table 7) were also indirectly quantified by intrinsic fluorescence assay of aminoacids present in T20 and T1249 peptides, using the supernatants collected during the three washing and centrifugation steps of PLGA-PEG NPs.

Table 7 – Entrapment efficiency (EE, % (w/w)) and loading capacity (LC, µg/mg) of the HIV-1 peptides (T20 and T1249) entrapped-PLGA-PEG nanoparticles, determined by intrinsic fluorescence assay (mean ± SD; N≥3; n=3). Statistical analysis: one-way ANOVA and Turkey's post test. Relative to PLGA-PEG_PL_T20_T1249 formulation (between peptides): * $p < 0.05$, ** $p < 0.01$ and *** $p < 0.001$. Relative to PLGA-PEG_PL for each peptide formulation (between external phases): $^{\#}$ $p < 0.05$, $^{\#\#}$ $p < 0.01$ and $^{\#\#\#}$ $p < 0.001$. Relative to PLGA-PEG_GCs for each peptide formulation (between internal phases): ^{o} $p < 0.05$, ^{oo} $p < 0.01$ and ^{ooo} $p < 0.001$.

FORMULATION	EE (% (w/w)) Fluorescence	LC (µg/mg) Fluorescence
PLGA-PEG_PVA_T20	80.36±15.72$^{\#}$	16.07±3.14$^{\#}$
PLGA-PEG_PVA_T1249	78.22±8.84$^{\#}$	15.64±1.77$^{\#}$
PLGA-PEG_PVA_T20_T1249	86.30±1.53^{oo}	17.26±0.31^{oo}
PLGA-PEG_GCs_T20	88.80±3.76$^{\#}$	17.76±0.75$^{\#}$
PLGA-PEG_GCs_T1249	82.49±6.80$^{\#\#}$	16.50±1.36$^{\#\#}$
PLGA-PEG_GCs_T20_T1249	92.65±1.78$^{\#\#}$	18.53±0.36$^{\#\#}$
PLGA-PEG_PL_T20	66.66±2.67*^{o}	13.33±0.53*^{o}
PLGA-PEG_PL_T1249	48.39±9.84**$^{;oo}$	9.68±1.97**$^{;oo}$
PLGA-PEG_PL_T20_T1249	85.35±0.36^{oo}	17.07±0.07^{oo}

Overall, NPs were able to co-entrap different HIV-1 antigens, presenting EE and LC values above 78 % (w/w) and 15 µg/mg, respectively. These values were similar to those obtained for carriers entrapping each antigen individually. On the other hand, the entrapment of those antigens appear to be dependent on the nature of the surfactant present in the external aqueous phase, showing higher EE and LC for formulations prepared using PVA. Internal aqueous phase composition also influenced EE and LC, where higher values were obtained for formulations developed using GCs. In addition, the highest EE and LC close to 93 % (w/w) and 19 µg/mg, were obtained when both HIV-1 antigens, T20 and T1249 peptides, were co-entrapped into PLGA-PEG_GCs NPs.

The EE (% (w/w)) and LC (µg/mg) of PLGA-PEG NPs entrapping each HIV peptide individually were significantly affected by the composition of the external or

internal phases ($p < 0.05$). On the other hand, no differences were observed for EE (% (w/w)) and LC (μg/mg) presented by NPs entrapping different HIV-1 antigens, except for PLGA-PEG_PL ($p < 0.05$; one-way ANOVA and Turkey's post test).

4.2. Cell viability assay

An AlamarBlue® assay was performed to determine the effect of plain PLGA-PEG NPs on the viability of murine immature BMDCs. Cells were incubated with crescent concentrations of the three different PLGA-PEG-based NPs (PLGA-PEG_PVA, PLGA-PEG_GCs and PLGA-PEG_PL) (0.125, 0.25, 0.5 and 1 mg/mL) for 24, 48 and 72 h. Triton X-100 was used as positive control. Cell viability (%) was normalized using PBS as negative control (100 %).

As it can be seen in Figure 4, no cytotoxic effect was observed on BMDCs, over a wide range of concentrations of the three groups of PLGA-PEG NPs, at 24, 48 and 72 h post incubation.

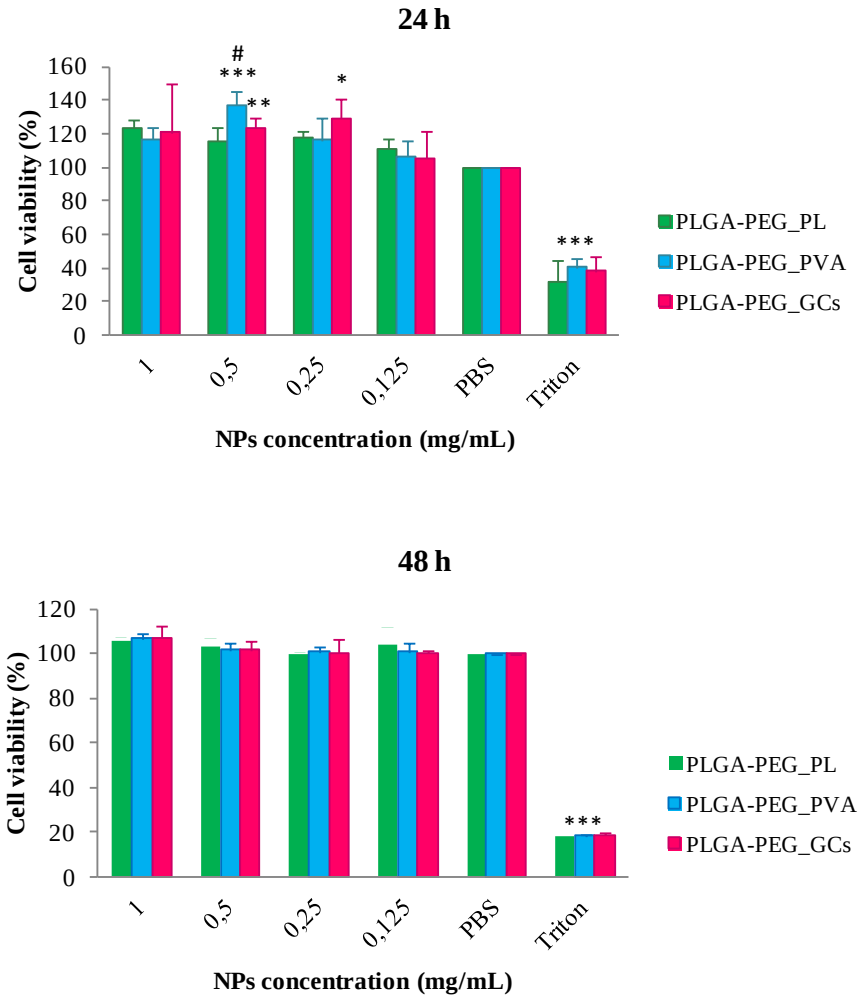

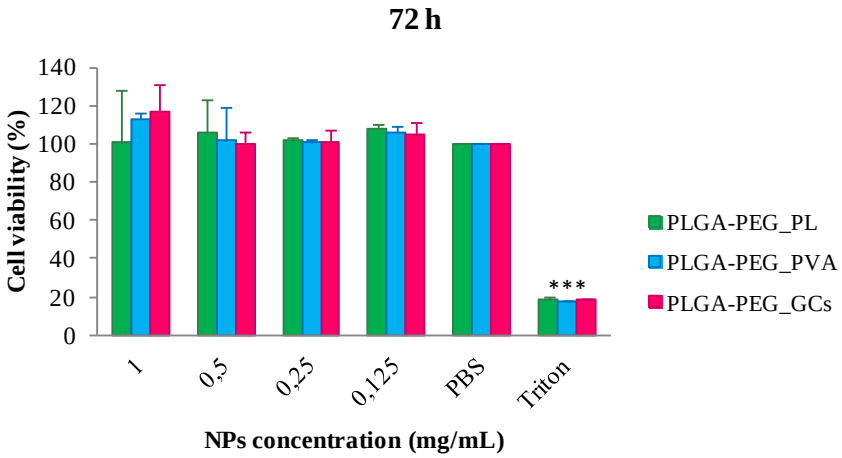

Figure 4 – Cell viability (%) determined by AlamarBlue® assay with increasing concentrations (0.125-1 mg/mL) of three different groups of PLGA-PEG nanoparticles (PLGA-PEG_PVA, PLGA-PEG_GCs and PLGA-PEG_PL) on murine immature bone marrow dendritic cells (JAW SII, ATCC®CRL-11904™), after 24, 48 and 72 hours of incubation (mean ± SD; N=3; n=6). Statistics: one-way ANOVA and Tukey's post test. Relative to negative control (PBS): * $p < 0.05$, ** $p < 0.01$ and *** $p < 0.001$. Between different concentrations for each formulation: # $p < 0.05$, ## $p < 0.01$ and ### $p < 0.001$.

Indeed, cell viability remained close to 100 % and thus similar to the negative control PBS, even after 72 h of incubation with the three groups of PLGA-PEG NPs in concentrations ranging from 0.125 mg/mL to 1 mg/mL. Cell viability was thus independent of external and internal aqueous phase composition, NP concentration and incubation time. Moreover, the levels of cell viability obtained after 48 h and 72 h of incubation with nanoparticulate formulations were not statistically different from the negative control (PBS). Contrary, a mean viability of 20 % was observed for positive control (cells treated with 0.05 % (v/v) Triton X-100), which was significantly different ($p < 0.001$; one-way ANOVA and Turkey's post test) than the one presented by cells after incubation with whichever nanoparticulate system under study and PBS. In addition, no statistically significant differences were seen between the cell viability obtained for the different concentrations tested for different types of formulations, with the exception of the one quantified after 24 h of incubation with 0.5 mg/mL of PLGA-PEG_PVA NPs ($p < 0.05$; one-way ANOVA and Turkey's post test).

4.3. Evaluation of peptide integrity

Having in consideration the higher EE and LC values obtained for PLGA-PEG formulation containing GCs, as well as the absence of cytotoxic effect on BMDCs, this formulation was selected to assess the effect of formulation procedure on HIV-1 peptide structural integrity. The integrity of T20 and T1249 individually or co-entrapped into PLGA-PEG_GCs NPs was evaluated by PAGE, using SDS as denaturing agent (16 % resolving gel) (Figure 5).

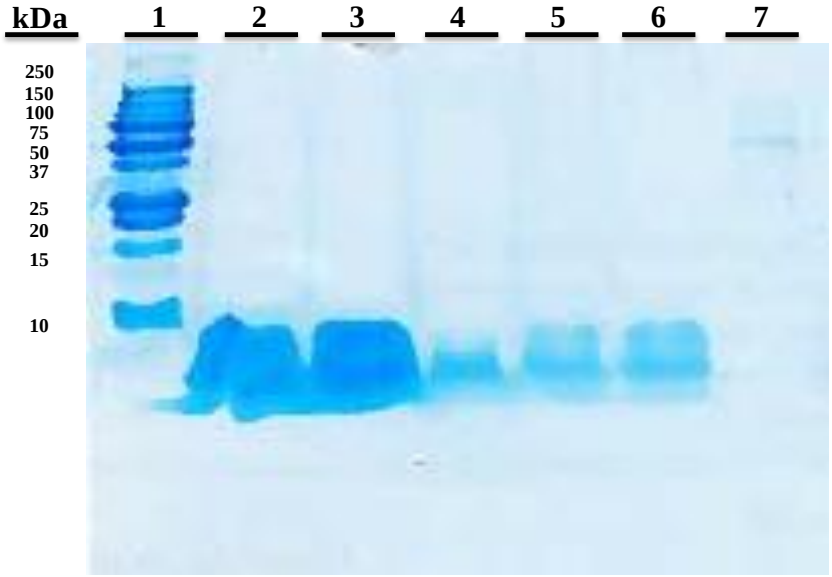

Figure 5 – Evaluation of the integrity of HIV-1 peptides, T20 and T1249, entrapped in PLGA-PEG_GCs nanoparticles (NPs) by sodium dodecyl sulfate-polyacrylamide gel electrophoresis (16 % resolving gel). (1) Standard molecular weight markers (10-250 kDa); (2) and (3) positive controls: T1249 and T20 solutions (0.75 mg/mL), respectively; (4) PLGA-PEG_GCs_T1249 NPs; (5) PLGA-PEG_GCs_T20 NPs; (6) PLGA-PEG_GCs_T20_T1249 NPs; and (7) negative control: PLGA-PEG_GCs_plain NPs.

It is possible see that all HIV-1 peptide-loaded NPs (loaded in wells 4, 5 and 6) have a similar pattern of migration and present a single band below the lower limit of the Mw marker (10 kDa), correspondent to HIV-1 peptides (T20 and T1249), which have molecular weights close to 5 kDa. In fact, the structure of the HIV-1 antigens entrapped into PLGA-PEG_GCs NPs seem not to be affected by the formulation procedure due to the presence of an unique band at a molecular weight similar to the one observed for positive controls, T20 and T1249 solutions (0.75 mg/mL), loaded in wells 2 and 3; as well as the absence of additional bands suggestive of peptide

fragmentation. Moreover, the previous results are corroborated by the non-existence of this band in plain NPs used as negative control (loaded in well 7).

4.4. Uptake and intracellular trafficking of nanoparticles

In order to verify the uptake of PLGA-PEG NPs by DCs, their intracellular trafficking and consequent ability to process and present antigens complexed with MHC class I and/or II molecules, confocal microscopy imaging studies were performed. BMDCs were incubated with fluorescent PLGA-PEG_GCs_plain NPs prepared using Rho-grafted PLGA (NPs-Rho), which presented physicochemical properties similar to non fluorescent PLGA_PEG_GCs_plain NPs. Thereafter, anti-EEA1 and anti-calnexin antibodies were added to BMDCs to visualize early endosomes and ER, respectively.

Representative images of BMDCs obtained after 1, 5 and 20 h of incubation with NPs-Rho (red) and staining of subcellular organelles (green), as well as the colocalized pixels (in white) arised from the red-green merged images, are shown on Figure 6A. Qualitatively, it was possible to infer that a small number of NPs were taken up by BMDCs after 1 h of incubation, being a considerable amount of NPs adsorbed onto cell membranes (EEA1, 1 h). However, the intracellular internalization of NPs by BMDCs increased after 5 h of incubation (EEA1 and Calnexin, 5 h), confirming the further uptake of those NPs previously adsorbed onto cell membranes. After 20 h of incubation, the amount of NPs taken up by cells seem to be lower (EEA1 and Calnexin, 20 h) than the one observed 5 h after of incubation, being still higher than those observed inside the cells after 1 h of incubation. Moreover, it was observed that the number of early endosomes increased with time (EEA1, 5 and 20 h). Regarding the intracellular localization, internalized NPs were localized in the perinuclear space as well as in the cytosol. Slightly orange regions resulting from the overlay of red and green channels indicate the colocalization of NPs-Rho (red) within acidic organelles (green), like early endosomes.

Quantitative analysis was also performed. The percentage of colocalization of NPs-Rho with each organelle is represented on Figure 6B (left). After 1 h, NPs-Rho presented 19.7±15.4 % and 34.7±25.3 % of colocalization with EEA1 and calnexin, respectively. After 5 h, the colocalization of NPs-Rho with organelles increased to 59.7±7.8 % and 65.6±2.1 % for EEA1 and calnexin, respectively. Finally, after 20 h, the colocalization percentage of NPs-Rho with EEA1 and calnexin decreased to 56.3±5.3 %

and 53.7±19.1 %, respectively. The obtained results suggest that after 1 h of incubation, NPs achieved the endo-lysosomal pathway, being possible to observe NPs colocalized with organelles. During the following 4 h, colocalization levels were increased for both organelles, being then lower at 20 h. According to the colocalization percentage of the organelles with NPs-Rho, which ranged from 12.4±4.5 % to 66.9±2.1 %, saturation of organelles with NPs did not take place (Figure 6B, right). On Figure 6C (left), M1 coefficient was found to be in accordance with the colocalization percentage of the red and green channels. The behavior of M2 coefficient is similar to M1, suggesting the dependence of the staining of NPs and organelles (Figure 6C, right). High correlation levels between NPs and organelle stains were observed through Rr values, which remained higher than 0.5, at all time points (Figure 6D).

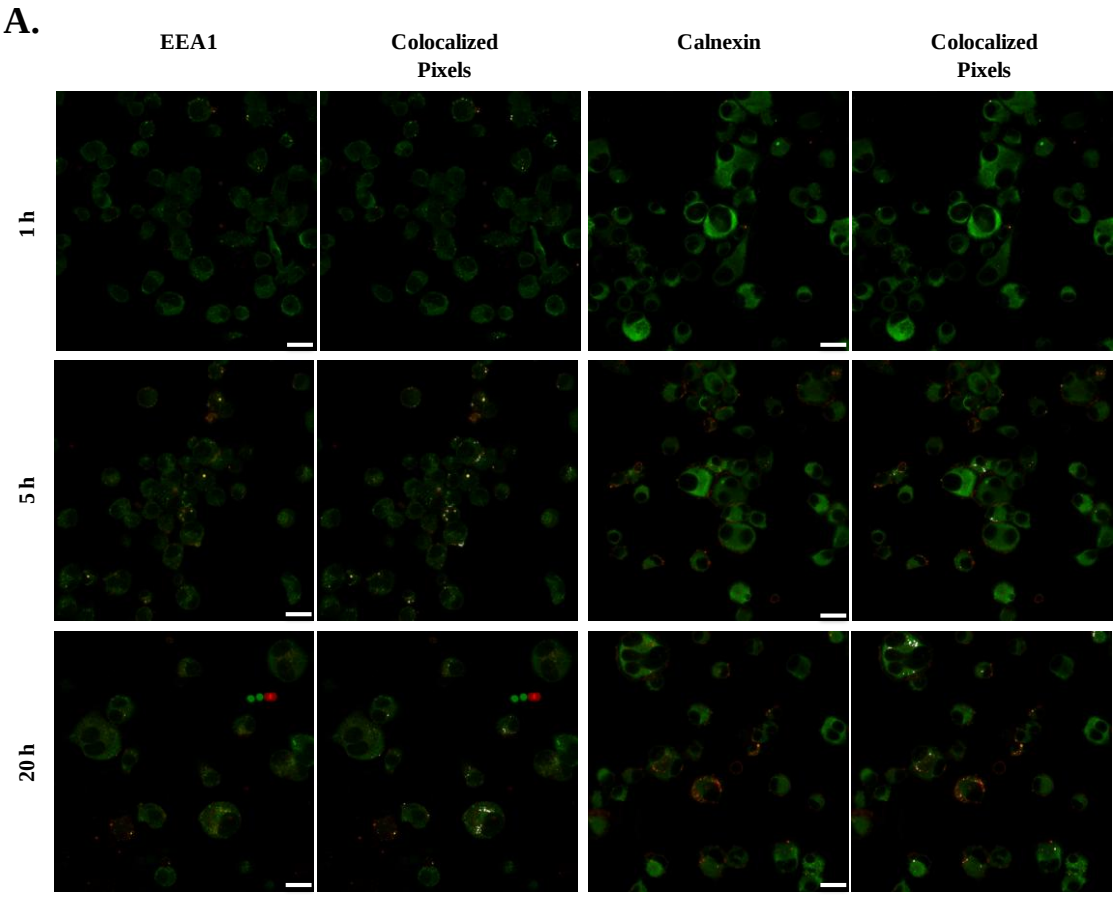

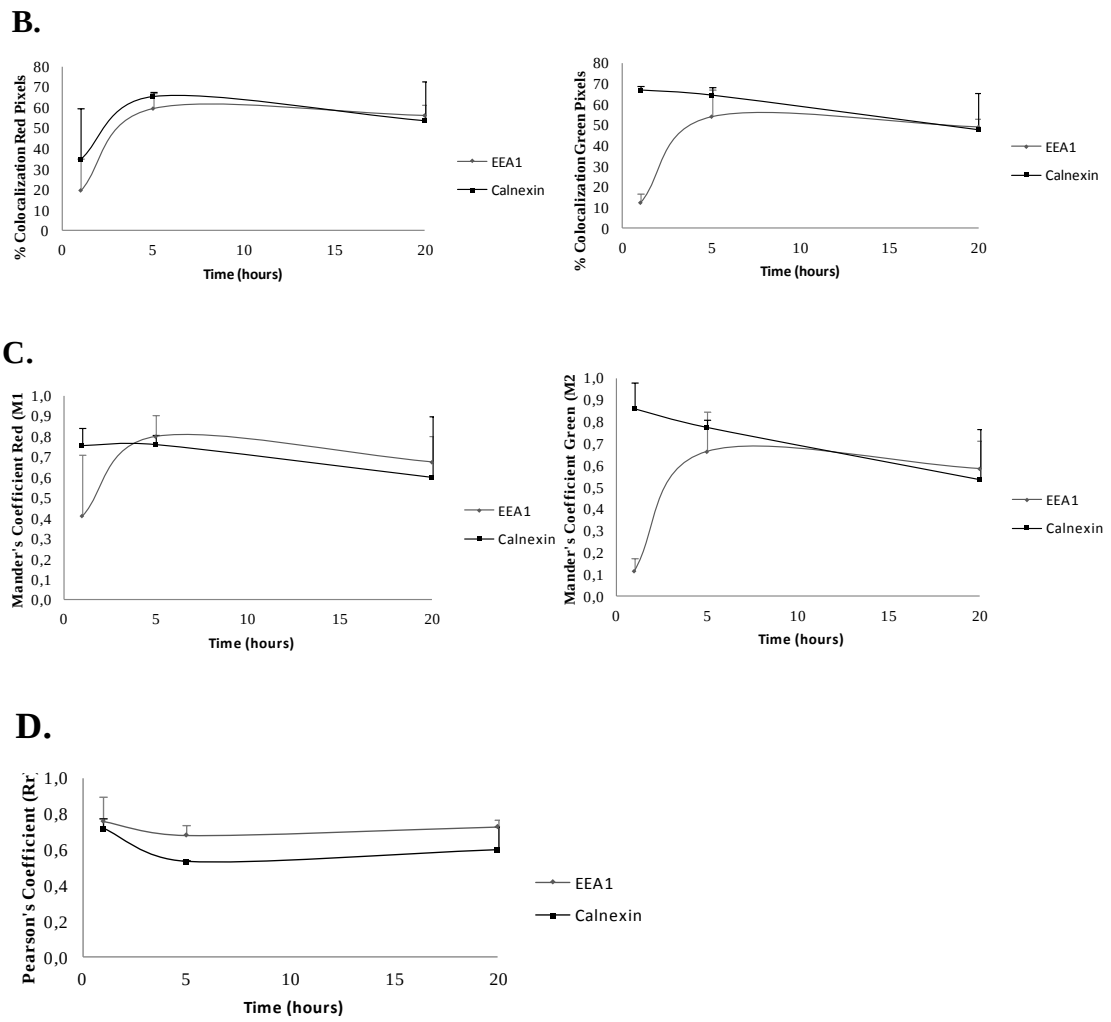

Figure 6 – Uptake and intracellular trafficking of nanoparticles (NPs) by murine immature bone marrow dendritic cells (BMDCs), and colocalization analysis. (A) Confocal microscopy images of rhodamine-labeled NPs (Red) incubated with BMDCs for 1, 5 and 20 h. Early endosomes and endoplasmic reticulum were stained with rabbit anti-mouse anti-EEA1 and anti-calnexin, respectively, and then labeled with goat anti-rabbit IgG Alexa Fluor 488® (green). Scale bars = 20 µm. WCIF ImageJ software was used to obtain the colocalized pixels in white, from red and green channels (on right of the respective image), as well as, to quantify the percentage of colocalization of NPs (red pixels) with each organelle-staining antibody (green pixels) and vice versa (B, left and right, respectively), the Mander's coefficient of red (M1) and green (M2) channels (C, left and right, respectively) and the Pearson's correlation coefficient, Rr (D). Mean ± SD from at least 40 cells from three independent images is represented.

5. Discussion

New preventive and/or therapeutic strategies against HIV-1 infection are urgently needed to avoid the continuous increase in the AIDS incidence rates observed around the world (192). The goal essentially comprises the control and eradication of HIV-1 infection through the development of an effective, safe and inexpensive vaccine with prophylactic/therapeutic properties, where both cellular and humoral immune responses are required. In fact, not only antibody and $CD4^+$ Th lymphocyte-mediated immune responses are crucial, but also the induction of both virus-specific neutralizing antibodies, at the site of viral entry, and $CD8^+$ Tc lymphocyte with cytotoxic effect seem to be crucial to impair the dissemination of this virus (193). Different vaccine strategies have been employed. Live attenuated or whole inactivated traditional vaccines were described as unsafe, causing unwanted side effects. More recent vaccines composed by part of the pathogen, such as recombinant/synthetic proteins or peptides, or DNA enconding for these proteins, have been described as safe approaches, but also as poorly immunogenic, requiring the use of adjuvants to induce potent immune responses (194). Polymeric NPs have been widely investigated as a promising strategy for HIV vaccine delivery systems, acting as adjuvant by enhancing the antigen uptake by APCs that will elicit effective humoral and cellular immune responses, and protecting antigens from unfavorable *in vivo* environment after administration (195, 196).

This project aimed to develop biodegradable and biocompatible PLGA nanoparticulate systems as vaccine candidates to deliver entrapped HIV-1 gp41 antigenic peptides to target highly specialized APCs, as DCs, in order to ultimately elicit an effective humoral and cellular immune responses, essentially with the production of neutralizing antibodies. It included the production and characterization of these antigen-loaded NPs, as well as the evaluation of their uptake and intracellular trafficking by target cells.

5.1. Composition of nanoparticles

The physicochemical properties of the selected materials and the formulation procedure used to prepare polymeric NPs play an important role in their physiochemical characteristics as well as in their *in vitro* and *in vivo* behavior. PLGA-based NPs have been widely used to carry antiretroviral drugs and for siRNA vaginal delivery aiming

HIV prophylaxis (178, 197, 198). PLGA is an FDA and European Medicine Agency (EMA) approved biocompatible and biodegradable polymer acceptable for different applications, including drug delivery. This polymer presents a residual cytotoxicity due to its metabolization via Krebs cycle after chemical hydrolysis into PLA and poly(glycolic acid) (PGA) monomers (199). PLGA NPs have the ability to interact and destabilize vesicular membranes that successfully result in the escape from endolysosomal route and in the delivery of entrapped cargo into cytoplasm (200, 201). The surface modification of PLGA NPs with PEG chains has also been reported to increase their intravaginal retention and reach an augment delivery of cargo, being useful for long-term prophylaxis (202). PEG is a hydrophilic, non-toxic and flexible molecule approved by the FDA for human use (203). The "PEGylation" process consists in coating NP surface with a hydrophilic layer and has been used not only to stabilize the formulation but especially to avoid the recognition of hydrophobic polymers by cells in the reticuloendothelial system (RES) as foreign, increasing their circulation half-life in bloodstream. In fact, this recognition process resultant from binding of opsonins is presented as one of the biggest barriers to the controlled delivery by NPs. Moreover, the linkage of specific ligands to the NP surface via PEG-grafted polymers has been applied for the targeting specific organs or subcellular organelles (204). PEG-grafted NPs were also reported to decrease the interaction of these carriers with digestive enzymes after oral administration (205). Different polymers have been used in the formulation of particulate vaccine delivery systems for HIV prophylaxis, such as PMMA (98), PG (99) and PLA (101). The potential use of PLGA was demonstrated by Zhu *et al*. (2012) who developed Eudragit microparticles encapsulated with HIV antigen-loaded PLGA NPs for oral administration (100). In addition, adjuvant properties of different polymeric NPs have been demonstrated by successful eliciting systemic and mucosal immune responses, as reviewed by Aline *et al*. (2009) and Caputo *et al*. (2009) (98, 206). Taking advantage of the unusual development of HIV vaccine delivery nanocarriers based on PLGA polymer and its higher biodegradation rate and lower hydrophobicity *in vivo* than other polymers such as PLA, PLGA and PLGA-PEG polymers were explored a NPs' matrix in this study.

Several methods such as solvent evaporation, salting-out, dialysis and supercritical fluid technology can be used to prepare polymeric NPs and their choice depends on several aspects, namely the type of polymeric system, route of administration, nature of active molecules and size distribution (207). PLGA NPs are

commonly prepared by emulsification-solvent evaporation technique, where two main strategies are used for those formulations: w/o single emulsion for hydrophobic drug encapsulation and w/o/w double emulsion to encapsulate hydrophilic entities, such as peptides, proteins and nucleic acids. In both cases, this technique consists in adding an aqueous phase, containing the stabilizer or surfactant, to an oil phase, composed by the polymer previously dissolved in an organic solvent (e.g., DCM). The formation of nanosized droplets is achieved by supplying energy to the system through high-speed homogenization or ultrasonication methods. In the specific case of a w/o/w emulsion, the first w/o emulsion is then added to a large volume of an external aqueous phase, containing a specific surfactant which will allow the formation of NPs. Thereafter, the active molecule-loaded solid nanospheres formed during solvent evaporation under continuous magnetic stirring at room temperature, or reduced pressure, can be collected by ultracentrifugation and washed to remove the excess of surfactants. Lately, NPs can be lyophilized (208). In this study, polymeric NPs were formulated using a modified w/o/w solvent evaporation method, originally described by Ogawa *et al*. (1988) (209).

The various biomaterials used as internal or external aqueous phases were chosen in order to compare their influence in the physicochemical properties of NPs, such as size, surface charge, stability, EE (% (w/w)) and LC (µg/mL), as well as their cytotoxicity *in vitro*. Therefore, PLGA or PLGA-PEG-based NPs were produced by utilizing PVA as the internal and external stabilizing agent. PVA is a nonionic water-soluble polymeric surfactant with excellent emulsifying properties (ampiphilic character), commonly used to stabilize the formulation of PLGA NPs and reduce emulsion surface tension (210). Lemoine and Préat (1998) observed that NPs' size decreased when PVA was used in the internal aqueous phase. On the contrary, a residual influence was seen when this polymer was used in the external aqueous phase (211). However, some studies have shown adverse effects in animals, such as hypertension, organ lesions, anemia and depression of the central nervous system, from PVA subcutaneous and intravenous administration (212). Furthermore, there are still some concerns about PVA carcinogenicity (213). Consequently, residual PVA should be always removed by repetitive washing and centrifugation procedures. Moreover, PL was also used as an alternative surfactant to PVA, in the external aqueous phase. PL is a non-ionic triblock copolymer surfactant, also commonly used for PLGA-based NP formulation, which presents low toxicity and immunogenicity (214). Menon *et al*. (2011) prepared PLGA NPs coated with different pluronic surfactants, observing that

Pluronic F127 was the most biocompatible, which support this alternative choice (215). Chitosan is a highly biocompatible and biodegradable polysaccharide obtained from chitin deacetylation, found in exoskeleton of shellfish. This cationic polymer is usually studied as gene delivery system, due to its ability to complex with negatively charged DNA (216). Cs-containing microparticles have been shown to elicit protective immune responses, after IN immunization (217). Moreover, Beletti *et al.* (2012) demonstrated that the addition of Cs in the inner phase of the primary emulsion increased the EE of tenofovir loaded into PLGA NPs (218). According to this evidence, GCs was also used in the internal aqueous phase, in combination with PVA, in order to attain a higher EE and LC of antigens.

In this study, PLGA and PLGA-PEG NPs formulation procedure was firstly optimized using OVA, as a model antigen. OVA is an albumin protein from chicken egg white of 45 kDa that has been widely studied as a model antigen (219, 220). After NP characterization and optimization, OVA was replaced by HIV-1 antigens, T20 and T1249 peptides. T20 or enfuvirtide is the only FDA approved HIV-1 fusion inhibitor since 2003 composed by 36 amino acids engineered directly from HIV-1 gp41 CHR sequence. It has the following amino acid sequence: CH_3CO-Tyr-Thr-Ser-Leu-Ile-His-Ser-Leu-Ile-Glu-Glu-Ser-Gln-Asn-Gln-Gln-Glu-Lys-Asn-Glu-Gln-Glu-Leu-Leu-Glu-Leu-Asp-Lys-Trp-Ala-Ser-Leu-Trp-Asn-Trp-Phe-NH_2 and a molecular weight of 4492 Da (160, 221). T1249 is another strong inhibitor of HIV-1 composed by 39-mer peptide derived from CHR consensus sequences. It amino acid sequence is: CH_3CO-Trp-Gln-Glu-Trp-Glu-Gln-Lys-Ile-_-_-_-_-_-_-_-_-Thr-Ala-Leu-Leu-Glu-Gln-Ala-Gln-Ile-Gln-Gln-Glu-Lys-Asn-Glu-Tyr-Glu-Leu-Gln-Lys-Leu-Asp-Lys-Trp-Ala-Ser-Leu-Trp-Glu-Trp-Phe-NH_2 and presents a molecular weight around 5000 Da (160).

Note that formulations of all nanoparticulate carriers were performed in triplicate in order to attain reliable statistical correlations.

5.2. Physicochemical characterization of nanoparticles

The goal of vaccination aims the induction of an appropriate immune response to confer protection against pathogen. Moreover, the delivery of antigens to APCs, especially DCs that are highly specialized to take up and process antigens, is crucial for the induction of T cell responses and the development of a protective immune response (105). In addition, the efficiency of antigen uptake into DCs has been shown to be

higher when encapsulated in NPs. However, it has been shown that the physicochemical properties of nanocarriers, such as size, surface charge and surface morphology, play an important role in the interaction between particles and APCs (222).

The size is an important factor that affects the cellular uptake of particulate antigen carriers. However, the ideal size for NPs uptake by APCs remains an utopian issue, several studies indicate that these cells are able capture and process any antigen with similar dimensions of viruses (20-100 nm), bacteria or even cells (micrometer range) (104). Size of soluble or particulate material also influences the mechanism of entry and consequently the subsequent endocytic pathway. Commonly, virus particles range from 20 to 200 nm can be taken up via clathrin-dependent endocytosis (size < 200 nm) (223) or via caveolae-mediated endocytosis (size range 50-100 nm) (224). Moreover, to elicit an effective and long-lasting immune response, antigen-loaded NPs should also migrate through the lymphatic system, being size an important determinant. While particles larger than 200-500 nm require to be transported by DCs, taking 24 hours to achieved the lymphoid organs, NPs smaller than 200 nm travel directly through lymph drainage reaching the lymphoid organs within hours after administration, besides being also transported by DCs (225). PLGA NPs demonstrated higher uptake levels than microparticles (226). Moreover, effective cellular immune responses have been elicited by NPs encapsulating HIV-1 antigens and presenting an average mean diameter close to 200 nm (97, 206).

Cellular uptake is also influenced by shape or surface morphology of these nanodelivery systems. According this fact, spherical gold NPs have been more efficiently taken up than rod-shaped NPs (227). In addition, PLGA elliptical particles took a longer period of time to be endocytosed by endothelial cells than spherical particles (228). Therefore, the latter constitutes a promising shape to be considered for vaccine delivery development.

Finally, surface charge presents an important role on internalization ability, and shows to be dependent on the chemical nature of polymer and stabilizing agent, as well as on pH of dispersant. Apparently, as a result of ionic interactions established between positively charged particles and negatively charged cell membranes, cationic NPs present a higher extent of internalization than negatively or neutrally charged ones (229, 230). In addition, it is believed that the internalization of anionic NPs occurs through the non-specific binding and aggregation of particles on cellular cationic sites, followed by endocytosis. Moreover, in order to increase the circulation time of these

nanocarriers, neutral charge may prevent unwanted interactions with cells (226). The surface charge of anionic delivery systems can be simply shifted to neutral by surface coating with PEG copolymer (231). Additionally, cationic NPs can also escape from lysosomal compartment after the internalization process, exhibiting perinuclear localization, whereas anionic or neutral particles are preferentially accumulated at lysosomes (232). However, NPs positively or negatively charged adsorb proteins present in the biological medium at higher extent than neutral carriers (233). Moreover, as reported by Albanese *et al*. (2012)**,** the binding of charged NPs to a lipid bilayer can induce alterations, local gelation (anionic particles) or fluidity (cationic particles) in cell membranes, being responsible for some toxicity and adjustments on normal cell metabolism (234).

Considering the main strategy of the present study to deliver HIV-1 antigenic peptides encapsulated into biodegradable and biocompatible nanocarriers that will target *in vivo* the professional antigen-presenting cells, namely DCs, polymeric NPs presenting ideal properties related to size, surface charge and morphology were successfully produced by a modified double emulsion-solvent evaporation method (190) using both polymers PLGA and PLGA-PEG. A model antigen was entrapped in those NPs to characterize NP physicochemical properties and optimize formulation procedure.

Actually, with the exception of PLGA_PL unstable formulation, all formulated NPs analyzed by DLS and LDE, presented a mean hydrodynamic diameter less than 200 nm, ranging between 170 and 187 nm, as well as a slightly negative surface charge, close to neutrality, with zeta potential values ranging from -1.22 to -3.27 mV (Table 2 and 3). Moreover, the monodispersity of this nanoparticulate population was proved by lower PdI values, which were smaller than 0.15. In addition, it was also proved the high reproducibility of NP formulation method, observing the low SD obtained. The stability inherent to this nano-emulsion that ultimately lead to solid NPs, is principally evidenced by the absence of the flocculation phenomenon, naturally prevented by the steric stabilization of the sub-micrometric droplet size (235). AFM analysis for PLGA_PVA formulation (Figure 3) revealed a homogeneous population of NPs with spherical shape and a mean size close to 170 m, corroborating DLS results. Surface morphology was shown to be smooth for plain NPs. On the other hand, OVA-loaded NPs presented a slight roughness surface, which is thought to be due to the presence of antigen adsorbed onto NP surface that is supported by the modest amount of non-entrapped OVA detected in the supernatants. Adsorbed molecules onto NP surface have been shown to

be responsible for the non-desired burst release effect of antigens from NPs, corresponding to the initially increased release rate. This phenomenon was reported for PLGA-based NPs and is caused by the high hydrophobicity of this polymer associated with highly hydrophilic entrapped molecules, being closely related to the lost of efficacy when cargo attains the target site (236). Regarding antigen entrapment, NPs were prepared in the absence of antigen (plain NPs), to be used as control for antigen-loaded nanocarrier composed by the different biomaterials under evaluation. The formulation process was shown to be antigen-independent, maintaining the stability of NPs when OVA was previously dissolved in the internal aqueous phase, since no statistically significant differences were observed ($p > 0.05$) between Z-Ave values obtained for OVA-loaded and plain NPs. As previously mentioned, different surfactants and polymers were tested as stabilizers in internal and external phases. The IP was modified by the addition of a water soluble Cs (GCs) to promote antigen entrapment. In addition, two different surfactants, 0.25 % (w/v) PVA and 0.125 % (w/v) PL solutions, were tested as EP in order to achieve the best stability and physicochemical characteristics suitable for antigen delivery. Previously optimized in our lab, PL and PVA concentrations had to be modified in order to obtain a highly stable formulation, inferred namely through their particulate size distribution and surface charge. The concentration of both polymers happened to be very different which was expected due to their distinct molecular weight, nature and consequent distinct physicochemical characteristics. Results obtained did not shown statistically significant differences ($p > 0.05$) between the different biopolymers used for particle formulation. This fact supports previous findings (215), by indicating that the stability of nanoparticulate formulations seems not to be affected by the chemical structure/composition of either internal or external phases. The yield percentage was however significantly higher (~ 75 % (w/w)) for formulations prepared with GCs at the internal phase than the others stabilized by both surfactants (~ 50 % (w/w)).

After the physicochemical characterization of the nanoparticulate systems formulated in this research project, it is possible to postulate that the developed modified double emulsion method was highly reproducible and that the resultant particles constitute promising antigens delivery systems. As a result and according to the previously mentioned advantages of PEGylation *in vivo*, PLGA-PEG polymer was selected to proceed with the experimental work and thus to entrap HIV-1 peptides, T20 and T1249. It is important to highlight that, to the best of our knowledge, this is the first

time that these HIV-1 peptides have been associated to a particulate delivery system. These NPs have been prepared following the same formulation method and testing the biomaterials previously used for OVA-loaded PLGA-PEG NPs. Moreover, HIV-1 peptides were entrapped individually or co-entrapped into NPs to evaluate a potential synergistic effect between both immunogens, due to their delivery to a single immune cell. As expected, all HIV-1 antigen-loaded PLGA-PEG NPs presented a mean hydrodynamic diameter close to 170 nm (ranging from 163-178 nm), a surface charge close to neutrality (ranging from -1.17 to -2.36 mV) and a PdI below 0.1 (Table 5). Although statistical differences were observed between size and zeta potential ($p < 0.05$) of HIV-1 antigen-loaded NPs and plain or OVA-loaded nanocarriers, HIV peptide-loaded NPs proved to be stable and not affected by the type of HIV-1 antigen entrapped or the nature of both internal and external aqueous phases ($p > 0.05$). Moreover, preliminary stability studies showed that formulations entrapping HIV-1 antigens remained physicochemically unaltered for one month (Table 6), but additional studies should be performed following International Conference Guidelines (ICH) stability testing guidelines Q1A (237). Even though, the low SD values obtained for size biodistribution and surface charge (Z-Ave, PdI and ZP) of developed HIV-1 peptide-loaded nanocarriers indicate that their production method is highly reproducible. In addition, their physicochemical properties evidence their potential extensive uptake by DCs, entrapped antigen delivery, as well as ability to be transported through the lymphatic system, reaching the lymph nodes, where a high number of DCs are found, after peripheral injection.

5.3. Antigen loading analysis

The administration of proteins or peptides alone has presented real pitfalls as their limited oral bioavailability, due to epithelial barriers of the gastrointestinal tract, their gastrointestinal degradation by digestive enzymes, their short half-life *in vivo* and their non-diffusion across some biological barriers. Moreover, their rapid degradation and elimination supports the need for repeated injections through invasive routes, such as subcutaneous, to attain effective levels (238). To overcome these concerns, the encapsulation of proteins and peptides in NPs has arisen as a promising tool, contributing with additional benefits such as the protection of proteins against enzymatic and hydrolytic degradation *in vivo*, the maintenance of their integrity and

activity, the improvement of their bioavailability and the target of specific organs, cell or even subcellular organelles for cargo delivery. Moreover, antigens can be loaded into NPs by two different methods: (1) the incorporation of antigen into NPs, during the production method and (2) the adsorption of antigen onto NP surface, after their formulation. Studies for delivery of vaccines for HIV using polymeric NPs have relied in both methods (99, 239). As explained before, in the experimental work under discussion, the antigens OVA (model antigen) and HIV-1 peptides were entrapped into polymeric NPs during the formulation process. The loading analysis was performed indirectly by determining the EE, (% (w/w)) and LC (μg/mg) of NPs through the quantification of the amount of antigen that remained dissolved in the supernatants collected during the three washing and centrifugation steps. Indeed, ultracentrifugation is classified as the most appropriate way to separate NPs from non entrapped antigens. High EE (percentage of loaded amount of entrapped antigen relative to the total amount used in NP formulation) and LC (loaded amount of entrapped antigen per total amount of polymer) are need to allow low number of administrations but also to obtain nanoparticulate suspensions presenting low viscosity, which is important to have in consideration specially when the vaccine is intended to be administered through a parenteral route. However, unlike high EE, the poor loading of drugs (around 1 %, meaning that NPs are carrying 1 mg of active molecule per 100 mg polymer) have been reported for PLGA-based NPs (236).

For model antigen, OVA, EE and LC were determined by MicroBCA™ protein assay and HPLC method. MicroBCA™ protein assay is based on the determination of total protein concentration which is revealed by a proportional color change from green to purple and measured at 560 nm using a colorimetric technique, according to manufacturer instructions. Indeed, the MicroBCA™ assay is based on the detection of Cu^{+} by bicinchoninic acid (BCA), after the reduction of Cu^{2+} by protein in alkaline conditions (240). The quantification of the protein present in supernatants is attained by the use of a standard calibration curve prepared using the same protein used in NP formulation. The HPLC method has been widely reported for the isolation and quantification of proteins or peptides of interest (241) and was applied in this study using a size-exclusion column for OVA isolation. The presence of this protein in supernatants was detected at 220 nm by spectrophotometric analysis, after 8-9 min of run. The supernatants of plain NPs were used as controls. Significantly higher EE and LC values were obtained using both methods, for all PLGA and PLGA-PEG NPs (Table

4). However, HPLC method reached the highest results (EE: 84-93 % (w/w); LC: 21-23 μg/mg) against the MicroBCA™ determination (EE: 41-64 % (w/w); LC: 10-16 μg/mg). The loading parameters appear to be independent of the presence of PEG polymer in PLGA polymeric chains, since no statistically significant differences were seen ($p > 0.05$) for EE (% (w/w)) and LC (μg/mg) obtained for PLGA-PEG and PLGA NPs correspondent NPs. Likewise, the surfactant present in the external aqueous phase, PVA or PL, did not affect antigen entrapment by PEGylated and non-PEGylated NPs. Unlike, higher values of EE (~ 63 % (w/w)) and LC (~ 16 μg/mg) were observed for formulations that used GCs in internal aqueous phase in comparison with formulations stabilized by PVA surfactant (PVA and PL formulations), which presented an EE in the range of 42-53 % (w/w) and LC ranging from 10 to 13 μg/mg, analyzed by MicroBCA™. Thus, EE (% (w/w)) and LC (μg/mg) were shown to be dependent on the internal aqueous phase composition, having statistical significance ($p < 0.05$). These results also suggested that Cs interfere with the antigen entrapment in PLGA and PLGA-PEG NPs, increasing the capacity of NPs to entrap higher amounts of antigen. Curiously, the loading analysis for PLGA-PEG_GCs obtained using HPLC method has also shown to be dependent on the internal phase, but in reverse order. Formulations developed using only PVA as an internal aqueous phase stabilizer presented higher values for EE (91-92 % (w/w)) and LC (23 μg/mg) than the correspondent formulation that also contained GCs in this primary emulsion phase (EE: 84 % (w/w); LC: 21 μg/mg). Besides being less expensive and a rapid process, not requiring higher sample or mobile phase volumes, MicroBCA™ protein assay is less sensitive than HPLC method. Moreover, MicroBCA™ solution can interfere with several substances, as chelating agents and strong acids or bases, which are commonly present in the supernatants obtained from NP formulation process (242).

The EE (% (w/w)) and LC (μg/mg) were also indirectly quantified for HIV-1 antigens entrapped into PLGA-PEG NPs, by intrinsic fluorescence assay of aminoacid residues present into peptides T20 and T1249 structures. Fluorescence is described as the photon emission by molecules, after being transiently stimulated to a higher excitation state, with radiant energy from an outside source. The release of the adsorbed energy as a fluorescent photon happen during the process of energy collapse, where the excited electron return to its initial ground state, almost immediately after its excitation (243). The molecules able to fluorescing are called fluorophores, being proteins and peptides included. Into proteins and peptides, tryptophan, tyrosine and phenylalanine

residues are accepted as intrinsic fluorophores that can emit fluorescence. Specifically, tryptophan, tyrosine and phenylalanine residues present a maximum wavelength (λ_{max}) of absorption/excitation at 280, 274 and 257 nm and emission at 348, 303 and 282 nm, respectively. However, tryptophan and tyrosine can be simultaneously excited at 280 nm. In addition, tryptophan is an excellent probe to distinguish native and unfolded proteins because it is very sensitive to the polarity of surrounded environment (244).

In general, higher EE (~ 78 % (w/w)) and LC (~ 15 μg/mg) values were observed for the entrapment or co-entrapment of HIV-1 peptides into PLGA-PEG NPs (Table 7). However, the loading parameters were shown to be dependent on the internal and external aqueous phases composition. When PVA was used as external phase stabilizer, instead of PL, in formulation process, higher EE (% (w/w)) and LC (μg/mg) were obtained, presenting values that varied between 78-93 % (w/w) for EE and 16-19 μg/mg for LC. Unlike, when GCs is included in the internal phase, NPs were able to entrap higher amounts of antigens (EE: 83-93 % (w/w); LC: 17-19 μg/mg) than those prepared using only PVA (EE: 48-86 % (w/w); LC: 10-17 μg/mg). Indeed, statistically significant differences have been observed for EE (% (w/w)) and LC (μg/mg), when different NPs stabilized by distinct external or internal phases are compared with each other for each entrapped HIV-1 antigen ($p < 0.05$). Moreover, the best results accomplished for loading parameters were obtained with the co-entrapment of T20 and T1249 peptides into PLGA-PEG_GCs NPs (EE: 93 % (w/w) and LC: 19 μg/mg). It is still important to refer that all results were obtained in triplicate from three isolated assays. Giving credibility to previous results, Wang *et al.* (2008) reported a LC of γ-PGA NPs (~ 200 nm) entrapping the recombinant HIV-1 p24 of 25 μg/mg, which was determined by the Lowry method (245). In addition, Himeno *et al*. (2010) also quantified the amount of encapsulated recombinant HIV-1 gp120 into γ-hPG (γ-PG-*graft*-Phe) NPs (200 nm) as 10 μg per mg NP, by the previous reported method (99).

5.4. Cytotoxic effect of nanoparticles

Long-term *in vitro* cytotoxicity experiments were designed to determine whether any of the components used for the production of PLGA-PEG NPs compromised the viability of murine immature BMDCs. Indeed, BMDCs were incubated with crescent concentrations (0.125-1 mg/mL) of PLGA-PEG_plain NPs (PLGA-PEG_PVA, PLGA-PEG_GCs and PLGA-PEG_PL), and their viability was quantified by AlamarBlue® assay after 24, 48 and 72 h of incubation. This bioassay allows inferring about the

cytotoxicity of substances within several chemical classes, measuring quantitatively the cellular proliferation based on the detection of mitochondrial dehyrogenase metabolic activity. In response to chemical reduction of growth medium resulting from cell growth, the fluorescent/colorimetric redox indicator incorporated into AlamarBlue® reagent changes its color from oxidized (non-fluorescent, blue) to reduced (fluorescent, pink) form. AlamarBlue® assay presents several advantages against MTT (thiazolyl blue tetrazolium bromide) assay such as i) its solubility in water, not requiring extraction steps; ii) stability allowing the continuous cell growth monitoring; iii) non-toxicity to cells, not interfering with normal metabolism and not compromising technician health. Moreover, AlamarBlue® reagent can be reduced by $FMNH_2$, FADHs, NADH, NADPH (higher reducing power) and cytochromes (lower reducing power) unlike the MTT reagent which cannot be reduced by the latter (246).

Quantification of cellular proliferation was performed by spectrophotometric analysis, monitoring absorbance at 570 nm (reduced/pink) and 600 nm (oxidized/blue). Triton X-100 and PBS were used as positive and negative controls, respectively. Cell viability (%) was normalized for negative control, PBS (100 %). All PLGA-PEG_plain formulations did not show long-term toxicity to BMBCs over the 72 hours time period (Figure 4). Moreover, cell viability was close to 100 %, analogous to the negative control PBS, for the lowest (0.125 mg/mL) to the highest (1 mg/mL) NP concentration, after 72 h of incubation. The AlamarBlue® assay did not shown any statistically significant effect ($p > 0.05$) on cell viability between the distinct formulation components used in external (PVA or PL) and internal (PVA or GCs) aqueous phases, for all tested concentrations and incubation periods, comparing to negative control (PBS). On the other hand, and as expected, a decrease on cell viability of 20 % was observed for cells treated with 0.05 % (v/v) Triton X-100, employed as positive control, being observed statistically significant differences ($p < 0.001$; one-way ANOVA and Turkey's post test) in the values obtained for all tested formulations and cell incubated with negative control.

These results support the fact that no toxic residues from the organic solvent (DCM) used in the formulation process remains in NPs, being completely evaporated after 1 hour of evaporation phase. The AlamarBlue® assay also confirmed that the different components used in internal or external aqueous phases during the formulation development allow the preparation of stable and non-toxic NPs. Moreover, these results also suggest that PVA has been completely washed through washing and centrifugation

steps, not reducing thus the safety of NPs. The results confirmed the statement that PLGA-PEG is biocompatible. However, the PEGylation of polymer might have also contributed to the absence of cytotoxicity due to its higher hydrophilicity and non-toxicity, also promoting NP biocompatibility (203).

According to the previous results obtained for PLGA-PEG formulation using GCs on internal aqueous phase, such as high EE (% (w/w)) and LC (µg/mg) and non-toxic effect, these specific NPs were used in the following studies.

5.5. Peptide integrity evaluation

The maintenance of integrity and antigenicity of proteins and peptides entrapped into NPs represents an essential feature on their bioavailability and ability to induce effective immune responses. Particularly, the encapsulation of proteins into PLGA particles or other polymeric release systems by the emulsion solvent evaporation method has presented some negative aspects. Instability problems of entrapped proteins and peptides due to the contact with organic solvents and the use of high-shear devices remain a challenge (247). Indeed, the formation of a water/organic solvent interface in the first step of the double emulsion procedure has been recognized as a major destabilizing factor for proteins, resulting in their interfacial adsorption onto the hydrophobic polymer, followed by protein denaturation and aggregation. Moreover, the protein unfolding can be easily achieved via shear stress caused by temperature extremes, with the use of sonicators or homogenizers predominantly during the formation of the primary emulsion (248). Additionally, protein denaturation or aggregation may induce undesired side effects, such as immunogenicity or toxicity beyond its therapeutic inactivity (249). To solve these problems, research community has been focused in the optimization of the formulation process, in order to improve protein stability. The use of organic solvents less hydrophobic (250) and several stabilizer agents (251), the reduction of sonication time (252) as well as higher solvent evaporation rates (213) have been reported to reduce the risk of degradation of particle payload.

The integrity of HIV-peptides, T20 and T1249, entrapped individually or co-entrapped into PLGA-PEG_GCs NPs was evaluated by SDS-PAGE (16 % resolving gel). The PAGE method is used to separate proteins or peptides according to their charge, size and shape, in response to an electrical field via pores present in the gel matrix. Moreover, under denaturing conditions, protein sample is treated with SDS and

β-mercaptoethanol, attaining a primary structure charged negatively and the reduction of disulfide bonds formed by cysteines, respectively. Then, proteins will be separated electrophoretically moving through the polyacrylamide gel matrix toward the anode, according to their molecular weight (253, 254). In this assay, it was possible to see (Figure 5) that all antigens extracted from the different HIV-1 peptides-loaded NPs (PLGA-PEG_GCs_T1249, PLGA-PEG_GCs_T20 and PLGA PEG_GCs_T20_T1249) presented a similar pattern of migration, showing an unique band correspondent to HIV-1 peptides, T20 and T1249 (Mw ~ 5 kDa), below the lower limit of the molecular weight marker (10 kDa). Moreover, these migration patterns were identical to those obtained for positive controls, T20 and T1249 standard solution (0.75 mg/mL), which is supposed to present a single band at the Mw ~ 5 kDa. These similar patterns of migration and the absence of additional bands, suggestive of peptide fragmentation, indicated that HIV-1 antigens entrapped into PLGA-PEG_GCs NPs are not structurally affected by the double emulsion procedure, remaining intact. In addition, these observations were corroborated by the absence of the same band in the negative control, composed by PLGA-PEG_GCs_plain NPs.

According to the obtained results, it can be inferred that the formulation procedure used in NP preparation did not affect the structural integrity and the stability of HIV-1 peptides, entrapped individually or co-entrapped. However, nothing about the antigenicity of peptides was possible to conclude. Western blotting techniques could be performed in the future to provide this information.

5.6. Uptake and intracellular trafficking of nanoparticles

To verify if formulated NPs were internalized and to characterize their intracellular trafficking, BMDCs were incubated for 1, 5 and 20 h with fluorescent PLGA-PEG_GCs_plain NPs, due to the presence of Rho-grafted PLGA. Moreover, anti-EEA1 and anti-calnexin Abs were added to BMDCs to stain early endosomes (MHC class I and II pathways) and endoplasmic reticulum (MHC class I pathway), respectively that were further visualized by confocal microscopy. The study of the intracellular traffic of these polymeric delivery systems is only undoubtedly attained if fluorophores-grafted polymers are used for NP preparation. In fact, probes covalently linked to polymeric surface constitute a better option than the entrapment of soluble probes into NPs, due to probe leakage and the resulting misinterpretation.

DCs have demonstrated preference to taken up smaller particles, as viral size particles, whereas larger particles, as those within bacterial size range, are preferentially ingested by macrophages (144). The formulated Rho-NPs, presenting mean diameters lower than 200 nm, were taken up by BMDCs and higher internalization levels were observed with increasing incubation time (Figure 6). Furthermore, distinct intracellular pathways were observed for Rho-labeled NPs. Following NPs uptake by DCs, the entrapped antigens can be processed by different pathways. NPs can be hydrolyzed into endolysosomes, where proteins are processed by lysosomal proteases into peptides. These specific peptides are loaded onto MHC class II molecules to be presented on cell surface for recognition by $CD4^+$ Th cells – a pathway involved in Th cell activation (255). In the meantime, some of the phagocytosed particles can follow the endolysosomal escape, being slowly hydrolyzed, releasing its cargo into the cytosol. Released proteins are degraded by the proteosomes into smaller peptides that will be subsequently translocated into the ER by the TAP. There, the complex formed by peptides loaded onto MHC class I molecules migrates to the cell surface to be recognize by $CD8^+$ Tc cells (phagosome-to-cytosol cross presentation pathway) – a pathway involved in CTL activation (256). Results suggest that the uptake of NPs showed to increase with increasing incubation time, presenting high values of particle uptake after 5 and 20 h of incubation. The slow attainment of endolysosomes, with most of NPs are colocalized around the cell membrane after 1 h of incubation, may be due to the PEGylated surface of NPs, providing delayed NP recognition and uptake by targeted cells (203, 257). This delay in the uptake may however provide effective immune responses due to a longer exposition of antigen. Moreover, the significant colocalization levels (50 to 60 %) with early endosome protein marker EEA1 support the hypothesis that this nanocarrier can travel mainly through endolysosomal vesicles pathway, inducing the antigen presentation on cell surface via MHC class II molecules to $CD4^+$ Th cells. In addition, the high colocalization levels (50 to 70 %) with the ER protein marker calnexin confirmed the suspicion that cross-presentation of antigens to $CD8^+$ cells via MHC class I molecules was also achieved. The concrete mechanism of endolysosomal escape is not clear, although two mechanisms are proposed for PLGA-based NPs. The first mechanism is based on the pH change via acidification of PLGA NPs into endosomes, through the formation of hydrogen bonds between hydronium ions and carboxyl groups of lactic (pKa 3.1) and glycolic (pKa 3.8) acids, which leads to the alteration of PLGA surface charge, from negative in neutral pH to positive in acidic pH.

This phenomenon results in the local interaction between positively charged NPs and negatively charged endosomal membranes and allow the release of NPs into the cytoplasm (200). Otherwise, the osmotic pressure can be increased due to the influx of hydronium and chloride ions during endosomal acidification, leading to the rupture of the endosomal membrane and release of its content in the cytoplasm (258). Additionally, the decrease of colocalization levels of NPs with early endosomes from 5 to 20 h after incubation can suggest the escape of NPs from these vesicles, their acumulation in the cytosol and the prolonged release of entrapped antigens over time, suggesting the potential use of these NPs as a single-dose vaccine.

These observations propose that the developed HIV-1-loaded NPs are in fact promising vaccine delivery systems to present antigens by MHC class I and II pathways, promoting a complete and harmonized immune response.

6. Conclusions and Future Prospects

The main goal of the present study is the development and characterization of a prophylactic vaccine for HIV-1, possibly also with immunotherapeutic application, using biodegradable and biocompatible polymeric NPs to deliver HIV-1 antigenic peptides. These studies will allow the selection of most promising delivery systems to *in vivo* target DCs, which are professional APCs of the immune system able to capture antigens and initiate coordinated innate and adaptative immune responses.

During this year, PLGA and PLGA-PEG NPs were primarily prepared and optimized using the model antigen OVA. The physicochemical properties of these nanocarriers were further evaluated, namely through the assessment of their mean size distribution, surface charge and morphology, EE and LC. The composition of internal and external aqueous phases was varied by the addition different biopolymers as GCs and PVA or PL, in order to achieve the best antigen entrapment and formulation stability, respectively. Overall, except for the PLGA_PL unstable formulation, the results demonstrated that the nanocarriers presented ideal size and surface charge for cellular uptake, and high EE and LC, values. Moreover, NP stability was shown to be independent from the composition of both internal and external phases. Taking into account the high reproducibility obtained using the modified double emulsion method to prepare these promising antigens-loaded nanocarriers and the advantages of PEGylation *in vivo*, HIV-1 peptides (T20 and T1249) were further entrapped individually or in association into PLGA-PEG NPs, using the same methodology and varying the internal and external aqueous phase, as reported above. The physicochemical characterization (Z-Ave, PdI and ZP) has shown that HIV-1 peptide-loaded nanocarriers are highly reproducible and present physicochemical properties adequate for an extensive uptake by DCs, promoting antigen recognition, processing and presentation. Moreover, the highest values for EE (% (w/w)) and LC (µg/mg) were obtained when PVA and GCs are used in external and internal phase, respectively. In addition, no toxic effect on targeted DCs was observed for all formulations tested for HIV-1 antigens entrapment, during 72 h of incubation.

Considering all the referred results, the PLGA-PEG nanocarriers prepared using GCs and PVA on internal and external aqueous phase, respectively, were recognized as the most promising system, being thus selected for following studies. Fluorescent PLGA-PEG_GCs_plain NPs formulated with Rho-grafted PLGA were internalized by

DCs and have been shown to follow distinct intracellular pathways: i) endolysosomal pathway for the antigen presentation on cell surface via MHC class II molecules to $CD4^+$ cells and ii) cross-presentation pathway via ER for the antigen presentation on cell surface to $CD8^+$ cells via MHC class I molecules. Furthermore, the HIV-1 antigens entrapped or co-entrapped into PLGA-PEG_GCs NPs remained intact and stable, not being affected structurally by the formulation procedure.

These observations suggest that the PLGA-PEG_GCs NPs constitute a promising platform for the delivery of HIV-1 antigens to DCs acting as vaccine delivery systems to promote an efficient immune response.

In the future, different experiments are needed to confirm the potential of this formulation and therefore to achieve a long-awaited vaccine against HIV-1.

6.1. Evaluation of peptide antigenicity by Imunoblotting

In order to confirm the maintenance of the antigenicity or activity of entrapped HIV-1 peptides into PLGA-PEG_GCs NPs, a western blotting assay should be performed. Primarily, HIV-1 peptide samples will be separated by SDS-PAGE using the process described in Materials and Methods section for the evaluation of peptide integrity. In addition, peptides negatively charged will be transferred and immobilized on nitrocellulose membrane positively charged. The membrane will be incubated with primary antibody which will bind to the peptide, forming the complex antibody-peptide. Thereafter, a conjugated secondary antibody (antibody-enzyme) will be used to bind to primary antibody. Enzymes as alkaline phosphatase (AP) and peroxidase will function as a molecular signaling of complex primary antibody-peptide, allowing the visualization of detected peptide. An added chromogenic substrate will be degraded by secondary antibody-conjugated enzyme giving an insoluble precipitate colocalized with the primary antibody bounded to the peptide.

6.2. Cellular uptake and intracellular trafficking studies of peptide-loaded NPs

The cellular uptake of peptide-loaded NPs prepared by w/o/w method and the intracellular trafficking and fate of NPs and peptides separately inside murine immature BMDCs will be assessed by flow cytometry and confocal microscopy. For this purpose, NPs and HIV-1 antigens will be labeled with different fluorescent probes.

6.2.1. Flow cytometry analysis

BMDCs will be seeded in plates and incubated overnight to allow cell attachment. After old medium removal, fluorescent PLGA_PEG_GCs NPs in fresh medium will be added in triplicates and incubated for 1, 5 and 20 h. Negative and positive controls will be composed by cells in medium, without NPs, and fluorescent NPs, respectively. Thereafter, medium will be removed, wells washed and cells harvested by trypsinization and centrifuged. Finally, cells will be resuspended in flow cytometry buffer and stored at 4 ºC until analysis. The percentage of fluorescent cells in the population will be measured using a flow cytometer.

6.2.2. Confocal microscopy imaging analysis

The procedure will be similar to that reported previously in the section Materials and Methods. BMDCs will be seeded on coverslips previously covered with PLL, and incubated overnight, allowing cell attachment. Without removing the medium, fluorescent PLGA-PEG_GCs NPs with entrapped fluorescent HIV-1 peptides will be added to cells and incubated for 1, 5 and 20 h. After incubation, cells will be washed, fixed and lastly permeabilized for antibody staining. Moreover, a blocking solution will also be used to prevent antibody unspecific binding. Cells will be stained with primary rabbit anti-mouse Abs, anti-EEA1 for early endosomes, anti-Rab7a for early and late endosomes, anti-LAMP1 for late endosomes and lysosomes and anti-calnexin for ER, being then labeled with secondary goat anti-rabbit antibody. Cell plasma membrane and nucleus will be also labeled. Finally, confocal microscopy preparations will be assembled and analyzed. The co-localization of fluorescent NPs or peptides with fluorescent organelles will evidence their intracellular location.

6.3. Study of endocytic pathways involved in NPs internalization

BMDCs will be seeded in plates for flow cytometry and confocal microscopy analysis. After cellular incubation with one of the following molecules: cytochalasin D, rottlerin, chlorpromazine, dynasore, genistein, nystatin and sucrose, NPs will be added for 1, 5 or 20 h at 37 °C. Analyses will be performed by confocal microscopy or flow cytometry as described. After treatment of BMDCs with the inhibitors, OVA Alexa Fluor® 647 will be used as control for clathrin-mediated endocytosis.

6.4. *In vivo* assay testing HIV-1 prophylactic effect

Animals will be allowed to acclimate to the new environment for 1 week prior vaccination. Female 4-6 weeks old BALB/c mice (n = 5/group) will be subcutaneously (s.c.) immunized on day 1 and boosted twice at days 14 and 28, with 100 µL of 10 µg of T20 and/or T1249 dissolved in saline, entrapped or co-entrapped into PLGA-PEG_GCs nanospheres, or admixed with CpG adjuvant (10 µg). Tail vein blood samples will be collected at day 0 prior immunization and at days 7, 21, and 43 after immunization, and spleens isolated at the end of the experiment for immunological assays. Serum will be prepared from clotted blood and stored at -20 ºC until analysis (190).

6.4.1. Serology

The presence of antigen specific antibodies (IgG, IgG1 and IgG2a) in sera and at mucosal (IgA, IgG) vaginal and lung lavages will be searched by Enzyme Linked Immunosorbent Assay (ELISA) on mice samples tested individually.

6.4.2. Cytokines assays

Spleens will be removed at the end of the experiment and cell homogenisates be prepared. Supernatants will be used for the quantification of secreted Th1/Th2 cytokines (IL-2, IL-4, IL-5, IL-6, IL- 10, TNF-α and IFN-γ) using an ELISA kit.

6.5. Antibody reactivity against HIV-1 peptides

ELISA plates will be coated overnight with recombinant HIV-1 peptides, T20 and T1249. Plates will be washed with ELISA-washing buffer and blocking solution. Mice antiserum will be added to the microplates and incubated for 1 h at room temperature. After another wash, AP-conjugated goat anti-mouse IgG or IgA will be added as a secondary antibody, for 1h at 37 ºC. After a final washing step, a colorimetric reaction is developed with the addition of p-nitrophenylphosphate (pNPP) substrate and read at 405 nm on a microplate reader. Negative and positive controls will be serum from pre-immune mice and from HIV-1-infected individuals, respectively. In this case, the secondary antibody will be AP-conjugated anti-human IgG or IgA (193).

6.6. Neutralizing assay

Primary virus isolates will be obtained from HIV-1-infected Portuguese patients. A single-round viral infectivity assay will be performed using a luciferase reporter gene assay to assess the neutralizing activity of mice serum against HIV-1 primary isolates. Cells will be added to culture plates overnight in complete growth medium, allowing their attachment before the addition of serum and virus dilutions. Thereafter, a mixing of heat-inactivated mice sera with virus will be incubated with cells for 1 h at 37°C. After culture medium removal from each well, cells will be lysed directly in the plate with One-Glow luciferase assay substrate reagent. Plates will be immediately analyzed for luciferase activity on a luminometer, using target cells and medium as controls. Virus neutralization titer is defined by the maximal dilution of plasma required to decrease virus production by 50 % two days after infection and is exhibited as the percent inhibition of viral infection (luciferase activity) at each serum dilution: % inhibition = [1 – (luciferase serum samples/luciferase without serum samples)] x 100 (193).

6.7. Lyophilization process optimization and NPs stability studies

Lyophilization process will be optimized in order to evaluate the stability of those antigen-entrapped NPs. For this purpose, different lyoprotectants at different proportions and cycles of lyophilization should be tested. The optimization of this procedure will be guided by Differential Scanning Calorimetry, which is a thermal analyze methodology that will for example allow the prevention of collapse, consequence of high temperatures, through the previous determination of glass transition temperature and collapse temperature. Moreover, the stability of NPs with entrapped or co-entrapped HIV-1 antigens (T20 and T1249) should be assess for at least six months, measuring physicochemical parameters (Z-Ave, PdI and ZP) as well as their EE (% (w/w)) and LC (µg/mL), month after month (237).

7. References

1. Gallo RC, Montagnier L. The chronology of AIDS research. Nature. 1986;326(6112):435-6.
2. Stover J, Bollinger L. The economic impact of AIDS. The Policy Project Manuscript. 1999.
3. UNAIDS W. Report on the global AIDS epidemic. Global Summary. 2008.
4. Levy JA. HIV and the Pathogenesis of AIDS: ASM press Washington, DC, USA:; 2007.
5. Haseltine WA. Molecular biology of the human immunodeficiency virus type 1. The FASEB journal. 1991;5(10):2349-60.
6. Reeves JD, Gallo SA, Ahmad N, Miamidian JL, Harvey PE, Sharron M, et al. Sensitivity of HIV-1 to entry inhibitors correlates with envelope/coreceptor affinity, receptor density, and fusion kinetics. Proceedings of the National Academy of Sciences. 2002;99(25):16249-54.
7. Bour S, Strebel K. HIV accessory proteins: multifunctional components of a complex system. Advances in pharmacology. 2000;48:75-120.
8. Thomson MM, Nájera R. Molecular epidemiology of HIV-1 variants in the global AIDS pandemic: an update. AIDS Rev. 2005;7(4):210-24.
9. de Silva TI, Cotten M, Rowland-Jones SL. HIV-2: the forgotten AIDS virus. Trends in microbiology. 2008;16(12):588-95.
10. Teixeira C, Gomes JR, Gomes P, Maurel F. Viral surface glycoproteins, gp120 and gp41, as potential drug targets against HIV-1: brief overview one quarter of a century past the approval of zidovudine, the first anti-retroviral drug. European journal of medicinal chemistry. 2011;46(4):979-92.
11. Borrego P, Calado R, Marcelino JM, Pereira P, Quintas A, Barroso H, et al. An ancestral HIV-2/simian immunodeficiency virus peptide with potent HIV-1 and HIV-2 fusion inhibitor activity. AIDS. 2013;27(7):1081-90.
12. Haase A. Population biology of HIV-1 infection: viral and CD4+ T cell demographics and dynamics in lymphatic tissues. Annual review of immunology. 1999;17(1):625-56.
13. Eckert DM, Kim PS. Mechanisms of viral membrane fusion and its inhibition. Annual review of biochemistry. 2001;70(1):777-810.
14. Rizzuto CD, Wyatt R, Hernández-Ramos N, Sun Y, Kwong PD, Hendrickson WA, et al. A conserved HIV gp120 glycoprotein structure involved in chemokine receptor binding. Science. 1998;280(5371):1949-53.
15. Cooley LA, Lewin SR. HIV-1 cell entry and advances in viral entry inhibitor therapy. Journal of clinical virology. 2003;26(2):121-32.
16. Doms RW, Moore JP. HIV-1 Membrane Fusion Targets of Opportunity. The Journal of cell biology. 2000;151(2):F9-F14.
17. Weissenhorn W, Dessen A, Harrison S, Skehel J, Wiley D. Atomic structure of the ectodomain from HIV-1 gp41. Nature. 1997;387(6631):426-30.
18. Chan DC, Fass D, Berger JM, Kim PS. Core structure of gp41 from the HIV envelope glycoprotein. Cell. 1997;89(2):263-73.
19. Jiang S, Debnath AK. Development of HIV entry inhibitors targeted to the coiled-coil regions of gp41. Biochemical and biophysical research communications. 2000;269(3):641-6.
20. Götte M, Li X, Wainberg MA. HIV-1 reverse transcription: A brief overview focused on structure–function relationships among molecules involved in initiation of the reaction. Archives of biochemistry and biophysics. 1999;365(2):199-210.
21. Farnet CM, Haseltine WA. Determination of viral proteins present in the human immunodeficiency virus type 1 preintegration complex. Journal of virology. 1991;65(4):1910-5.
22. Sierra S, Kupfer B, Kaiser R. Basics of the virology of HIV-1 and its replication. Journal of clinical virology. 2005;34(4):233-44.
23. Jaffe HW, Bregman DJ, Selik RM. Acquired immune deficiency syndrome in the United States: the first 1,000 cases. Journal of Infectious Diseases. 1983;148(2):339-45.
24. Levy JA. HIV pathogenesis: 25 years of progress and persistent challenges. Aids. 2009;23(2):147-60.

25. Collins KB, Patterson BK, Naus GJ, Landers DV, Gupta P. Development of an in vitro organ culture model to study transmission of HIV-1 in the female genital tract. Nature medicine. 2000;6(4):475-9.
26. Miller CJ, Shattock RJ. Target cells in vaginal HIV transmission. Microbes and infection. 2003;5(1):59-67.
27. Geijtenbeek TB, Kwon DS, Torensma R, van Vliet SJ, van Duijnhoven GC, Middel J, et al. DC-SIGN, a Dendritic Cell–Specific HIV-1-Binding Protein that Enhances< i> trans</i>-Infection of T Cells. cell. 2000;100(5):587-97.
28. Wilkinson J, Cunningham AL. Mucosal transmission of HIV-1: first stop dendritic cells. Current drug targets. 2006;7(12):1563-9.
29. Soto-Ramirez LE, Renjifo B, McLane MF, Marlink R, O'Hara C, Sutthent R, et al. HIV-1 Langerhans' cell tropism associated with heterosexual transmission of HIV. Science. 1996;271(5253):1291-3.
30. Lackner AA, Veazey RS. Current concepts in AIDS pathogenesis: insights from the SIV/macaque model. Annu Rev Med. 2007;58:461-76.
31. Gupta P, Balachandran R, Ho M, Enrico A, Rinaldo C. Cell-to-cell transmission of human immunodeficiency virus type 1 in the presence of azidothymidine and neutralizing antibody. Journal of virology. 1989;63(5):2361-5.
32. Mothes W, Sherer NM, Jin J, Zhong P. Virus cell-to-cell transmission. Journal of virology. 2010;84(17):8360-8.
33. Jolly C, Kashefi K, Hollinshead M, Sattentau QJ. HIV-1 cell to cell transfer across an Env-induced, actin-dependent synapse. The Journal of experimental medicine. 2004;199(2):283-93.
34. Schiffner T, Sattentau QJ, Duncan CJ. Cell-to-cell spread of HIV-1 and evasion of neutralizing antibodies. Vaccine. 2013;31(49):5789-97.
35. McDonald D. Dendritic cells and HIV-1 trans-infection. Viruses. 2010;2(8):1704-17.
36. Mehandru S, Poles MA, Tenner-Racz K, Horowitz A, Hurley A, Hogan C, et al. Primary HIV-1 infection is associated with preferential depletion of CD4+ T lymphocytes from effector sites in the gastrointestinal tract. The Journal of experimental medicine. 2004;200(6):761-70.
37. Guadalupe M, Reay E, Sankaran S, Prindiville T, Flamm J, McNeil A, et al. Severe CD4+ T-cell depletion in gut lymphoid tissue during primary human immunodeficiency virus type 1 infection and substantial delay in restoration following highly active antiretroviral therapy. Journal of virology. 2003;77(21):11708-17.
38. Quinn TC, Wawer MJ, Sewankambo N, Serwadda D, Li C, Wabwire-Mangen F, et al. Viral load and heterosexual transmission of human immunodeficiency virus type 1. New England journal of medicine. 2000;342(13):921-9.
39. Pilcher CD, Eron JJ, Galvin S, Gay C, Cohen MS. Acute HIV revisited: new opportunities for treatment and prevention. The Journal of clinical investigation. 2004;113(113 (7)):937-45.
40. Brenchley JM, Price DA, Schacker TW, Asher TE, Silvestri G, Rao S, et al. Microbial translocation is a cause of systemic immune activation in chronic HIV infection. Nature medicine. 2006;12(12):1365-71.
41. Bluestone JA, Abbas AK. Natural versus adaptive regulatory T cells. Nature Reviews Immunology. 2003;3(3):253-7.
42. Card CM, McLaren PJ, Wachihi C, Kimani J, Plummer FA, Fowke KR. Decreased immune activation in resistance to HIV-1 infection is associated with an elevated frequency of CD4+ CD25+ FOXP3+ regulatory T cells. Journal of Infectious Diseases. 2009;199(9):1318-22.
43. Jiang Q, Zhang L, Wang R, Jeffrey J, Washburn ML, Brouwer D, et al. FoxP3+ CD4+ regulatory T cells play an important role in acute HIV-1 infection in humanized Rag2−/− γC−/− mice in vivo. Blood. 2008;112(7):2858-68.
44. Sempere JM, Soriano V, Benito JM. T regulatory cells and HIV infection. AIDS Rev. 2007;9(1):54-60.
45. Boettler T, Cunha-Neto E, Kalil J, von Herrath M. Can an immune-regulatory vaccine prevent HIV infection? 2012.
46. Pantaleo G, Fauci A. Immunopathogenesis of HIV infection. Annual review of microbiology. 1996;50(1):825-54.

47. Buchbinder S, Vittinghoff E. HIV-infected long-term nonprogressors: epidemiology, mechanisms of delayed progression, and clinical and research implications. Microbes and infection. 1999;1(13):1113-20.
48. Huang Y, Paxton WA, Wolinsky SM, Neumann AU, Zhang L, He T, et al. The role of a mutant CCR5 allele in HIV-1 transmission and disease progression. Nature medicine. 1996;2(11):1240-3.
49. Blankson JN, Persaud D, Siliciano RF. The challenge of viral reservoirs in HIV-1 infection. Annual review of medicine. 2002;53(1):557-93.
50. Venzke S, Keppler OT. Role of macrophages in HIV infection and persistence. 2006.
51. Schrager LK, D'Souza MP. Cellular and anatomical reservoirs of HIV-1 in patients receiving potent antiretroviral combination therapy. Jama. 1998;280(1):67-71.
52. Burton DR. Antibodies, viruses and vaccines. Nature Reviews Immunology. 2002;2(9):706-13.
53. Aasa-Chapman MM, Holuigue S, Aubin K, Wong M, Jones NA, Cornforth D, et al. Detection of antibody-dependent complement-mediated inactivation of both autologous and heterologous virus in primary human immunodeficiency virus type 1 infection. Journal of virology. 2005;79(5):2823-30.
54. Hessell AJ, Hangartner L, Hunter M, Havenith CE, Beurskens FJ, Bakker JM, et al. Fc receptor but not complement binding is important in antibody protection against HIV. Nature. 2007;449(7158):101-4.
55. Wei X, Decker JM, Wang S, Hui H, Kappes JC, Wu X, et al. Antibody neutralization and escape by HIV-1. Nature. 2003;422(6929):307-12.
56. Stamatatos L, Morris L, Burton DR, Mascola JR. Neutralizing antibodies generated during natural HIV-1 infection: good news for an HIV-1 vaccine? Nature medicine. 2009;15(8):866-70.
57. Rosenberg ES, Billingsley JM, Caliendo AM, Boswell SL, Sax PE, Kalams SA, et al. Vigorous HIV-1-specific CD4+ T cell responses associated with control of viremia. Science. 1997;278(5342):1447-50.
58. McMichael AJ, Rowland-Jones SL. Cellular immune responses to HIV. Nature. 2001;410(6831):980-7.
59. Almeida JR, Price DA, Papagno L, Arkoub ZA, Sauce D, Bornstein E, et al. Superior control of HIV-1 replication by CD8+ T cells is reflected by their avidity, polyfunctionality, and clonal turnover. The Journal of experimental medicine. 2007;204(10):2473-85.
60. Bernardin F, Kong D, Peddada L, Baxter-Lowe LA, Delwart E. Human immunodeficiency virus mutations during the first month of infection are preferentially found in known cytotoxic T-lymphocyte epitopes. Journal of virology. 2005;79(17):11523-8.
61. Lichterfeld M, Kaufmann DE, Xu GY, Mui SK, Addo MM, Johnston MN, et al. Loss of HIV-1–specific CD8+ T cell proliferation after acute HIV-1 infection and restoration by vaccine-induced HIV-1–specific CD4+ T cells. The Journal of experimental medicine. 2004;200(6):701-12.
62. Granich R, Crowley S, Vitoria M, Smyth C, Kahn JG, Bennett R, et al. Highly active antiretroviral treatment as prevention of HIV transmission: review of scientific evidence and update. Current Opinion in HIV and AIDS. 2010;5(4):298.
63. Yarchoan R, Broder S. Development of antiretroviral therapy for the acquired immunodeficiency syndrome and related disorders. A progress report. The New England journal of medicine. 1987;316(9):557-64.
64. Autran B, Carcelain G, Li TS, Blanc C, Mathez D, Tubiana R, et al. Positive effects of combined antiretroviral therapy on CD4+ T cell homeostasis and function in advanced HIV disease. Science. 1997;277(5322):112-6.
65. Carcelain G, Debré P, Autran B. Reconstitution of CD4+ T lymphocytes in HIV-infected individuals following antiretroviral therapy. Current opinion in immunology. 2001;13(4):483-8.
66. Friis-Moller N, Reiss P, Sabin CA, Weber R, Monforte A, El-Sadr W, et al. Class of antiretroviral drugs and the risk of myocardial infarction. New Engl J Med. 2007;356(17):1723-35.
67. Hawkins T. Understanding and managing the adverse effects of antiretroviral therapy. Antiviral research. 2010;85(1):201-9.
68. Aghokeng AF, Ayouba A, Mpoudi-Ngole E, Loul S, Liegeois F, Delaporte E, et al. Extensive survey on the prevalence and genetic diversity of SIVs in primate bushmeat provides insights into

risks for potential new cross-species transmissions. Infection, Genetics and Evolution. 2010;10(3):386-96.
69. Johnson VA, Brun-Vézinet F, Clotet B, Gunthard H, Kuritzkes DR, Pillay D, et al. Update of the drug resistance mutations in HIV-1: Spring 2008. Top HIV Med. 2008;16(1):62-8.
70. Rerks-Ngarm S, Pitisuttithum P, Nitayaphan S, Kaewkungwal J, Chiu J, Paris R, et al. Vaccination with ALVAC and AIDSVAX to prevent HIV-1 infection in Thailand. New England Journal of Medicine. 2009;361(23):2209-20.
71. Walker BD, Burton DR. Toward an AIDS vaccine. science. 2008;320(5877):760-4.
72. Douek DC, Kwong PD, Nabel GJ. The rational design of an AIDS vaccine. Cell. 2006;124(4):677-81.
73. Wijesundara DK, Jackson RJ, Ramshaw IA, Ranasinghe C. Human immunodeficiency virus-1 vaccine design: where do we go now&quest. Immunology and cell biology. 2010;89(3):367-74.
74. Hirbod T, Broliden K. Mucosal immune responses in the genital tract of HIV-1-exposed uninfected women. Journal of internal medicine. 2007;262(1):44-58.
75. Mascola JR, Stiegler G, VanCott TC, Katinger H, Carpenter CB, Hanson CE, et al. Protection of macaques against vaginal transmission of a pathogenic HIV-1/SIV chimeric virus by passive infusion of neutralizing antibodies. Nature medicine. 2000;6(2):207-10.
76. Genescà M. Characterization of an Effective CTL Response against HIV and SIV Infections. BioMed Research International. 2011;2011.
77. McElrath MJ, Haynes BF. Induction of immunity to human immunodeficiency virus type-1 by vaccination. Immunity. 2010;33(4):542-54.
78. Day CL, Walker BD. Progress in defining CD4 helper cell responses in chronic viral infections. The Journal of experimental medicine. 2003;198(12):1773-7.
79. Zhao Z, Leong K. Controlled delivery of antigens and adjuvants in vaccine development. Journal of pharmaceutical sciences. 1996;85(12):1261-70.
80. Bettinger T, Carlisle RC, Read ML, Ogris M, Seymour LW. Peptide-mediated RNA delivery: a novel approach for enhanced transfection of primary and post-mitotic cells. Nucleic acids research. 2001;29(18):3882-91.
81. Pascolo S. Vaccination with messenger RNA (mRNA). Toll-Like Receptors (TLRs) and Innate Immunity: Springer; 2008. p. 221-35.
82. Storni T, Kündig TM, Senti G, Johansen P. Immunity in response to particulate antigen-delivery systems. Advanced drug delivery reviews. 2005;57(3):333-55.
83. Marciani DJ. Vaccine adjuvants: role and mechanisms of action in vaccine immunogenicity. Drug discovery today. 2003;8(20):934-43.
84. Kazzaz J, Singh M, Ugozzoli M, Chesko J, Soenawan E, O'Hagan DT. Encapsulation of the immune potentiators MPL and RC529 in PLG microparticles enhances their potency. Journal of controlled release. 2006;110(3):566-73.
85. Gupta RK. Aluminum compounds as vaccine adjuvants. Advanced drug delivery reviews. 1998;32(3):155-72.
86. Goto N, Kato H, Maeyama J-i, Eto K, Yoshihara S. Studies on the toxicities of aluminium hydroxide and calcium phosphate as immunological adjuvants for vaccines. Vaccine. 1993;11(9):914-8.
87. Campbell A. The potential role of aluminium in Alzheimer's disease. Nephrology Dialysis Transplantation. 2002;17(suppl 2):17-20.
88. Chen X, Kim P, Farinelli B, Doukas A, Yun S-H, Gelfand JA, et al. A novel laser vaccine adjuvant increases the motility of antigen presenting cells. PLoS One. 2010;5(10):e13776.
89. Heikenwalder M, Polymenidou M, Junt T, Sigurdson C, Wagner H, Akira S, et al. Lymphoid follicle destruction and immunosuppression after repeated CpG oligodeoxynucleotide administration. Nature medicine. 2004;10(2):187-92.
90. O'Hagan DT, Valiante NM. Recent advances in the discovery and delivery of vaccine adjuvants. Nature Reviews Drug Discovery. 2003;2(9):727-35.
91. O'Hagan DT, Lavelle E. Novel adjuvants and delivery systems for HIV vaccines. Aids. 2002;16:S115-S24.

92. Pinto Reis C, Neufeld RJ, Ribeiro AJ, Veiga F. Nanoencapsulation I. Methods for preparation of drug-loaded polymeric nanoparticles. Nanomedicine: Nanotechnology, Biology and Medicine. 2006;2(1):8-21.
93. Pinto Reis C, Neufeld RJ, Ribeiro AJ, Veiga F. Nanoencapsulation II. Biomedical applications and current status of peptide and protein nanoparticulate delivery systems. Nanomedicine: Nanotechnology, Biology and Medicine. 2006;2(2):53-65.
94. Beaudette TT, Bachelder EM, Cohen JA, Obermeyer AC, Broaders KE, Fréchet JM, et al. In vivo studies on the effect of co-encapsulation of CpG DNA and antigen in acid-degradable microparticle vaccines. Molecular pharmaceutics. 2009;6(4):1160-9.
95. Zolnik BS, González-Fernández Á, Sadrieh N, Dobrovolskaia MA. Minireview: nanoparticles and the immune system. Endocrinology. 2010;151(2):458-65.
96. Cohen S, Alonso MJ, Langer R. Novel approaches to controlled-release antigen delivery. International journal of technology assessment in health care. 1994;10(01):121-30.
97. Liard C, Munier S, Arias M, Joulin-Giet A, Bonduelle O, Duffy D, et al. Targeting of HIV-p24 particle-based vaccine into differential skin layers induces distinct arms of the immune responses. Vaccine. 2011;29(37):6379-91.
98. Caputo A, Castaldello A, Brocca-Cofano E, Voltan R, Bortolazzi F, Altavilla G, et al. Induction of humoral and enhanced cellular immune responses by novel core–shell nanosphere-and microsphere-based vaccine formulations following systemic and mucosal administration. Vaccine. 2009;27(27):3605-15.
99. Himeno A, Akagi T, Uto T, Wang X, Baba M, Ibuki K, et al. Evaluation of the immune response and protective effects of rhesus macaques vaccinated with biodegradable nanoparticles carrying gp120 of human immunodeficiency virus. Vaccine. 2010;28(32):5377-85.
100. Zhu Q, Talton J, Zhang G, Cunningham T, Wang Z, Waters RC, et al. Large intestine-targeted, nanoparticle-releasing oral vaccine to control genitorectal viral infection. Nature medicine. 2012;18(8):1291-6.
101. Lamalle-Bernard D, Munier S, Compagnon C, Charles M-H, Kalyanaraman VS, Delair T, et al. Coadsorption of HIV-1 p24 and gp120 proteins to surfactant-free anionic PLA nanoparticles preserves antigenicity and immunogenicity. Journal of controlled release. 2006;115(1):57-67.
102. Lisziewicz J, Kelly L, Lori F. Topical DermaVir vaccine targeting dendritic cells. Current drug delivery. 2006;3(1):83-8.
103. Lisziewicz J, Trocio J, Xu J, Whitman L, Ryder A, Bakare N, et al. Control of viral rebound through therapeutic immunization with DermaVir. Aids. 2005;19(1):35-43.
104. Bachmann MF, Jennings GT. Vaccine delivery: a matter of size, geometry, kinetics and molecular patterns. Nature Reviews Immunology. 2010;10(11):787-96.
105. Banchereau J, Steinman RM. Dendritic cells and the control of immunity. Nature. 1998;392(6673):245-52.
106. de Jong EC, Smits HH, Kapsenberg ML, editors. Dendritic cell-mediated T cell polarization. Springer seminars in immunopathology; 2005: Springer.
107. Randolph GJ, Angeli V, Swartz MA. Dendritic-cell trafficking to lymph nodes through lymphatic vessels. Nature Reviews Immunology. 2005;5(8):617-28.
108. Adams S, O'Neill DW, Bhardwaj N. Recent advances in dendritic cell biology. Journal of clinical immunology. 2005;25(2):87-98.
109. Luster AD. The role of chemokines in linking innate and adaptive immunity. Current opinion in immunology. 2002;14(1):129-35.
110. Demento SL, Siefert AL, Bandyopadhyay A, Sharp FA, Fahmy TM. Pathogen-associated molecular patterns on biomaterials: a paradigm for engineering new vaccines. Trends in biotechnology. 2011;29(6):294-306.
111. Seong S-Y, Matzinger P. Hydrophobicity: an ancient damage-associated molecular pattern that initiates innate immune responses. Nature Reviews Immunology. 2004;4(6):469-78.
112. Ingulli E, Mondino A, Khoruts A, Jenkins MK. In vivo detection of dendritic cell antigen presentation to CD4+ T cells. The Journal of experimental medicine. 1997;185(12):2133-41.

113. De Temmerman M-L, Rejman J, Demeester J, Irvine DJ, Gander B, De Smedt SC. Particulate vaccines: on the quest for optimal delivery and immune response. Drug discovery today. 2011;16(13):569-82.
114. McGreal EP, Miller JL, Gordon S. Ligand recognition by antigen-presenting cell C-type lectin receptors. Current opinion in immunology. 2005;17(1):18-24.
115. Pierre P, Turley SJ, Gatti E, Hull M, Meltzer J, Mirza A, et al. Developmental regulation of MHC class II transport in mouse dendritic cells. Nature. 1997;388(6644):787-92.
116. Chefalo PJ, Harding CV. Processing of exogenous antigens for presentation by class I MHC molecules involves post-Golgi peptide exchange influenced by peptide-MHC complex stability and acidic pH. The Journal of Immunology. 2001;167(3):1274-82.
117. Song R, Harding CV. Roles of proteasomes, transporter for antigen presentation (TAP), and beta 2-microglobulin in the processing of bacterial or particulate antigens via an alternate class I MHC processing pathway. The Journal of Immunology. 1996;156(11):4182-90.
118. Gagnon E, Duclos S, Rondeau C, Chevet E, Cameron PH, Steele-Mortimer O, et al. Endoplasmic reticulum-mediated phagocytosis is a mechanism of entry into macrophages. Cell. 2002;110(1):119-31.
119. Bousso P, Robey E. Dynamics of CD8+ T cell priming by dendritic cells in intact lymph nodes. Nature immunology. 2003;4(6):579-85.
120. Perez VL, Van Parijs L, Biuckians A, Zheng XX, Strom TB, Abbas AK. Induction of peripheral T cell tolerance in vivo requires CTLA-4 engagement. Immunity. 1997;6(4):411-7.
121. Harrington LE, Mangan PR, Weaver CT. Expanding the effector CD4 T-cell repertoire: the Th17 lineage. Current opinion in immunology. 2006;18(3):349-56.
122. Constant SL, Bottomly K. Induction of Th1 and Th2 CD4+ T cell responses: the alternative approaches. Annual review of immunology. 1997;15(1):297-322.
123. Netea MG, Van der Meer JW, Sutmuller RP, Adema GJ, Kullberg B-J. From the Th1/Th2 paradigm towards a Toll-like receptor/T-helper bias. Antimicrobial agents and chemotherapy. 2005;49(10):3991-6.
124. Arens R, Schoenberger SP. Plasticity in programming of effector and memory CD8+ T-cell formation. Immunological reviews. 2010;235(1):190-205.
125. Sallusto F, Geginat J, Lanzavecchia A. Central memory and effector memory T cell subsets: function, generation, and maintenance. Annu Rev Immunol. 2004;22:745-63.
126. Young HA, Hardy K. Role of interferon-gamma in immune cell regulation. Journal of leukocyte biology. 1995;58(4):373-81.
127. Opferman JT, Ober BT, Ashton-Rickardt PG. Linear differentiation of cytotoxic effectors into memory T lymphocytes. Science. 1999;283(5408):1745-8.
128. Johansen P, Stamou P, Tascon RE, Lowrie DB, Stockinger B. CD4 T cells guarantee optimal competitive fitness of CD8 memory T cells. European journal of immunology. 2004;34(1):91-7.
129. Donaghy H, Gazzard B, Gotch F, Patterson S. Dysfunction and infection of freshly isolated blood myeloid and plasmacytoid dendritic cells in patients infected with HIV-1. Blood. 2003;101(11):4505-11.
130. Granelli-Piperno A, Golebiowska A, Trumpfheller C, Siegal FP, Steinman RM. HIV-1-infected monocyte-derived dendritic cells do not undergo maturation but can elicit IL-10 production and T cell regulation. Proceedings of the National Academy of Sciences of the United States of America. 2004;101(20):7669-74.
131. Naicker DD, Wang B, Losina E, Zupkosky J, Bryan S, Reddy S, et al. Association of IL-10-promoter genetic variants with the rate of CD4 T-cell loss, IL-10 plasma levels, and breadth of cytotoxic T-cell lymphocyte response during chronic HIV-1 infection. Clinical Infectious Diseases. 2011:cir811.
132. Huber S, Gagliani N, Esplugues E, O'Connor Jr W, Huber FJ, Chaudhry A, et al. Th17 cells express interleukin-10 receptor and are controlled by Foxp3− and Foxp3+ regulatory CD4+ T cells in an interleukin-10 dependent manner. Immunity. 2011;34(4):554.

133. Rock KL, Shen L. Cross-presentation: underlying mechanisms and role in immune surveillance. Immunological reviews. 2005;207(1):166-83.
134. Lanzavecchia A. Mechanisms of antigen uptake for presentation. Current opinion in immunology. 1996;8(3):348-54.
135. Avraméas A, McIlroy D, Hosmalin A, Autran B, Debré P, Monsigny M, et al. Expression of a mannose/fucose membrane lectin on human dendritic cells. European journal of immunology. 1996;26(2):394-400.
136. Kaisho T, Akira S. Toll-like receptors as adjuvant receptors. Biochimica et Biophysica Acta (BBA)-Molecular Cell Research. 2002;1589(1):1-13.
137. Blander JM, Medzhitov R. Regulation of phagosome maturation by signals from toll-like receptors. Science. 2004;304(5673):1014-8.
138. Bauer S, Kirschning CJ, Häcker H, Redecke V, Hausmann S, Akira S, et al. Human TLR9 confers responsiveness to bacterial DNA via species-specific CpG motif recognition. Proceedings of the National Academy of Sciences. 2001;98(16):9237-42.
139. Alexopoulou L, Holt AC, Medzhitov R, Flavell RA. Recognition of double-stranded RNA and activation of NF-κB by Toll-like receptor 3. Nature. 2001;413(6857):732-8.
140. Pasare C, Medzhitov R. Toll pathway-dependent blockade of CD4+ CD25+ T cell-mediated suppression by dendritic cells. Science. 2003;299(5609):1033-6.
141. van Broekhoven CL, Parish CR, Demangel C, Britton WJ, Altin JG. Targeting Dendritic Cells with Antigen-Containing Liposomes A Highly Effective Procedure for Induction of Antitumor Immunity and for Tumor Immunotherapy. Cancer research. 2004;64(12):4357-65.
142. Lee H, Jang IH, Ryu SH, Park TG. N-terminal site-specific mono-PEGylation of epidermal growth factor. Pharmaceutical research. 2003;20(5):818-25.
143. Wilson NS, El-Sukkari D, Belz GT, Smith CM, Steptoe RJ, Heath WR, et al. Most lymphoid organ dendritic cell types are phenotypically and functionally immature. Blood. 2003;102(6):2187-94.
144. Gamvrellis A, Leong D, Hanley JC, Xiang SD, Mottram P, Plebanski M. Vaccines that facilitate antigen entry into dendritic cells. Immunology and cell biology. 2004;82(5):506-16.
145. Josephson L, Tung C-H, Moore A, Weissleder R. High-efficiency intracellular magnetic labeling with novel superparamagnetic-Tat peptide conjugates. Bioconjugate chemistry. 1999;10(2):186-91.
146. Liu Z, Cumberland WG, Hultin LE, Prince HE, Detels R, Giorgi JV. Elevated CD38 antigen expression on CD8+ T cells is a stronger marker for the risk of chronic HIV disease progression to AIDS and death in the Multicenter AIDS Cohort Study than CD4+ cell count, soluble immune activation markers, or combinations of HLA-DR and CD38 expression. JAIDS Journal of Acquired Immune Deficiency Syndromes. 1997;16(2):83-92.
147. Alpar HO. Strategies for vaccine delivery. Journal of drug targeting. 2003;11(8-10):459-61.
148. Montefiori D, Sattentau Q, Flores J, Esparza J, Mascola J, Enterprise aWGcbtGHV. Antibody-based HIV-1 vaccines: recent developments and future directions. PLoS medicine. 2007;4(12):e348.
149. Nagashima KA, Thompson DA, Rosenfield SI, Maddon PJ, Dragic T, Olson WC. Human immunodeficiency virus type 1 entry inhibitors PRO 542 and T-20 are potently synergistic in blocking virus-cell and cell-cell fusion. Journal of Infectious Diseases. 2001;183(7):1121-5.
150. Clercq ED. New anti-HIV agents and targets. Medicinal research reviews. 2002;22(6):531-65.
151. Esparza J. What Has 30 Years of HIV Vaccine Research Taught Us? Vaccines. 2013;1(4):513-26.
152. Moore JP, Doms RW. The entry of entry inhibitors: a fusion of science and medicine. Proceedings of the National Academy of Sciences. 2003;100(19):10598-602.
153. Wild CT, Shugars DC, Greenwell TK, McDanal CB, Matthews TJ. Peptides corresponding to a predictive alpha-helical domain of human immunodeficiency virus type 1 gp41 are potent inhibitors of virus infection. Proceedings of the National Academy of Sciences. 1994;91(21):9770-4.
154. Hardy H, Skolnik PR. Enfuvirtide, a new fusion inhibitor for therapy of human immunodeficiency virus infection. Pharmacotherapy: The Journal of Human Pharmacology and Drug Therapy. 2004;24(2):198-211.
155. Wild C, Greenwell T, Matthews T. A synthetic peptide from HIV-1 gp41 is a potent inhibitor of virus-mediated cell—cell fusion. AIDS research and human retroviruses. 1993;9(11):1051-3.

156. Eggink D, Berkhout B, W Sanders R. Inhibition of HIV-1 by fusion inhibitors. Current pharmaceutical design. 2010;16(33):3716-28.
157. Ketas TJ, Klasse PJ, Spenlehauer C, Nesin M, Frank I, Pope M, et al. Entry inhibitors SCH-C, RANTES, and T-20 block HIV type 1 replication in multiple cell types. AIDS research and human retroviruses. 2003;19(3):177-86.
158. Lazzarin A, Clotet B, Cooper D, Reynes J, Arasteh K, Nelson M, et al. Efficacy of enfuvirtide in patients infected with drug-resistant HIV-1 in Europe and Australia. New England Journal of Medicine. 2003;348(22):2186-95.
159. Johnson VA, Brun-Vézinet F, Clotet B, Gunthard H, Kuritzkes DR, Pillay D, et al. Update of the drug resistance mutations in HIV-1: December 2009. Top HIV Med. 2009;17(5):138-45.
160. Cai L, Jiang S. Development of Peptide and Small-Molecule HIV-1 Fusion Inhibitors that Target gp41. ChemMedChem. 2010;5(11):1813-24.
161. Gulick R. New antiretroviral drugs. Clinical microbiology and infection. 2003;9(3):186-93.
162. Chong CS, Cao M, Wong WW, Fischer KP, Addison WR, Kwon GS, et al. Enhancement of T helper type 1 immune responses against hepatitis B virus core antigen by PLGA nanoparticle vaccine delivery. Journal of controlled release. 2005;102(1):85-99.
163. Miller RA, Brady JM, Cutright DE. Degradation rates of oral resorbable implants (polylactates and polyglycolates): rate modification with changes in PLA/PGA copolymer ratios. Journal of biomedical materials research. 1977;11(5):711-9.
164. Molavi O, Mahmud A, Hamdy S, Hung RW, Lai R, Samuel J, et al. Development of a Poly (D, L-lactic-co-glycolic acid) Nanoparticle Formulation of STAT3 Inhibitor JSI-124: Implication for Cancer Immunotherapy. Molecular pharmaceutics. 2010;7(2):364-74.
165. Danhier F, Lecouturier N, Vroman B, Jérôme C, Marchand-Brynaert J, Feron O, et al. Paclitaxel-loaded PEGylated PLGA-based nanoparticles: in vitro and in vivo evaluation. Journal of Controlled Release. 2009;133(1):11-7.
166. Luo G, Jin C, Long J, Fu D, Yang F, Xu J, et al. RNA interference of MBD1 in BxPC-3 human pancreatic cancer cells delivered by PLGA-poloxamer nanoparticles. Cancer Biol Ther. 2009;8(7):594-8.
167. Wang Y, Ng YW, Chen Y, Shuter B, Yi J, Ding J, et al. Formulation of superparamagnetic iron oxides by nanoparticles of biodegradable polymers for magnetic resonance imaging. Advanced Functional Materials. 2008;18(2):308-18.
168. Lamprecht A, Yamamoto H, Takeuchi H, Kawashima Y. Nanoparticles enhance therapeutic efficiency by selectively increased local drug dose in experimental colitis in rats. Journal of Pharmacology and Experimental Therapeutics. 2005;315(1):196-202.
169. Higaki M, Ishihara T, Izumo N, Takatsu M, Mizushima Y. Treatment of experimental arthritis with poly (D, L-lactic/glycolic acid) nanoparticles encapsulating betamethasone sodium phosphate. Annals of the rheumatic diseases. 2005;64(8):1132-6.
170. Cartiera MS, Ferreira EC, Caputo C, Egan ME, Caplan MJ, Saltzman WM. Partial correction of cystic fibrosis defects with PLGA nanoparticles encapsulating curcumin. Molecular pharmaceutics. 2009;7(1):86-93.
171. Chappell JC, Song J, Burke CW, Klibanov AL, Price RJ. Targeted Delivery of Nanoparticles Bearing Fibroblast Growth Factor-2 by Ultrasonic Microbubble Destruction for Therapeutic Arteriogenesis. Small. 2008;4(10):1769-77.
172. Vorp DA, Maul T, Nieponice A. Molecular aspects of vascular tissue engineering. Front Biosci. 2005;10:768-89.
173. Liu J, Zhang S, Chen P, Cheng L, Zhou W, Tang W, et al. Controlled release of insulin from PLGA nanoparticles embedded within PVA hydrogels. Journal of Materials Science: Materials in Medicine. 2007;18(11):2205-10.
174. Pillai RR, Somayaji SN, Rabinovich M, Hudson MC, Gonsalves KE. Nafcillin-loaded PLGA nanoparticles for treatment of osteomyelitis. Biomedical Materials. 2008;3(3):034114.
175. Gregory AE, Titball R, Williamson D. Vaccine delivery using nanoparticles. Frontiers in cellular and infection microbiology. 2013;3.

176. Bharali DJ, Pradhan V, Elkin G, Qi W, Hutson A, Mousa SA, et al. Novel nanoparticles for the delivery of recombinant hepatitis B vaccine. Nanomedicine: Nanotechnology, Biology and Medicine. 2008;4(4):311-7.
177. Demento SL, Bonafé N, Cui W, Kaech SM, Caplan MJ, Fikrig E, et al. TLR9-targeted biodegradable nanoparticles as immunization vectors protect against West Nile encephalitis. The Journal of Immunology. 2010;185(5):2989-97.
178. Ham AS, Cost MR, Sassi AB, Dezzutti CS, Rohan LC. Targeted delivery of PSC-RANTES for HIV-1 prevention using biodegradable nanoparticles. Pharmaceutical research. 2009;26(3):502-11.
179. Steinbach JM, Weller CE, Booth CJ, Saltzman WM. Polymer nanoparticles encapsulating siRNA for treatment of HSV-2 genital infection. Journal of Controlled Release. 2012;162(1):102-10.
180. Zhang T, Sturgis TF, Youan B-BC. pH-responsive nanoparticles releasing tenofovir intended for the prevention of HIV transmission. European Journal of Pharmaceutics and Biopharmaceutics. 2011;79(3):526-36.
181. Date AA, Shibata A, Goede M, Sanford B, La Bruzzo K, Belshan M, et al. Development and evaluation of a thermosensitive vaginal gel containing raltegravir+efavirenz loaded nanoparticles for HIV prophylaxis. Antiviral Res. 2012;96(3):430-6.
182. Jiang W, Gupta RK, Deshpande MC, Schwendeman SP. Biodegradable poly (lactic-co-glycolic acid) microparticles for injectable delivery of vaccine antigens. Advanced drug delivery reviews. 2005;57(3):391-410.
183. Hamdy S, Molavi O, Ma Z, Haddadi A, Alshamsan A, Gobti Z, et al. Co-delivery of cancer-associated antigen and Toll-like receptor 4 ligand in PLGA nanoparticles induces potent CD8< sup>+</sup> T cell-mediated anti-tumor immunity. Vaccine. 2008;26(39):5046-57.
184. Shen H, Ackerman AL, Cody V, Giodini A, Hinson ER, Cresswell P, et al. Enhanced and prolonged cross-presentation following endosomal escape of exogenous antigens encapsulated in biodegradable nanoparticles. Immunology. 2006;117(1):78-88.
185. Diwan M, Elamanchili P, Cao M, Samuel J. Dose sparing of CpG oligodeoxynucleotide vaccine adjuvants by nanoparticle delivery. Current drug delivery. 2004;1(4):405-12.
186. Liu G, Zhang L, Zhao Y. Modulation of immune responses through direct activation of Toll-like receptors to T cells. Clinical & Experimental Immunology. 2010;160(2):168-75.
187. Cruz LJ, Tacken PJ, Fokkink R, Joosten B, Stuart MC, Albericio F, et al. Targeted PLGA nano-but not microparticles specifically deliver antigen to human dendritic cells via DC-SIGN in vitro. Journal of Controlled Release. 2010;144(2):118-26.
188. Mundargi RC, Babu VR, Rangaswamy V, Patel P, Aminabhavi TM. Nano/micro technologies for delivering macromolecular therapeutics using poly(D,L-lactide-co-glycolide) and its derivatives. Journal of controlled release : official journal of the Controlled Release Society. 2008;125(3):193-209.
189. Freichels H, Danhier F, Préat V, Lecomte P, Jérôme C. Fluorescent labeling of degradable poly (lactide-co-glycolide) for cellular nanoparticles tracking in living cells. The International journal of artificial organs. 2011;34(2):152-60.
190. Florindo HF, Pandit S, Gonçalves L, Videira M, Alpar O, Almeida AJ. Antibody and cytokine-associated immune responses to S. equi antigens entrapped in PLA nanospheres. Biomaterials. 2009;30(28):5161-9.
191. Florindo HF, Pandit S, Lacerda L, Gonçalves LMD, Alpar HO, Almeida AJ. The enhancement of the immune response against S. equi antigens through the intranasal administration of poly-ε-caprolactone-based nanoparticles. Biomaterials. 2009;30(5):879-91.
192. Letvin NL. Correlates of immune protection and the development of a human immunodeficiency virus vaccine. Immunity. 2007;27(3):366-9.
193. Marcelino JM, Borrego P, Rocha C, Barroso H, Quintas A, Novo C, et al. Potent and broadly reactive HIV-2 neutralizing antibodies elicited by a vaccinia virus vector prime-C2V3C3 polypeptide boost immunization strategy. Journal of virology. 2010;84(23):12429-36.
194. Greenland JR, Letvin NL. Chemical adjuvants for plasmid DNA vaccines. Vaccine. 2007;25(19):3731-41.

195. Bramwell VW, Perrie Y. Particulate delivery systems for vaccines: what can we expect? Journal of pharmacy and pharmacology. 2006;58(6):717-28.
196. Davis SS. The use of soluble polymers and polymer microparticles to provide improved vaccine responses after parenteral and mucosal delivery. Vaccine. 2006;24:S7-S10.
197. Woodrow KA, Cu Y, Booth CJ, Saucier-Sawyer JK, Wood MJ, Saltzman WM. Intravaginal gene silencing using biodegradable polymer nanoparticles densely loaded with small-interfering RNA. Nature materials. 2009;8(6):526-33.
198. Date AA, Shibata A, Goede M, Sanford B, La Bruzzo K, Belshan M, et al. Development and evaluation of a thermosensitive vaginal gel containing raltegravir+ efavirenz loaded nanoparticles for HIV prophylaxis. Antiviral research. 2012;96(3):430-6.
199. Kumari A, Yadav SK, Yadav SC. Biodegradable polymeric nanoparticles based drug delivery systems. Colloids and Surfaces B: Biointerfaces. 2010;75(1):1-18.
200. Panyam J, ZHOU W-Z, PRABHA S, SAHOO SK, LABHASETWAR V. Rapid endo-lysosomal escape of poly (DL-lactide-co-glycolide) nanoparticles: implications for drug and gene delivery. The FASEB Journal. 2002;16(10):1217-26.
201. Vasir JK, Labhasetwar V. Biodegradable nanoparticles for cytosolic delivery of therapeutics. Advanced drug delivery reviews. 2007;59(8):718-28.
202. Cu Y, Booth CJ, Saltzman WM. In vivo distribution of surface-modified PLGA nanoparticles following intravaginal delivery. Journal of Controlled Release. 2011;156(2):258-64.
203. Cruz LJ, Tacken PJ, Fokkink R, Figdor CG. The influence of PEG chain length and targeting moiety on antibody-mediated delivery of nanoparticle vaccines to human dendritic cells. Biomaterials. 2011;32(28):6791-803.
204. Betancourt T, Byrne JD, Sunaryo N, Crowder SW, Kadapakkam M, Patel S, et al. PEGylation strategies for active targeting of PLA/PLGA nanoparticles. Journal of Biomedical Materials Research Part A. 2009;91(1):263-76.
205. Tobıo M, Sanchez A, Vila A, Soriano I, Evora C, Vila-Jato J, et al. The role of PEG on the stability in digestive fluids and in vivo fate of PEG-PLA nanoparticles following oral administration. Colloids and Surfaces B: Biointerfaces. 2000;18(3):315-23.
206. Aline F, Brand D, Pierre J, Roingeard P, Séverine M, Verrier B, et al. Dendritic cells loaded with HIV-1 p24 proteins adsorbed on surfactant-free anionic PLA nanoparticles induce enhanced cellular immune responses against HIV-1 after vaccination. Vaccine. 2009;27(38):5284-91.
207. Nagavarma B, Hemant KY, Ayaz A, Vasudha L, Shivakumar H. Different techniques for preparation of polymeric nanoparticles-a review. Asian Journal of Pharmaceutical and Clinical Research. 2012;5(3):16-23.
208. Rao JP, Geckeler KE. Polymer nanoparticles: preparation techniques and size-control parameters. Progress in Polymer Science. 2011;36(7):887-913.
209. Ogawa Y, Yamamoto M, Okada H, Yashiki T, Shimamoto T. A new technique to efficiently entrap leuprolide acetate into microcapsules of polylactic acid or copoly(lactic/glycolic) acid. Chem Pharm Bull (Tokyo). 1988;36(3):1095-103.
210. Sahoo SK, Panyam J, Prabha S, Labhasetwar V. Residual polyvinyl alcohol associated with poly (D,L-lactide-co-glycolide) nanoparticles affects their physical properties and cellular uptake. Journal of controlled release : official journal of the Controlled Release Society. 2002;82(1):105-14.
211. Lemoine D, Préat V. Polymeric nanoparticles as delivery system for influenza virus glycoproteins. Journal of Controlled Release. 1998;54(1):15-27.
212. Wang Y-C, Wu Y-T, Huang H-Y, Yang C-S. Surfactant-free formulation of poly (lactic/glycolic) acid nanoparticles encapsulating functional polypeptide: a technical note. Aaps Pharmscitech. 2009;10(4):1263-7.
213. Zambaux M, Bonneaux F, Gref R, Maincent P, Dellacherie E, Alonso M, et al. Influence of experimental parameters on the characteristics of poly (lactic acid) nanoparticles prepared by a double emulsion method. Journal of Controlled Release. 1998;50(1):31-40.
214. Batrakova E, Li S, Elmquist W, Miller D, Alakhov VY, Kabanov A. Mechanism of sensitization of MDR cancer cells by Pluronic block copolymers: Selective energy depletion. British journal of cancer. 2001;85(12):1987.

215. Menon JU, Kona S, Wadajkar AS, Desai F, Vadla A, Nguyen KT. Effects of surfactants on the properties of PLGA nanoparticles. Journal of Biomedical Materials Research Part A. 2012;100(8):1998-2005.
216. Mansouri S, Lavigne P, Corsi K, Benderdour M, Beaumont E, Fernandes JC. Chitosan-DNA nanoparticles as non-viral vectors in gene therapy: strategies to improve transfection efficacy. European Journal of Pharmaceutics and Biopharmaceutics. 2004;57(1):1-8.
217. Iqbal M, Lin W, Jabbal-Gill I, Davis S, Steward M, Illum L. Nasal delivery of chitosan–DNA plasmid expressing epitopes of respiratory syncytial virus (RSV) induces protective CTL responses in BALB/c mice. Vaccine. 2003;21(13):1478-85.
218. Belletti D, Tosi G, Forni F, Gamberini MC, Baraldi C, Vandelli MA, et al. Chemico-physical investigation of tenofovir loaded polymeric nanoparticles. International journal of pharmaceutics. 2012;436(1):753-63.
219. Uto T, Akagi T, Toyama M, Nishi Y, Shima F, Akashi M, et al. Comparative activity of biodegradable nanoparticles with aluminum adjuvants: antigen uptake by dendritic cells and induction of immune response in mice. Immunology letters. 2011;140(1):36-43.
220. Wang X, Uto T, Akagi T, Akashi M, Baba M. Poly(gamma-glutamic acid) nanoparticles as an efficient antigen delivery and adjuvant system: potential for an AIDS vaccine. Journal of medical virology. 2008;80(1):11-9.
221. Fung HB, Guo Y. Enfuvirtide: a fusion inhibitor for the treatment of HIV infection. Clinical therapeutics. 2004;26(3):352-78.
222. Akagi T, Baba M, Akashi M. Biodegradable nanoparticles as vaccine adjuvants and delivery systems: regulation of immune responses by nanoparticle-based vaccine. Polymers in Nanomedicine: Springer; 2012. p. 31-64.
223. Ehrlich M, Boll W, van Oijen A, Hariharan R, Chandran K, Nibert ML, et al. Endocytosis by random initiation and stabilization of clathrin-coated pits. Cell. 2004;118(5):591-605.
224. Wang Z, Tiruppathi C, Minshall RD, Malik AB. Size and dynamics of caveolae studied using nanoparticles in living endothelial cells. ACS nano. 2009;3(12):4110-6.
225. Manolova V, Flace A, Bauer M, Schwarz K, Saudan P, Bachmann MF. Nanoparticles target distinct dendritic cell populations according to their size. European journal of immunology. 2008;38(5):1404-13.
226. Kumari A, Yadav SK. Cellular interactions of therapeutically delivered nanoparticles. Expert opinion on drug delivery. 2011;8(2):141-51.
227. Chithrani BD, Ghazani AA, Chan WC. Determining the size and shape dependence of gold nanoparticle uptake into mammalian cells. Nano letters. 2006;6(4):662-8.
228. Yoo JW, Doshi N, Mitragotri S. Endocytosis and intracellular distribution of PLGA particles in endothelial cells: effect of particle geometry. Macromolecular rapid communications. 2010;31(2):142-8.
229. Foged C, Brodin B, Frokjaer S, Sundblad A. Particle size and surface charge affect particle uptake by human dendritic cells in an in vitro model. International journal of pharmaceutics. 2005;298(2):315-22.
230. Vasir JK, Labhasetwar V. Quantification of the force of nanoparticle-cell membrane interactions and its influence on intracellular trafficking of nanoparticles. Biomaterials. 2008;29(31):4244-52.
231. Danhier F, Feron O, Préat V. To exploit the tumor microenvironment: Passive and active tumor targeting of nanocarriers for anti-cancer drug delivery. Journal of Controlled Release. 2010;148(2):135-46.
232. Yue Z-G, Wei W, Lv P-P, Yue H, Wang L-Y, Su Z-G, et al. Surface charge affects cellular uptake and intracellular trafficking of chitosan-based nanoparticles. Biomacromolecules. 2011;12(7):2440-6.
233. Saptarshi SR, Duschl A, Lopata AL. Interaction of nanoparticles with proteins: relation to bio-reactivity of the nanoparticle. J Nanobiotechnol. 2013;11(26).
234. Albanese A, Tang PS, Chan WC. The effect of nanoparticle size, shape, and surface chemistry on biological systems. Annual review of biomedical engineering. 2012;14:1-16.

235. Anton N, Benoit J-P, Saulnier P. Design and production of nanoparticles formulated from nano-emulsion templates—a review. Journal of Controlled Release. 2008;128(3):185-99.
236. Danhier F, Ansorena E, Silva JM, Coco R, Le Breton A, Préat V. PLGA-based nanoparticles: an overview of biomedical applications. Journal of controlled release. 2012;161(2):505-22.
237. Guideline IHT. Stability testing of new drug substances and products. Recommended for Adoption at Step. 2003;4.
238. Talmadge JE. The pharmaceutics and delivery of therapeutic polypeptides and proteins. Advanced drug delivery reviews. 1993;10(2):247-99.
239. Ataman-Önal Y, Munier S, Ganée A, Terrat C, Durand P-Y, Battail N, et al. Surfactant-free anionic PLA nanoparticles coated with HIV-1 p24 protein induced enhanced cellular and humoral immune responses in various animal models. Journal of controlled release. 2006;112(2):175-85.
240. Wiechelman KJ, Braun RD, Fitzpatrick JD. Investigation of the bicinchoninic acid protein assay: identification of the groups responsible for color formation. Analytical biochemistry. 1988;175(1):231-7.
241. Eberlein G. Quantitation of proteins using HPLC-detector response rather than standard curve comparison. Journal of pharmaceutical and biomedical analysis. 1995;13(10):1263-71.
242. Brown RE, Jarvis KL, Hyland KJ. Protein measurement using bicinchoninic acid: elimination of interfering substances. Analytical biochemistry. 1989;180(1):136-9.
243. Murphy DB, Davidson MW. Fundamentals of light microscopy and electronic imaging: John Wiley & Sons; 2012.
244. Eftink MR. Intrinsic fluorescence of proteins. Topics in fluorescence spectroscopy: Springer; 2000. p. 1-15.
245. Wang X, Uto T, Akagi T, Akashi M, Baba M. Poly (γ-glutamic acid) nanoparticles as an efficient antigen delivery and adjuvant system: Potential for an AIDS vaccine. Journal of medical virology. 2008;80(1):11-9.
246. Rampersad SN. Multiple applications of Alamar Blue as an indicator of metabolic function and cellular health in cell viability bioassays. Sensors. 2012;12(9):12347-60.
247. van de Weert M, Hennink WE, Jiskoot W. Protein instability in poly(lactic-co-glycolic acid) microparticles. Pharm Res. 2000;17(10):1159-67.
248. Giteau A, Venier-Julienne M-C, Marchal S, Courthaudon J-L, Sergent M, Montero-Menei C, et al. Reversible protein precipitation to ensure stability during encapsulation within PLGA microspheres. European Journal of Pharmaceutics and Biopharmaceutics. 2008;70(1):127-36.
249. Cleland JL, Powell MF, Shire SJ. The development of stable protein formulations: a close look at protein aggregation, deamidation, and oxidation. Critical reviews in therapeutic drug carrier systems. 1992;10(4):307-77.
250. Sah H. Protein instability toward organic solvent/water emulsification: implications for protein microencapsulation into microspheres. PDA Journal of Pharmaceutical Science and Technology. 1999;53(1):3-10.
251. Kumar PS, Saini TR, Chandrasekar D, Yellepeddi VK, Ramakrishna S, Diwan PV. Novel approach for delivery of insulin loaded poly (lactide-co-glycolide) nanoparticles using a combination of stabilizers. Drug delivery. 2007;14(8):517-23.
252. Zambaux M, Bonneaux F, Gref R, Dellacherie E, Vigneron C. Preparation and characterization of protein C-loaded PLA nanoparticles. Journal of controlled release. 1999;60(2):179-88.
253. Gallagher SR. One-dimensional SDS gel electrophoresis of proteins. Current protocols in molecular biology. 2006:10.2 A. 1-.2 A. 44.
254. Sarfo K, Moorhead GB, Turner RJ. A novel procedure for separating small peptides on polyacrylamide gels. Letters in Peptide Science. 2003;10(2):127-33.
255. Trombetta ES, Mellman I. Cell biology of antigen processing in vitro and in vivo. Annu Rev Immunol. 2005;23:975-1028.
256. Davis ID, Chen W, Jackson H, Parente P, Shackleton M, Hopkins W, et al. Recombinant NY-ESO-1 protein with ISCOMATRIX adjuvant induces broad integrated antibody and CD4+ and CD8+ T cell

responses in humans. Proceedings of the National Academy of Sciences of the United States of America. 2004;101(29):10697-702.
257. Shan X, Yuan Y, Liu C, Tao X, Sheng Y, Xu F. Influence of PEG chain on the complement activation suppression and longevity in vivo prolongation of the PCL biomedical nanoparticles. Biomedical microdevices. 2009;11(6):1187-94.
258. Pack DW, Hoffman AS, Pun S, Stayton PS. Design and development of polymers for gene delivery. Nature Reviews Drug Discovery. 2005;4(7):581-93.